

Best Available Copy

AD 667546

Best Available Copy

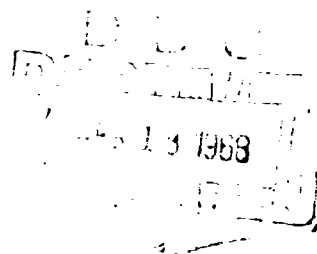
Reproduced by the
CLEARINGHOUSE
for Federal Scientific & Technical
Information Springfield Va. 22151

EM SHIELDING OF BUILDING MATERIALS

C. M. Brennan
et al

The Electro-Mechanics Company

This document has been approved
for public release and sale; its
distribution is unlimited.




FOREWORD

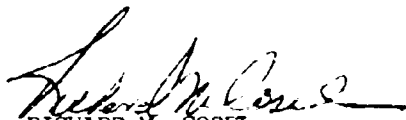
This final report was prepared by C.M. Brennan, C.C. Lambert, C.G. Conner, G.F. Roberts, W.T. Flannery and F.J. Morris of The Electro-Mechanics Company, P.O. Box 1546, Austin, Texas, under Contract AF30 (602)-4275, project number 4540, task number 454003. Reporting period covered May 1966 to June 1967. RADC project engineer is Wayne E. Woodward (EMCVI-2).

This report has been reviewed and is approved.


Approved:


WAYNE E. WOODWARD
Interf Anal & Control Sec
Vulnerability Reduction Branch

Approved:


RICHARD W. COSSELL
Colonel, USAF
Chief, Communications Division

FOR THE COMMANDER:


IRVING J. GABELMAN
Chief, Advanced Studies Group

ABSTRACT

This report covers the results of a program for measuring the shielding effectiveness (SE) of building materials. Part I of the report describes a number of techniques which were used to make radiated measurements of magnetic field SE from 10 Hz to 50 KHz and conductive measurements from 10 Hz to 1 GHz. A method was introduced for plotting the low frequency field distribution about various shaped ferromagnetic enclosures. Part II contains a group of the significant results of the radiated measurements on a variety of building materials. A collection of tables shows the measured electrical parameters and the calculated shielding obtainable from a cross-section of dielectric building materials.

TABLE OF CONTENTS

Foreword	ii
Abstract	iii

PART I

List of Illustrations	vi
List of Tables	viii
Part I — EM Shielding of Building Material	1
Introduction	1
Radiated Measurements	4
Conducted Measurements	30
Magnetic Field Pattern Shadowgraphs	37
Effects of Geometry and Construction Methods	54
Material Selection for Shielding	61

PART II

List of Illustrations	66
List of Tables	70
Part II — Handbook of Shielding	72
Introduction	72
Section 1 - General Conclusions	75
Section 2 - Graphed Results of Radiated Measurements	78
Section 3 - Tabulated Results of Conducted Measurements	127

LIST OF ILLUSTRATIONS

PART I

Fig. No.		Page
1	Block Diagram of MFIM.	6
2	Test Arrangement for Measuring Apparent Shielding Effectiveness of Metal Furniture	8
3	Apparent Shielding Effectiveness Caused by Metal Vending Machine Placed in Field Path	9
4	Test Arrangement for Measuring Field Distortion Caused by Office Furnishings	10
5	Apparent Field Attenuation vs Frequency Caused by Metal Filing Cabinet Field Barrier	11
6	Test Setup for Measuring Magnetic Field Attenuation Through Small Area Barriers	12
7	Test Arrangement for Measuring Shielding Through 4 x 8-Foot Metal Sheets	13
8	Equipment Configuration for Measuring Shielding Effectiveness of Small Enclosures	14
9	SE of a Sheet of 0.06-Inch Thick Aluminum at Various Distances from the Sensor	15
10	SE of One 0.06-Inch Thick Aluminum Sheet vs Spacing for Several Frequencies	16
11	SE Curve Variations as a Function of Barrier Placement	18
12	SE Curve Variations as a Function of Barrier Placement	19
13	SE of Two Aluminum Sheets .026- Inches Thick Separated Various Distances Between Source and Sensor	20
14	Closed Loop "Cage" Enclosures: 25 1-Foot-Square Loops per Cage, Each Loop on 1/2-Inch Centers	21
15	Shielding Effectiveness of Cage Made of 0.030-Inch Copper Wire	22
16	Shielding Effectiveness of Cage Made of 0.063-Inch Iron Wire	23
17	Shielding Effectiveness of Cage Made of 0.033-Inch Chromel "A" Wire	24

Fig. No.		Page
18	SE of a 1-Foot Cubed, Open-Ended Enclosure of 0.031-Inch Copper, All Seams Soldered	26
19	SE of 1-Foot Cubed, Open-Ended Enclosure of 0.055-Inch Galvanized Steel; All Seams Soldered	27
20	Shielding Effectiveness at Various Positions within a 4-Ft Cubical, 3/8-Inch Annealed Wrought Iron Box	28
21	Magnetic Field Shadowgraph Showing Field Distribution about a Square Cross-Section Barrier	29
22	Test Setup for Conducted Measurements	33
23	Device for Graphical Illustration of Magnetic Field Paths and Distortion	38
24	Field Vector Diagram	40
25	Field Vectors Calculated by Elliptical Integrals	44
26	Shadowgraph of the Magnetic Field Distribution about the Center of a Circular Coil	45
27	Plot of Calculated Field Distribution Printed over Magnetic Field Shadowgraph	46
28	60 Hz Field Along the Coil Axis	47
29	60 Hz Field Along Coil Axis	48
30	60 Hz Field Along Coil Axis	49
31	60 Hz Field Along Coil Axis	50
32	60 Hz Field at Edge of Coil	51
33	400 Hz Field at Edge of Coil	52
34	400 Hz Field Along Coil Axis	53
35	Shadowgraph of 60 Hz Field Distribution about a Circular Barrier	55
36	Shadowgraph of 60 Hz Field Distribution about a Circular Barrier Cut in Half and Butted Together	56
37	Shadowgraph of 60 Hz Field Distribution about Rejoined Halves of Circular Barrier, Showing Steel Weld and Brazed Joints	57
38	Magnetic Field SE of Two Sizes Expanded Steel	59

PART II

List of Illustrations	66
---------------------------------	----

LIST OF TABLES
PART I

Table		Page
I	Conducted Tests Equipment List	32

PART II

Alphabetical List of Tables	70
---------------------------------------	----

EVALUATION

The objective of this effort was to determine the shielding effectiveness of materials normally used in the construction of buildings housing electronic equipment. For the purpose of this effort the first order parameters were wall materials, configuration, and entry via seams, doors, windows, power lines, roofing and et cetera. Knowledge of the nature of basic construction materials with respect to behavior will allow the construction of buildings in which materials can be chosen on the basis of their composition and shielding properties as well as their structural properties.

Some of the high lights of this effort are as follows:

a. Shadowgraphs of the magnetic field distribution of miniaturized enclosures can yield valuable data during the design stage. This technique will show where to place or where not to place electronic equipment within an enclosure.

b. The use of reinforcing steel rods does not provide the proper degree of homogeneity in a wall to effect good shielding. Expanded metal plates have good homogeneous properties as well as strength and good bonding characteristics.

c. Ferromagnetic materials are needed for shielding at frequencies below 1 kHz. Conductive sheets or expanses of metals are responsible for shielding effectiveness at frequencies above several kHz.

d. Dielectric construction materials, such as concrete, brick, stone, plaster, etc. offer no significant shielding at frequencies below 100 MHz.

e. The presence of metal fixtures as furniture in an enclosure can cause apparent shielding which is not homogeneous throughout the enclosure. This can give misleading results when measuring shielding effectiveness of a building or room.

Wayne E. Woodward
WAYNE E. WOODWARD

EM SHIELDING OF BUILDING MATERIALS

PART I

Introduction:

Electrical and electronic equipment functioning normally may generate electrical, magnetic or electromagnetic signals of a fundamental or spurious nature. Since nearly all electronic circuits are influenced by induced signals, steps must be taken to keep the radiation from one apparatus from degrading the operation of another. Electronic interference is most likely to occur in large concentrations of electronic and electrical equipment. To prevent malfunction of control circuits, loss of security in intelligence systems and physical damage to delicate circuitry, it is necessary to provide a proper shield between installations of incompatible equipment.

In the past, shielding was a concern only when delicate, low level measurements were being made. Shielded enclosures were used to house equipment known to be interference generators, or the enclosures were used to house the equipment which had to be protected from interfering signals. The history of screen shielding consists of little more than a description of the use of copper screen enclosures with carefully soldered corner seams and with good electrical contact at door and window seams. In recent years more emphasis has been placed on shielding from magnetic fields as well as from electric and electromagnetic fields. The name "low impedance" is often given to magnetic fields in contrast to electric fields which are called high impedance fields.

The shielding of low impedance fields is considerably harder to accomplish than shielding of high impedance fields. Whereas electric field shielding is rather easily accomplished with a conductive enclosure, an effective shield for low frequency magnetic fields requires the use of magnetically permeable materials in massive amounts compared to the amount of materials necessary in high frequency shields. The shape and orientation of an enclosure with respect to its surroundings also play an important part in determining the shielding effectiveness (SE) of a barrier about a particular location. The shape, orientation, and distribution of material in a shield are all considered in the geometry of a shield.

The objective of the work on this program was to measure the SE of different building materials by two methods. Radiated or induced field measurements were made on a complete cross section of building materials. These measurements were made covering the

frequency range from 10Hz to 50KHz. Conducted measurements which measure the electrical characteristics of materials were made from 10Hz to 1GHz.

Radiated measurements indicate directly the reduction of signal strength due to the presence of an attenuating barrier. This reduction of signal strength is said to be the SE of the barrier. The conducted tests measure the electrical parameters of materials. By using the values of these parameters, the SE of the materials may be calculated.

The result of the measurements are tabulated in Part II of this report. These tabulations are arranged so as to be of help to building design architects and engineers. With comparative shielding data available, the designers and builders will have a choice of materials for construction and may determine the best for shielding.

Shielding measurements have been classified in three categories: 1) the attenuation of magnetic fields, 2) the attenuation of electric fields, and 3) the attenuation of plane waves. According to procedures in Military Standards for SE measurements, magnetic field measurements are made up to 200KHz using shielded loops. Electric field measurements are made using a tuned rod radiator and sensor. Electric field measurements are usually made between 100KHz and 100MHz. Above this frequency the plane wave measurements are made using tuned dipole or horn antennas.

Radiated measurements in this study were made using low frequency induction fields in the frequency range from 10Hz to 50KHz. The conducted measurements were made in the range of 10Hz to 1GHz with the intention of comparing SE made by both methods. A close correlation of SE values obtained by the two methods would indicate that methods of determining shielding without the usual problems involved in making radiated measurements were possible.

During the progress of measuring SE by the two methods described, it became apparent that very little shielding was effected through the use of dielectric building materials, unfortunately the largest category of building materials. Radiated tests measuring the attenuation of magnetic fields at low frequencies verify the results of conducted measurements at the low frequencies. They show that very little energy is absorbed as the field passes through dielectric barriers. Equations for calculating SE of dielectric materials from the conducted measurements show that shielding is heavily dependent on the frequency of the field. Because of this dependency, shielding caused by power consumption within the material does not become significant until the frequency increases above 100MHz.

A significant error is introduced into calculations of SE when conductive and ferromagnetic materials are used. One such error is apparent shielding, caused by field regeneration. When a time varying magnetic field impinges on a conductive surface, Lenz's Law states that a voltage is induced in the conductor in such a manner as to cause a current to flow, developing a magnetic field to oppose the incident field. The magnitude of this field is limited by the conductivity of the barrier, implying that ultimate shielding could be produced by a superconducting barrier.

Another type of apparent shielding takes place about a ferromagnetic barrier. A building or enclosure made of a material having a high magnetic permeability may drastically change the magnetic field distribution about the enclosure. The analysis of field distortion as an effect on the overall SE is very difficult. This problem of analyzing magnetic field distribution led to the study of making magnetic field pattern studies. In this technique, models of enclosures are made and low frequency magnetic fields are generated to show the field distribution about the enclosure. This test reveals the field direction, but it does not show the absolute magnitude of the field intensity in the pattern. However, the relative intensity of one area of field compared with another may be interpreted by the iron particle distribution in the pattern.

The behavior of magnetic fields about ferromagnetic barriers as well as other characteristics of fields are all influenced by the shape and distribution of materials within an enclosure. Magnetic field distribution patterns about sharp corners of an enclosure differ from those about streamlined shapes. The complete loop of a conductive material around the field lines of an incident field produce much more shielding than would be produced by a loop of a broken conductive path. The presence of several thin layers of a shield provide more shielding than one thick layer.

At high frequencies the wavelength of an electromagnetic signal becomes small. If a wavelength is small enough to equal any physical dimensions of a shielding enclosure or barrier, EM resonance may occur. This phenomenon may cause a very marked change in the shielding characteristics of a material. This phenomenon, as well as others which cause reflections or abnormal transmission characteristics in shielding materials, are called geometric effects.

Part II of this report is compiled as a handbook of shielding which is intended for use by structural designers and engineers so that materials and geometry may be combined efficiently into a structure or enclosure which could provide optimum shielding for the least cost. The shielding handbook takes into account the best materials, construction

methods and configurations for protection against magnetic fields, electric fields, and plane wave transmission.

Radiated Measurements:

Radiated measurements are defined as those dealing with the transmission of electromagnetic energy through a medium. In the language of those who measure the shielding characteristics of materials, radiated measurements are made using equipment to transmit and receive electromagnetic signals. Neither the transmitting element nor the receiver sensor are in contact with the shielding barrier. This type of measurement is in contrast with conducted measurements, involving direct contact with the materials being tested for the purpose of measuring their electrical parameters.

For many years radiated measurements have been made to test electromagnetic compatibility, measure SE, or to measure the frequency and power spectrum emanating from a source. Most measurements were made in the frequency range from 10KHz to 1 GHz. Since the advent of radar and the more general use of microwave frequencies, radiated measurements have included the frequency spectrum up to 10GHz and sometimes to even higher frequencies, but very little work has been done to extend the range of radiated measurements to frequencies below 10KHz. One limitation which has prevented both downward and upward spread of measurements has been the lack of equipment to make accurate measurements in these frequencies.

A requirement of this contract states that radiated SE measurements shall be made on a number of building materials including concretes, steels, woods, nonferrous materials and others. The tests shall measure the attenuation of the magnetic fields from 10Hz to 50KHz.

Previously, measurement of magnetic field attenuation has been done using two shielded loops, one loop acting as the radiator and the other as the sensor. In this manner the driven loop is energized with a signal generator and the receiving loop is fed to a field intensity meter or other low frequency receiver. The lowest measurable frequency using this type of equipment is limited to about 10KHz, the lower limit of the super-heterodyne receivers.

The development of the variable- μ Magnetic Field Intensity Meter (MFIM) by The Electro-Mechanics Company has increased the capability of making radiated measurements at frequencies below 10KHz. The EMCO Model 6640 MFIM was used for the

radiated tests performed on this contract. This instrument is capable of measuring time varying magnetic fields from less than 10 Hz up to 50 KHz. The high sensitivity of the instrument makes it capable of reading broadband signal intensities less than 10 milligammas (equivalent to 10^{-12} Teslas or 10^{-7} gauss) with a dynamic range of about 100 db.

The variable- μ MFIM operates in the following manner. A coil wound through an aperture in a ferrite rod of known incremental permeability acts as one element of a tuned oscillator circuit. A change in the magnetic field intensity about the ferrite rod changes the permeability of the rod, thereby changing the inductance of the coil. The variation in the magnetic field is indicated by a proportional shift in the oscillator frequency. A core and coil transducer in the inductance portion of a tuned circuit determines the oscillator frequency of the MFIM sensor. A servo control loop compensates for changes in component characteristics caused by temperature effects and slow variations in the earth's magnetic field. The compensation is provided by a voltage variable capacitor in the sensor electronics. This capacitor is controlled by an integrator system whose upper frequency response determines the lower frequency response of the entire system. An illustrative block diagram is shown in Fig. 1. A steady magnetic field, H , does not produce a shift in the sensor oscillator frequency because of the servo control. However, a time varying field, ΔH , causes a frequency shift varying at the same rate of change as the applied field. The magnitude of the frequency shift is proportional to the magnitude of ΔH . The modulated sensor frequency, f_s , is then mixed with a constant frequency, f_{LO} , from the local oscillator. The difference frequency, $f_{LO} - f_s = f_{IF}$, is demodulated to produce an analog voltage, V , which is proportional to the magnitude of ΔH and varies at the same time rate. The above response occurs within the passband, 0.1 Hz to 50 KHz, of the instrument.

The general arrangement for all radiated tests requires the use of a variable frequency signal generator, a power amplifier, and a circular coil for the magnetic field source. The MFIM measures the strength of the magnetic field produced by the source. Measuring the attenuation of a barrier consists of determining the field intensity in an area without the barrier in place and then measuring the field intensity with the barrier or enclosure in position.

In order to develop techniques to make meaningful radiated measurements, a number of tests were run. Several attenuation measurements were made to study the effect of varying the spacing between the source and barrier, and the spacing between the barrier and the sensor. Another group of tests were designed to study the effect of

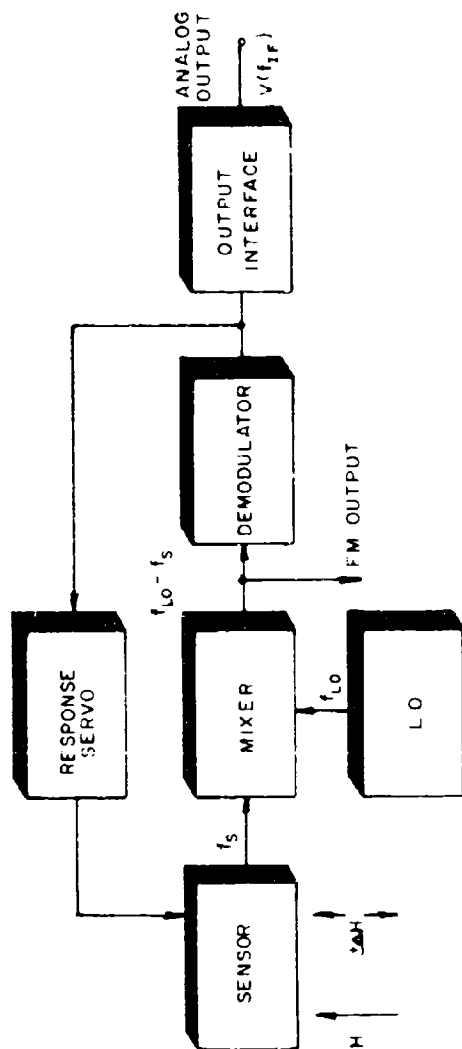


Fig. 1 Block Diagram of MFIM

the size of the barrier on the measured SE. Other tests were run to study the existence of magnetic field reflection from conductive barriers. Tests which involved ferromagnetic material enclosures were made to show variations in field intensities at several different sensor positions within the enclosure. The SE obtained from complete enclosures was compared with that obtained for plane surface barriers.

Some measurements were designed to study the effect of material thickness on its shielding characteristic. Other tests were run to examine the shielding variations caused by multilayered shielding materials in adjacent or separated configurations.

Erroneous SE measurements are likely to be made if there are metal obstacles in the test area. Fig. 2 shows a test setup which was used to investigate the apparent shielding by metal obstacles. The measured SE of the wall with and without the obstacle is shown in Fig. 3. A similar situation showing an apparent SE is illustrated in Figs. 4 and 5. The conclusion of these tests provided substantial evidence that SE measurements must be made carefully to avoid errors which could be caused by objects in the test area.

While making the radiated measurements, it became apparent that only conductive and ferromagnetic materials displayed any significant degree of shielding in the 10 Hz to 50 KHz range. A study was made using several configurations of materials and equipment in order to establish a reliable method of comparing SE of various materials. The test arrangements shown in Figs. 6, 7 and 8 illustrate the configuration of the source coil, barrier and sensor for measuring SE on 1-ft-square sheet samples, larger 4 ft by 8 ft sheets, and cubical enclosures. The results of nearly all tests done on the plane surface or sheet type barriers reveal that considerable error in the SE measurements starts in the upper frequency range of the radiated measurements, usually in the 5 KHz to 50 KHz range.

These errors prevent accurate SE data from being taken in the 10 KHz to 50 KHz frequency range, although comparison between different materials measured in the same manner show the shielding merits of one material relative to another. The test jig in Fig. 6 was useful in determining the effect of spacing between the source coil, barrier, and sensor. The greatest shielding was effected by placing the source coil and the sensor as close as possible and on opposite sides of the barrier material. The apparent shielding caused by the variations in spacing are shown in Figs. 9 and 10. In the tests, the source coil and sensor were separated by 12 inches. The curves show the magnetic field SE variation as the barrier is moved in 2-inch increments from the sensor to the source coil. The distances shown are measured from the center of the sensor. The size of the sensor case limits the axial distance to 2 inches. The barrier was not brought any closer than

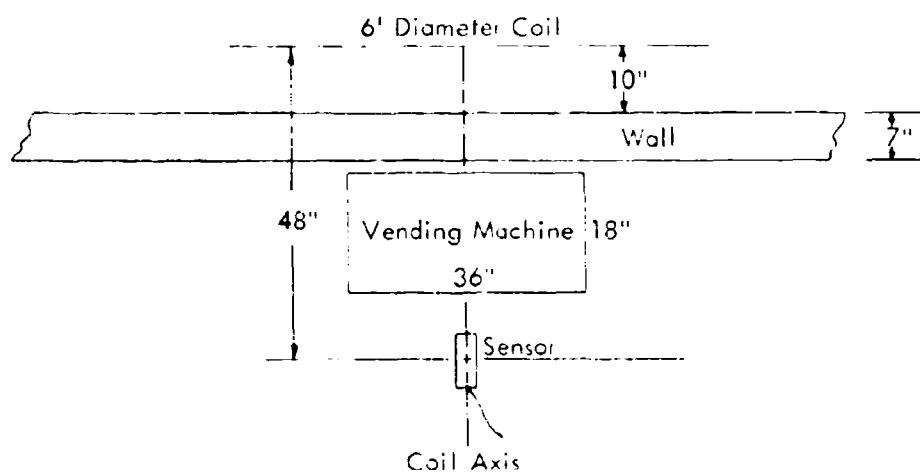


Fig. 2 Test Arrangement for Measuring
Apparent Shielding Effectiveness of Metal Furniture

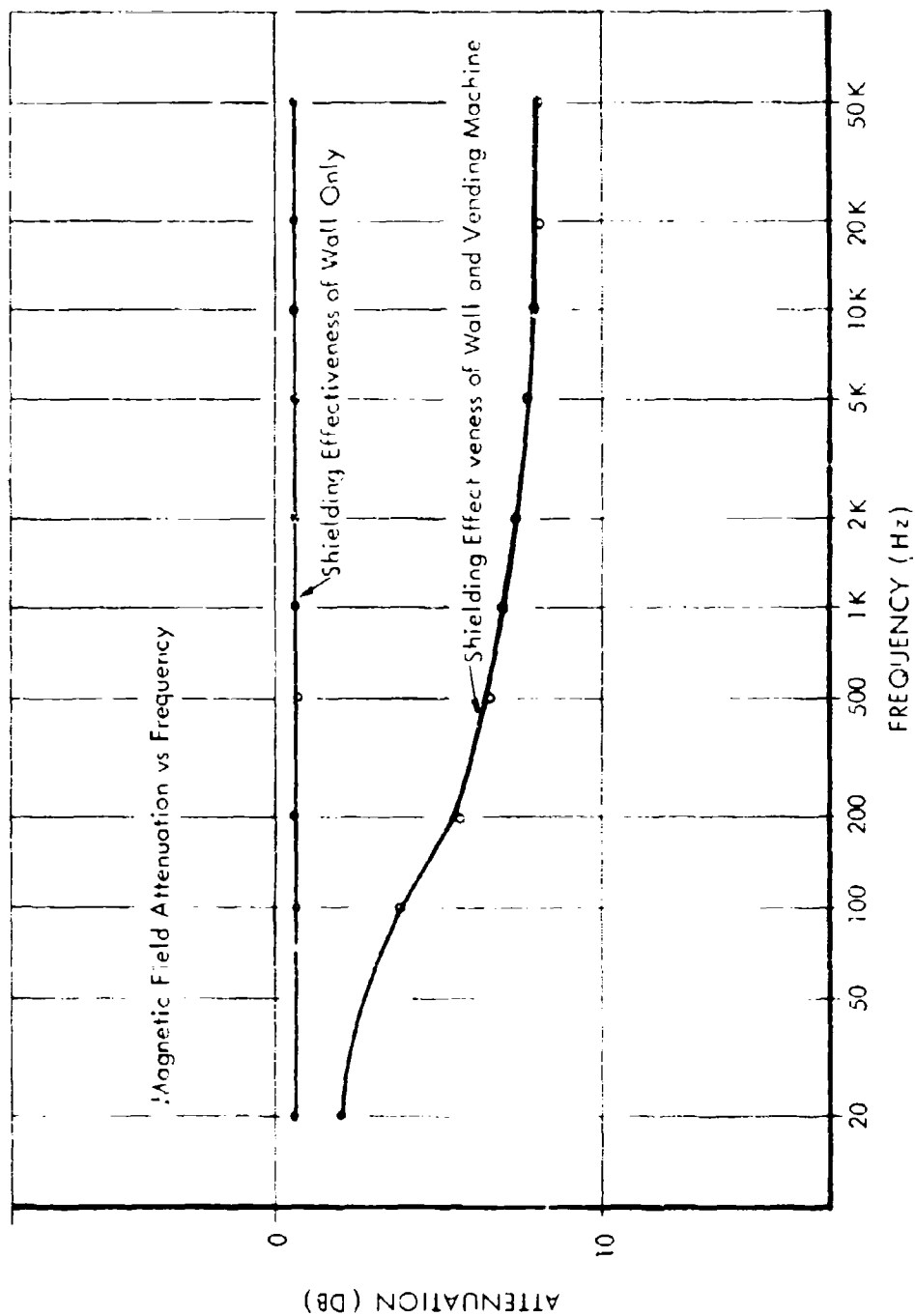


Fig. 3 Apparent Shielding Effectiveness Caused by Metal Vending Machine Placed in Field Path

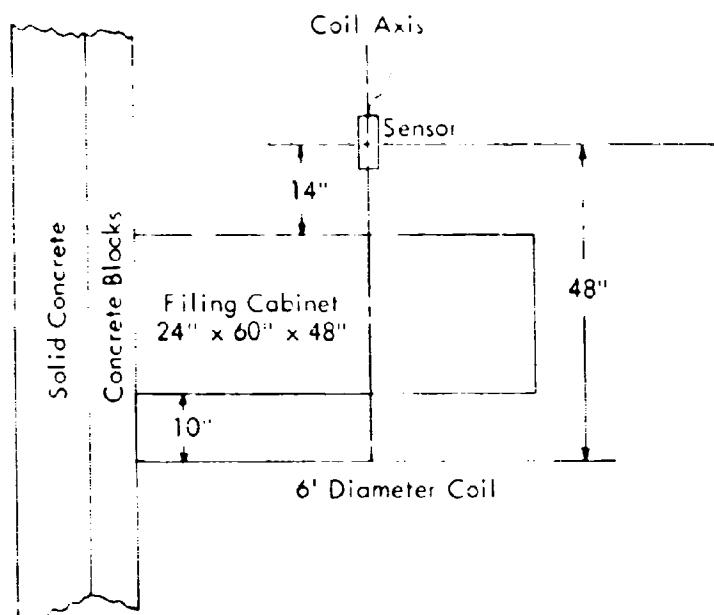


Fig. 4 Test Arrangement for Measuring Field Distortion
Caused by Office Furnishings

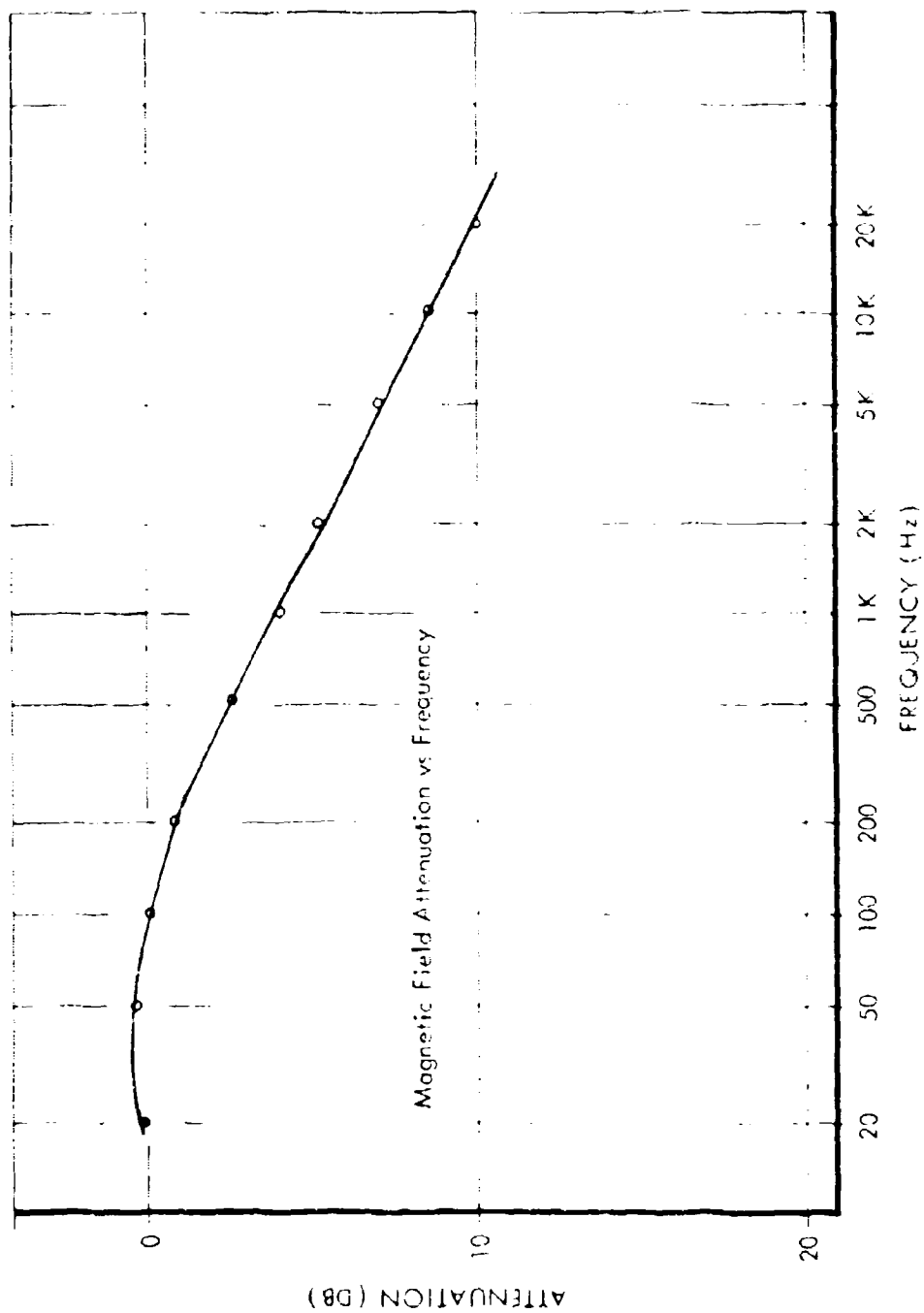


Fig. 5 Apparent Field Attenuation vs Frequency Caused by Metal Filing Cabinet Field Barrier

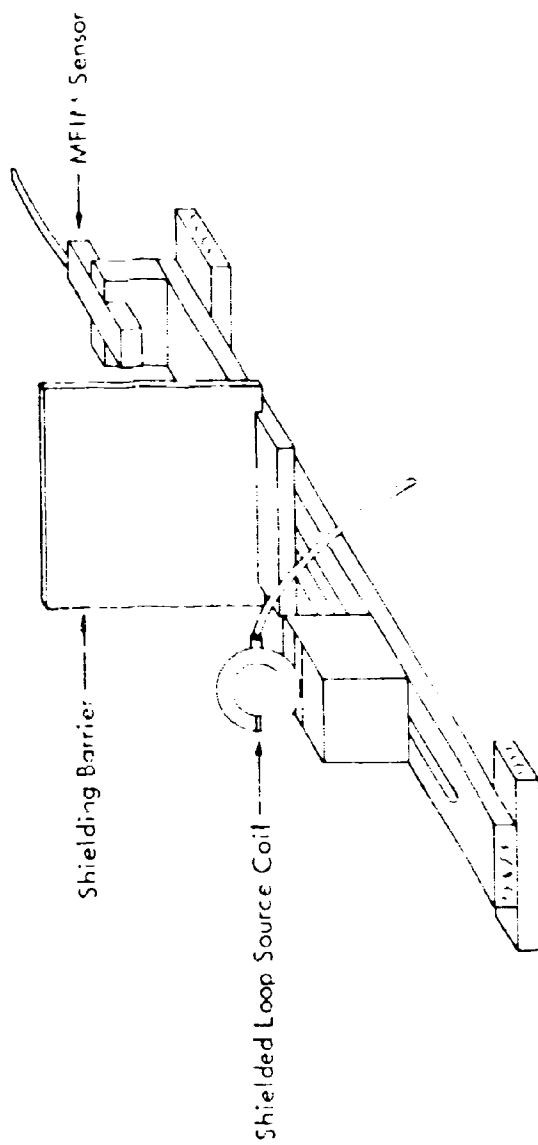


Fig. 6 Test Setup for Measuring Magnetic Field Attenuation Through Small Area Barriers

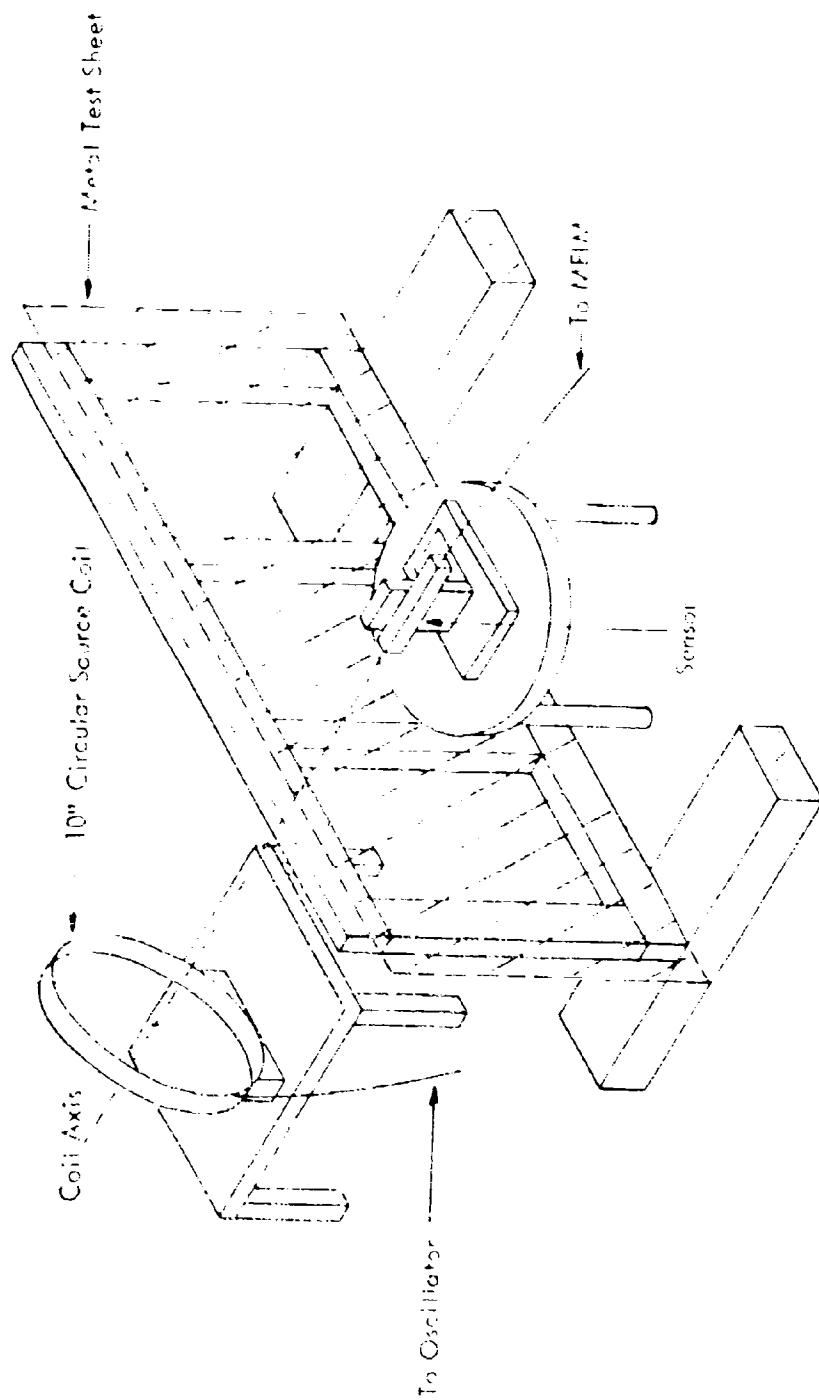


Fig. 7 Test Arrangement for Measuring Shielding Through 4 x 8-Foot Metal Sheet

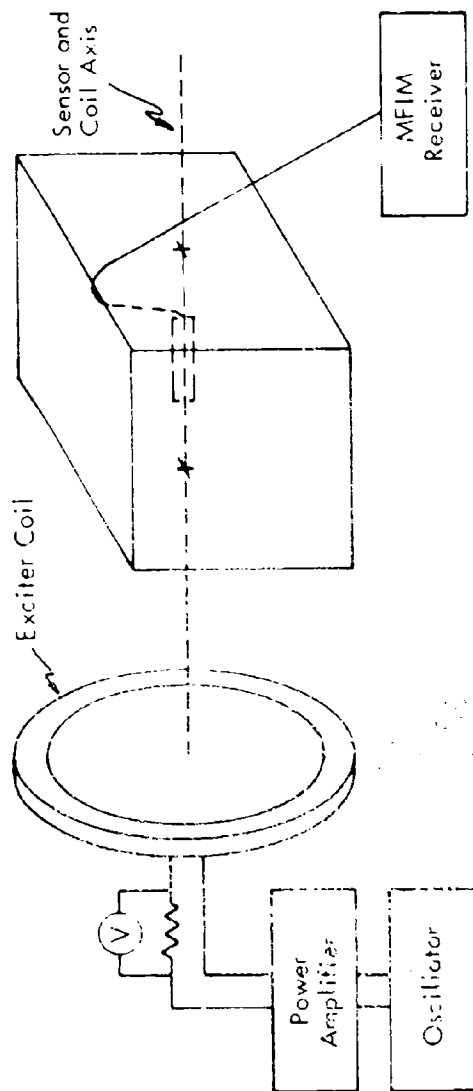


Fig. 8 Equipment Configuration for Measuring Shielding Effectiveness of Small Enclosures

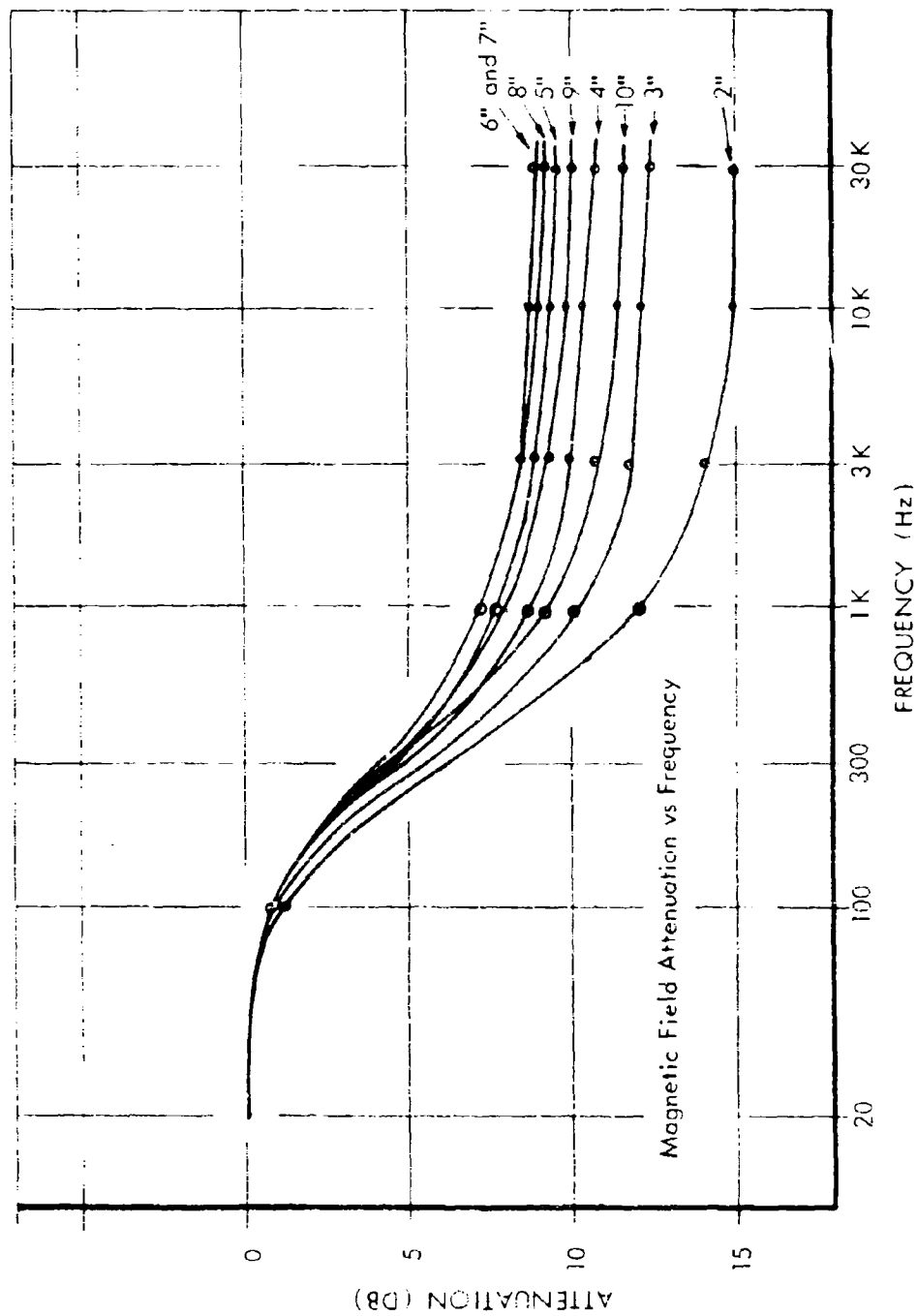


Fig. 9 SE of a Sheet of 0.06-Inch Thick Aluminum at Various Distances from the Sensor

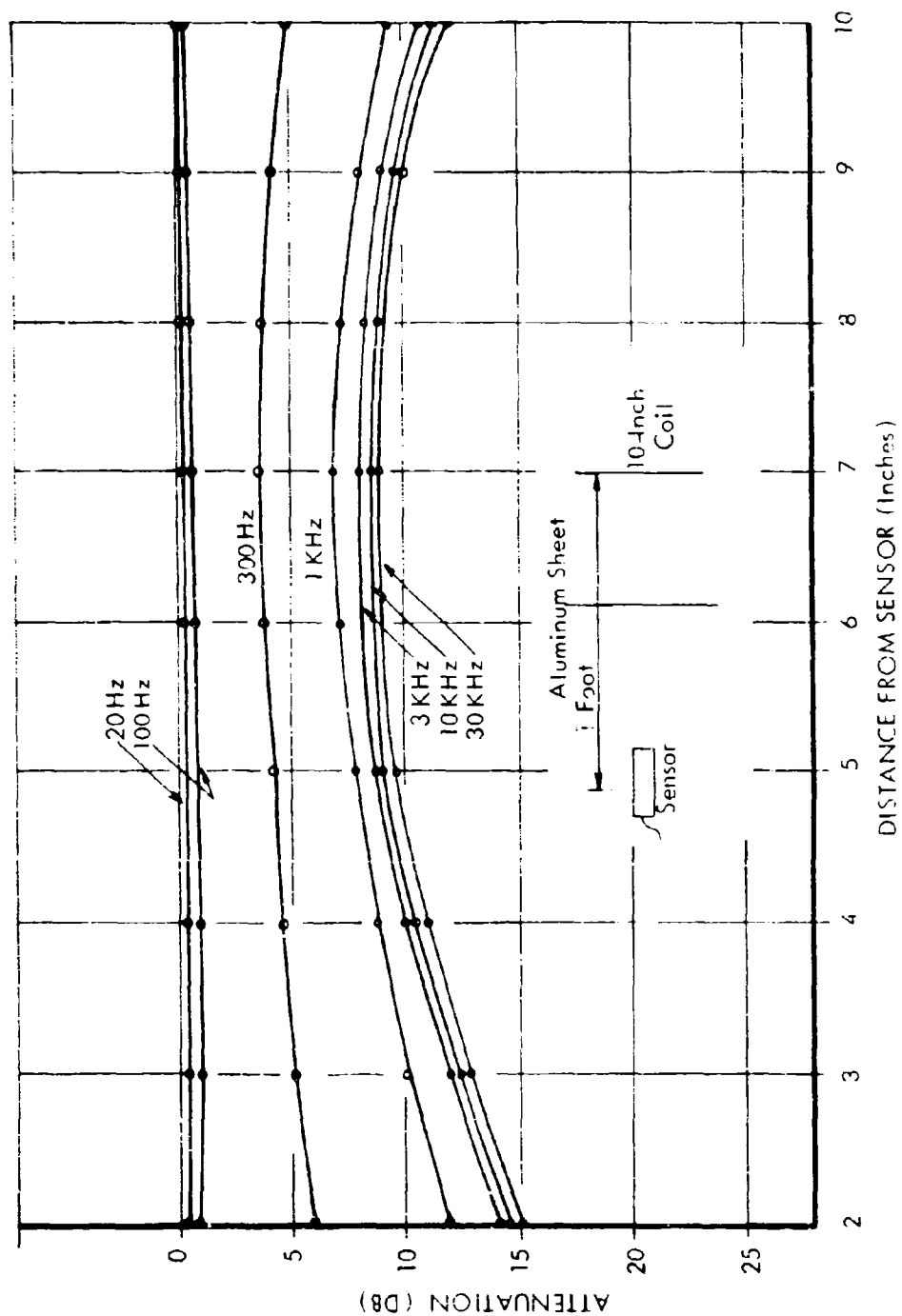


Fig. 10 SE of One 0.06-Inch Thick Aluminum Sheet vs Spacing for Several Frequencies

2 inches from the source coil because induced currents in the barrier caused a gross change in loading characteristics when the barrier was placed closer than 2 inches to the coil. A similar test which used two barriers, one fixed and the other movable, showed about the same results as using a single sheet except that slightly more SE was attainable. Figs. 11 and 12 show the result with the fixed plate 2 inches from the source coil and 2 inches from the sensor, respectively.

The curves in Fig. 13 show the variations of apparent SE caused by separating two aluminum sheet barriers in two inch increments. In these tests, the source coil and sensor were separated by a fixed distance of 12 inches and both plates were moved symmetrically away from the mid point between the source coil and sensor. The results, which are similar to those shown in Figs. 9 through 12, show the increase in SE as the barriers are placed close to the source and sensor.

In measuring the SE of conductive materials, it became apparent that the greatest amount of shielding was caused by the regeneration of magnetic fields by the principle of Lenz's Law. This indicates that the SE of a material is directly proportional to the conductivity of the material, especially for nonferrous materials. Several experiments were set up to investigate the degree of this effect. Three "cage" type enclosures were wound from different wire material on wooden frames. Each loop of wire closes on itself and does not contact the adjacent loop. Shielding tests were run with the plane of the loop perpendicular to the axis of the field and then with the plane of the loops parallel to the field. These arrangements are shown in Fig. 14. The cages were made of copper, iron, and Chromel "A" wire. These materials were chosen because they have different electrical resistances. Iron has six times the resistance of copper, and Chromel "A" has about 60 times the resistance of copper. Curves of the attenuation versus frequency are shown in Figs. 15, 16 and 17.

A similar group of tests has been run on solid sheet enclosures having an open side toward the source coil (see Part II, Fig. 45, pg. 123). The results indicate that the cage of copper wire shields better than the open-front sheet enclosure. This discrepancy is due partly to the higher broadband noise present during the measurement of the solid sheet enclosure. The broadband noise level was about 10 db higher, causing an overall upward shift in the flattened portion of the curves of Fig. 45. Since shielding is a function of frequency, the shielding curves should have a continued downward slope with increased frequency. Limitations of the test configuration in some of the measurements cause an apparent flattening in the shielding effectiveness above a certain frequency.

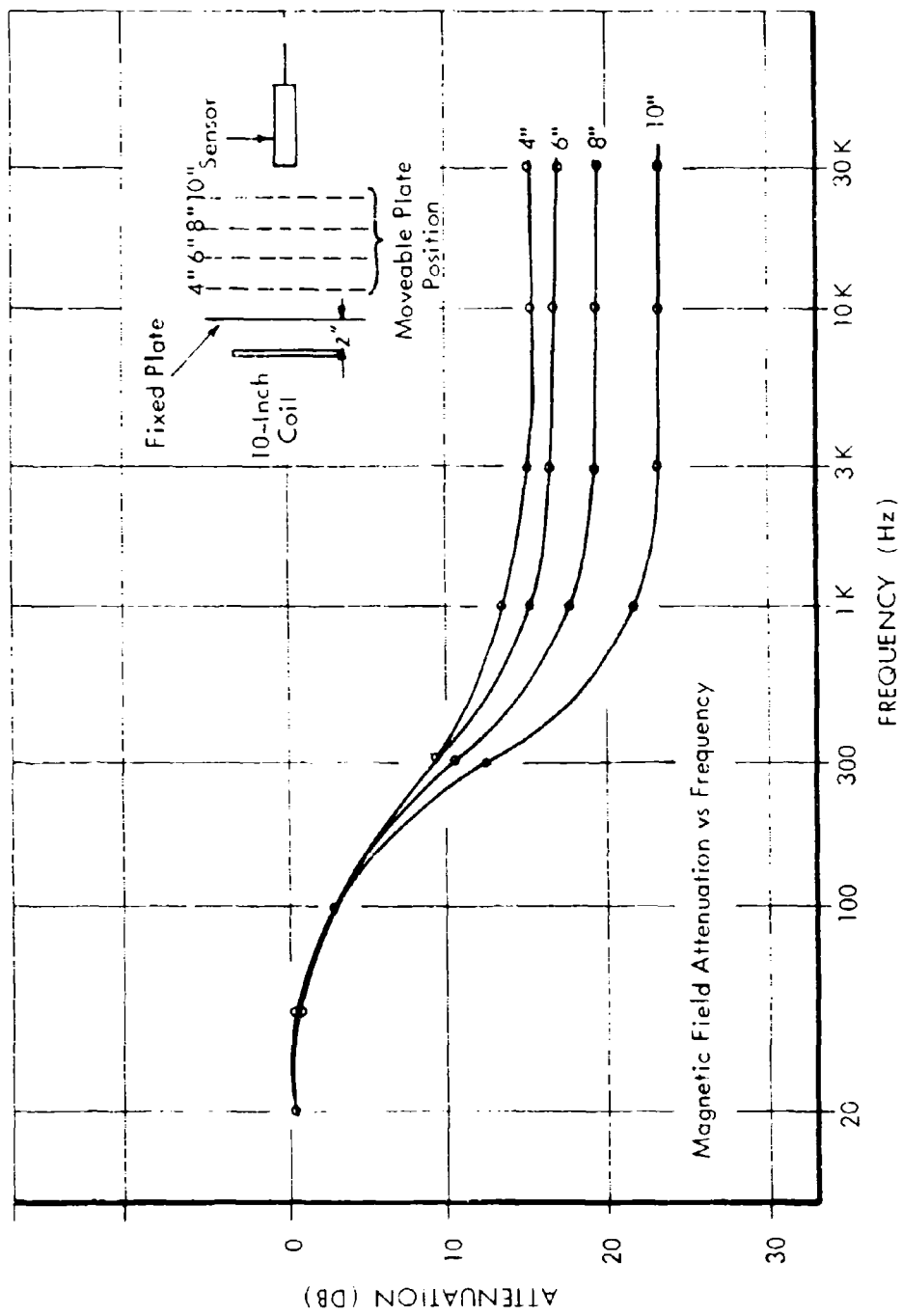


Fig. 11 SE Curve Variations as a Function of Barrier Placement

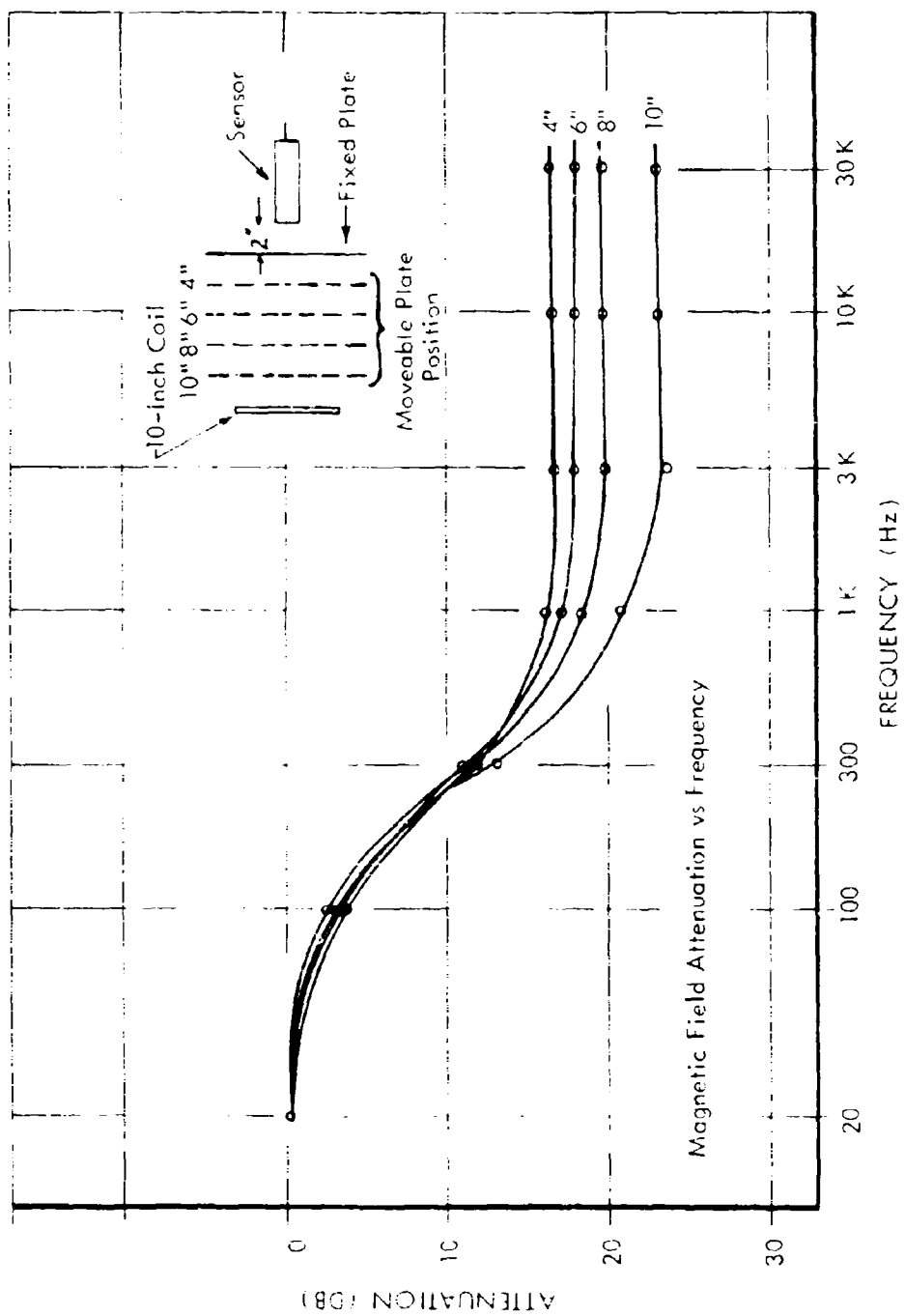


Fig. 12 SE Curve Variations as a Function of Barrier Placement

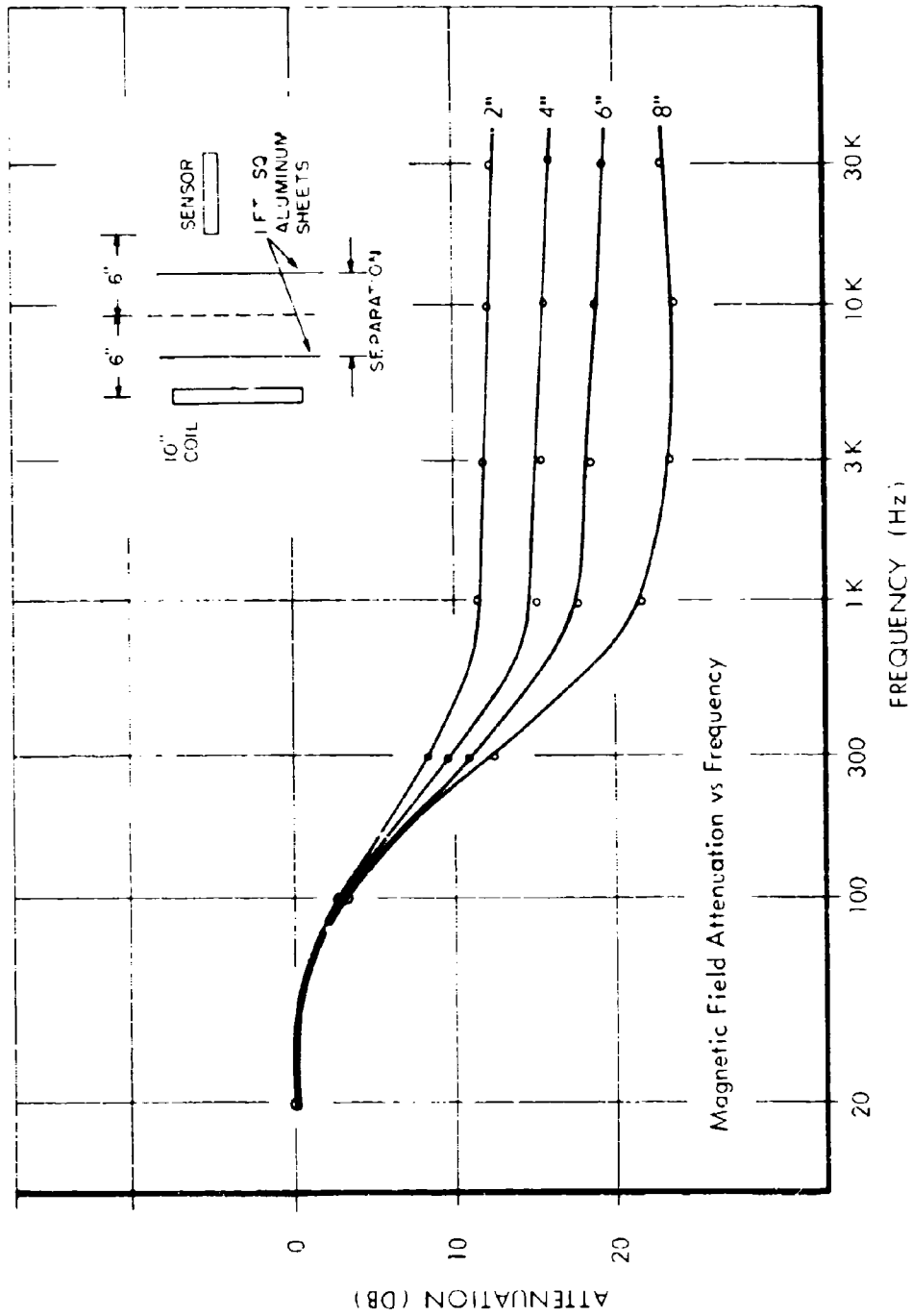


Fig. 13 SE of Two Aluminum Sheets .026 Inches Thick Separated Various Distances Between Source and Sensor

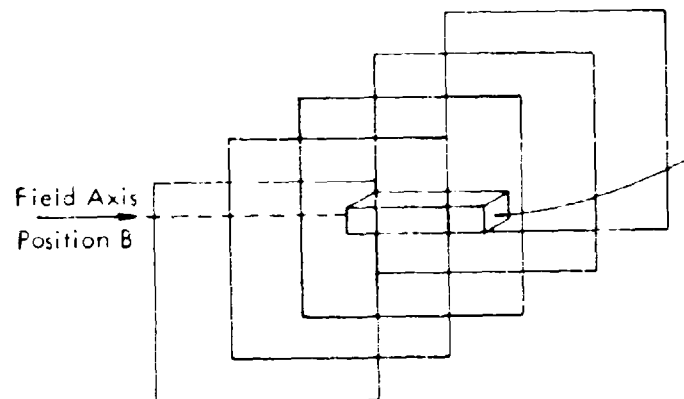
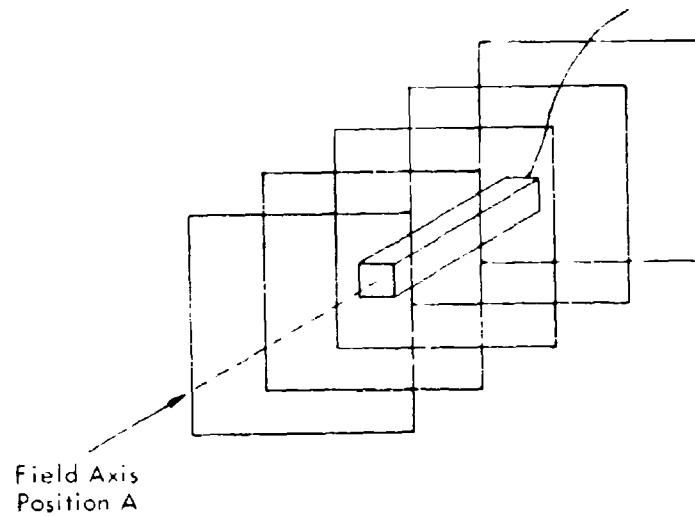


Fig. 14 Closed Loop "Cage" Enclosures:
25 1-Foot-Square Loops per Cage, Each Loop on 1/2-Inch Centers

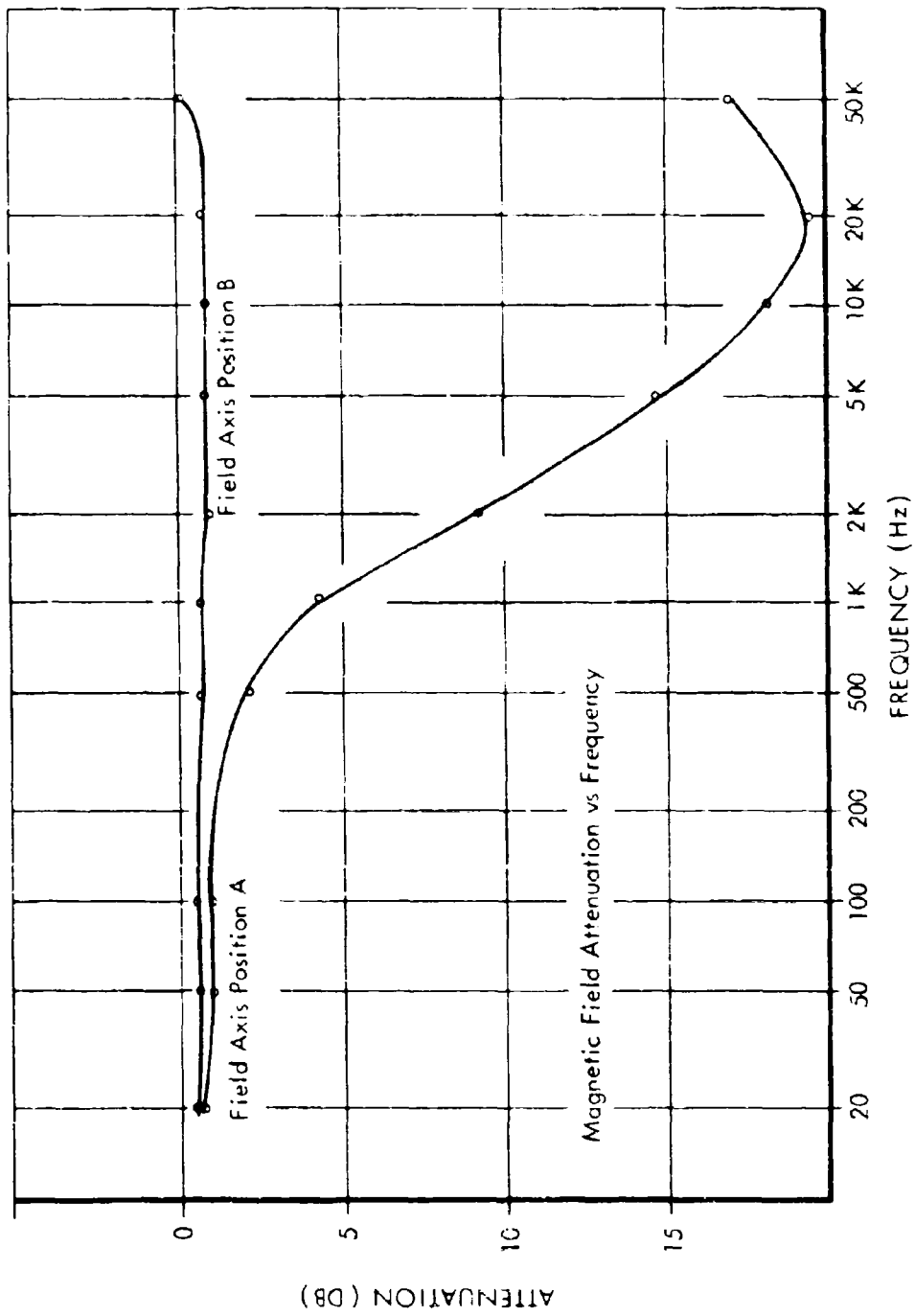


Fig. 15 Shielding Effectiveness of Cage Made of 0.030-Inch Copper Wire
(See Fig. 14)

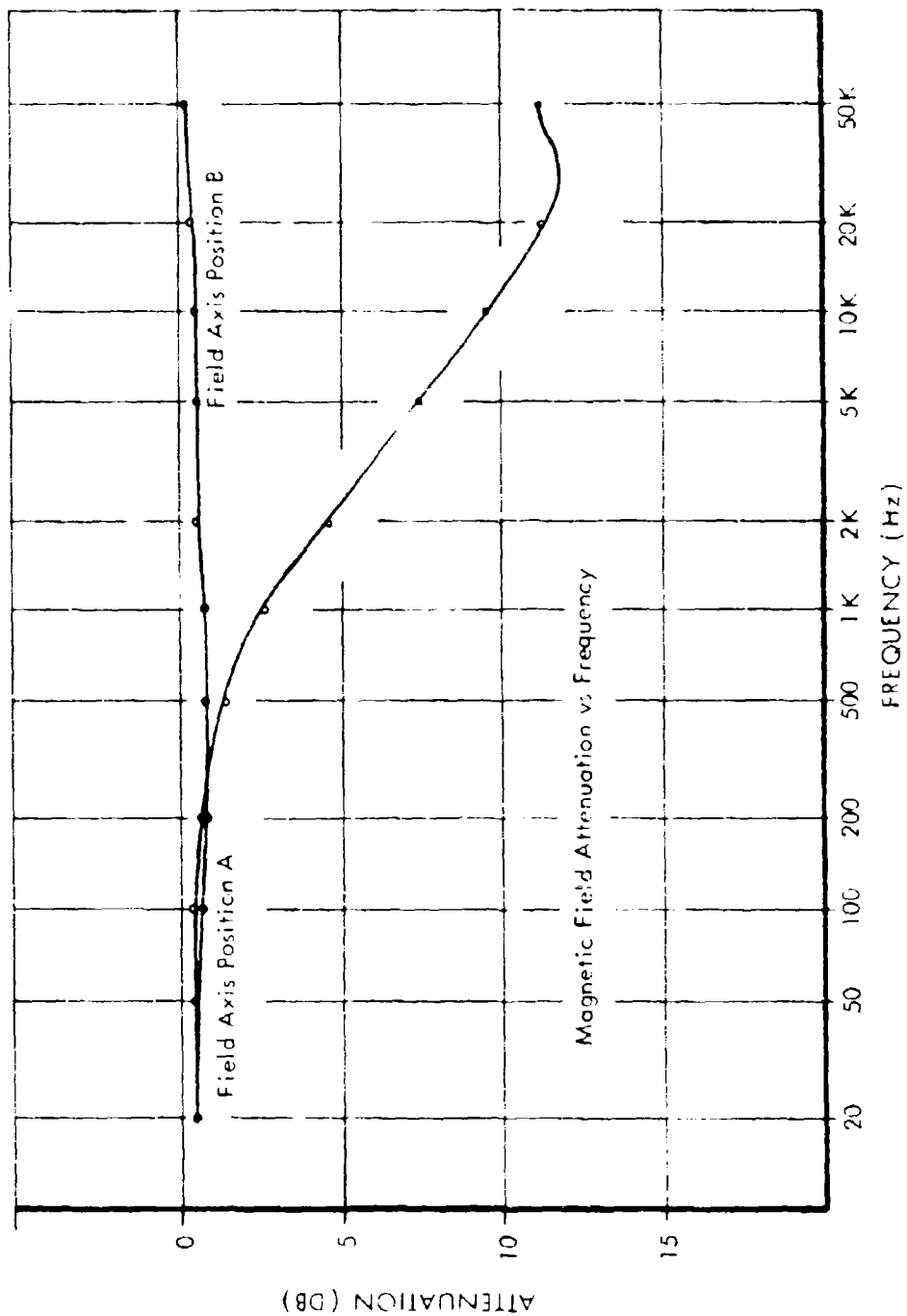


Fig. 16 Shielding Effectiveness of Cage Made of 0.063-Inch Iron Wire

(See Fig. 14)

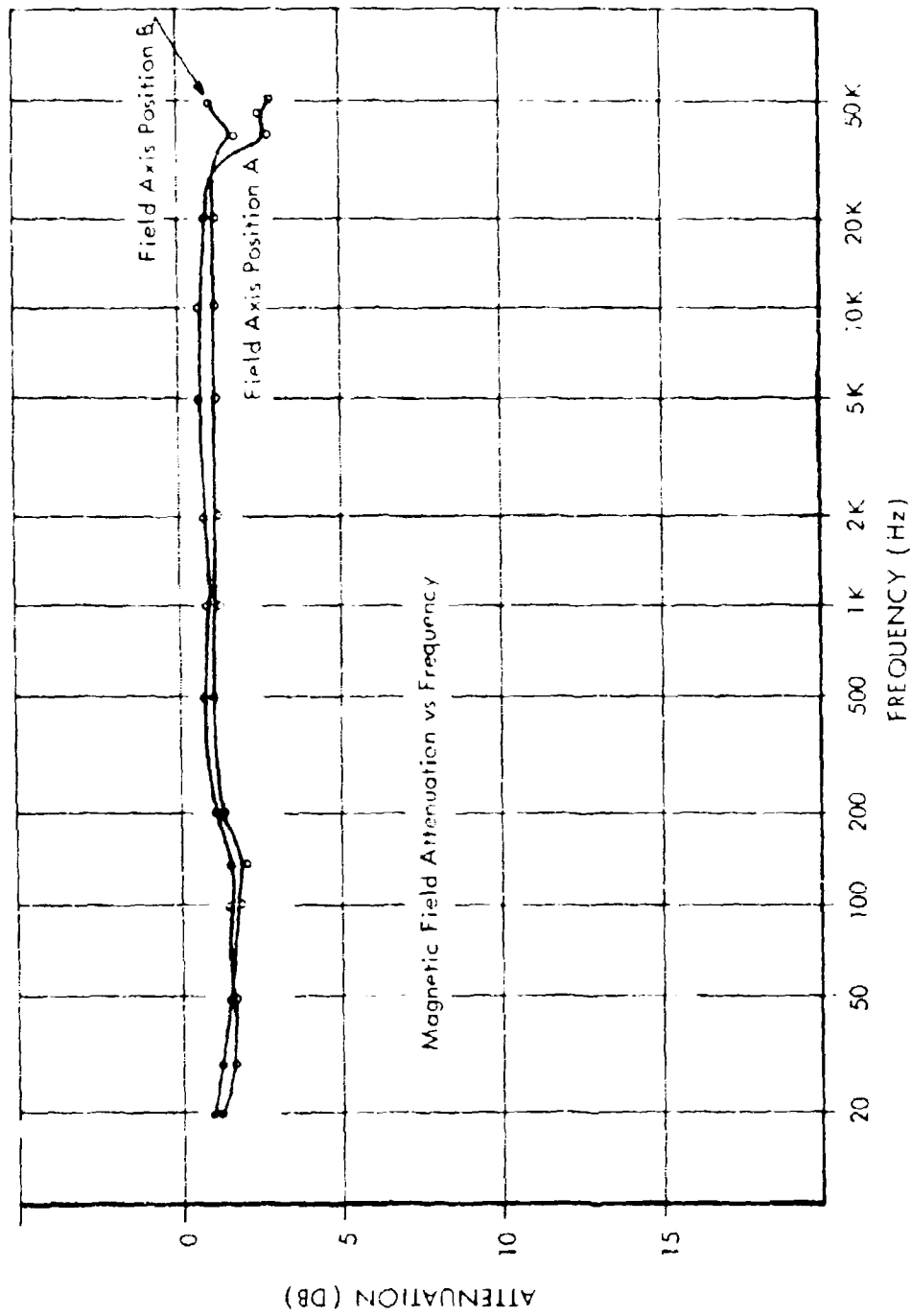


Fig. 17 Shielding Effectiveness of Cage Made of 0.033-Inch Chromel "A" Wire

(See Fig. 14)

This data should not be compared. A group of tests were run on cubical enclosures resembling the wire cages, but which were made of sheets of material rather than wire strips. The apparent shielding produced by these enclosures is shown in Figs. 18 and 19.

The shielding that occurs in conductive nonferrous enclosures seems to be homogeneous throughout the area. This is not true of the shielded area within a ferromagnetic enclosure. The magnetic field distribution within a ferromagnetic enclosure can have wide variations of field intensity from one part of the enclosure to the next. A measurement of the field intensities at various locations in a 4 ft cubical enclosure of wrought iron show that the fields near the walls are oriented perpendicular to the walls and that the fields within the enclosure are strongest just behind the front wall of the enclosure and just in front of the rear wall. Fig. 20 shows the variation of the fields in several locations of the enclosure. It is noteworthy to compare these measurements with the magnetic field shadowgraphs of a similarly shaped enclosure (see Fig. 21). Two characteristics of the MFIM measurements must be remembered in making the comparison. First, the MFIM is sensitive only to fields along its axis and will not respond to fields at right angles to the sensor axis. Second, the MFIM detects the normal weakening of the field as the distance from the sensor to the source coil increases. This change in intensity is not as apparent in the magnetic field shadowgraphs. Some change in behavior occurs at higher frequencies because the attenuation pattern at 1000 Hz is slightly different from that at 100 Hz. In the 100 Hz test, the No. 6 position shows the least attenuation. This is followed by Position 1 which has a slight reduction caused by the bending of the field lines near the side of the enclosure. The maximum attenuation takes place when the sensor is placed in the No. 4 position. This is accountable to the high field distortion and increased separation from the source coil at this point. The distortion is visible in Fig. 21 although it is difficult to discern the field intensity in the shadowgraph.

The graphed results of attenuation versus frequency for various building materials having significant shielding qualities are compiled in Part II of this report.

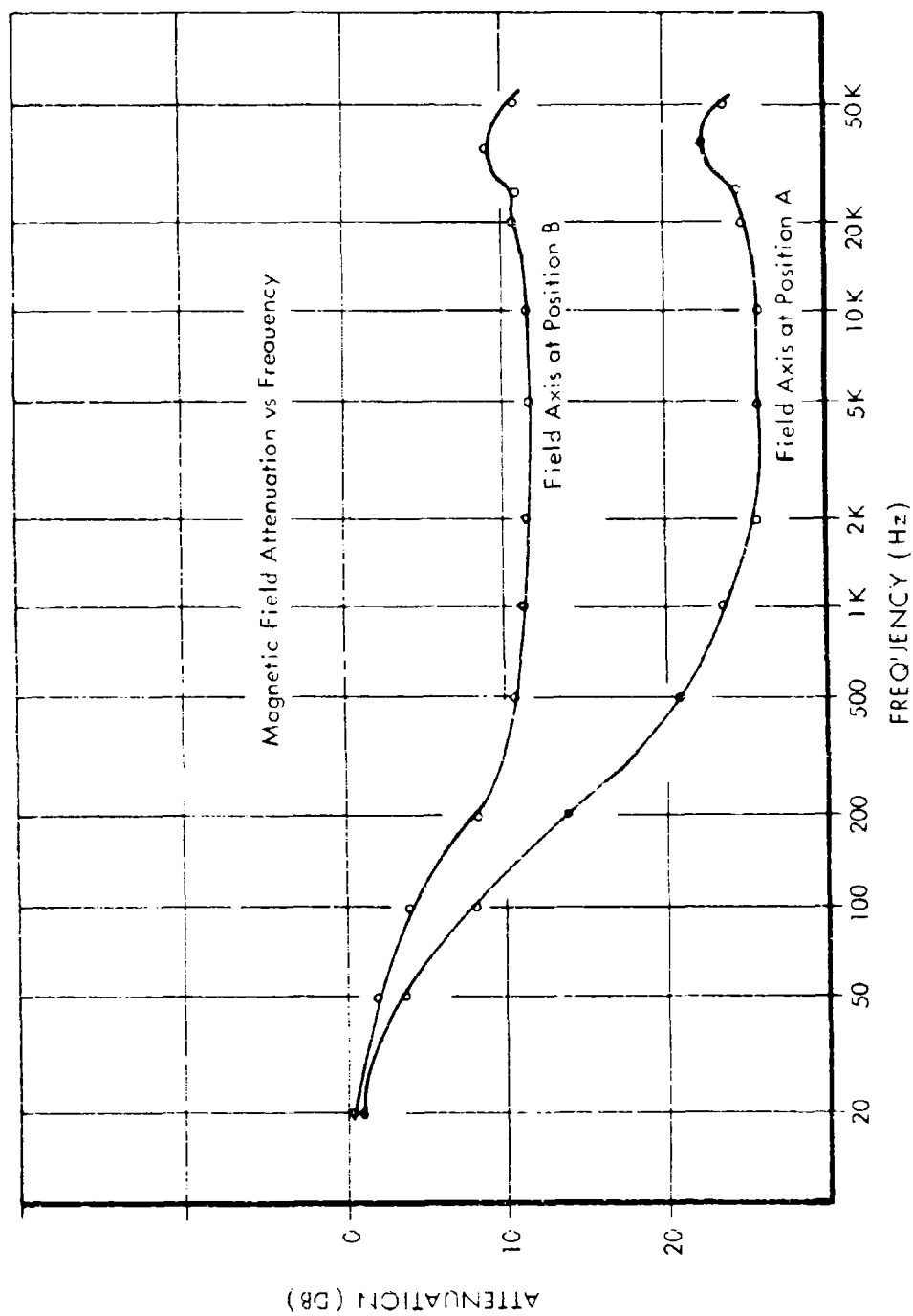


Fig. 18 SE of a 1-foot Cubed, Open-Ended Enclosure of 0.031-Inch Copper, All Seams Soldered

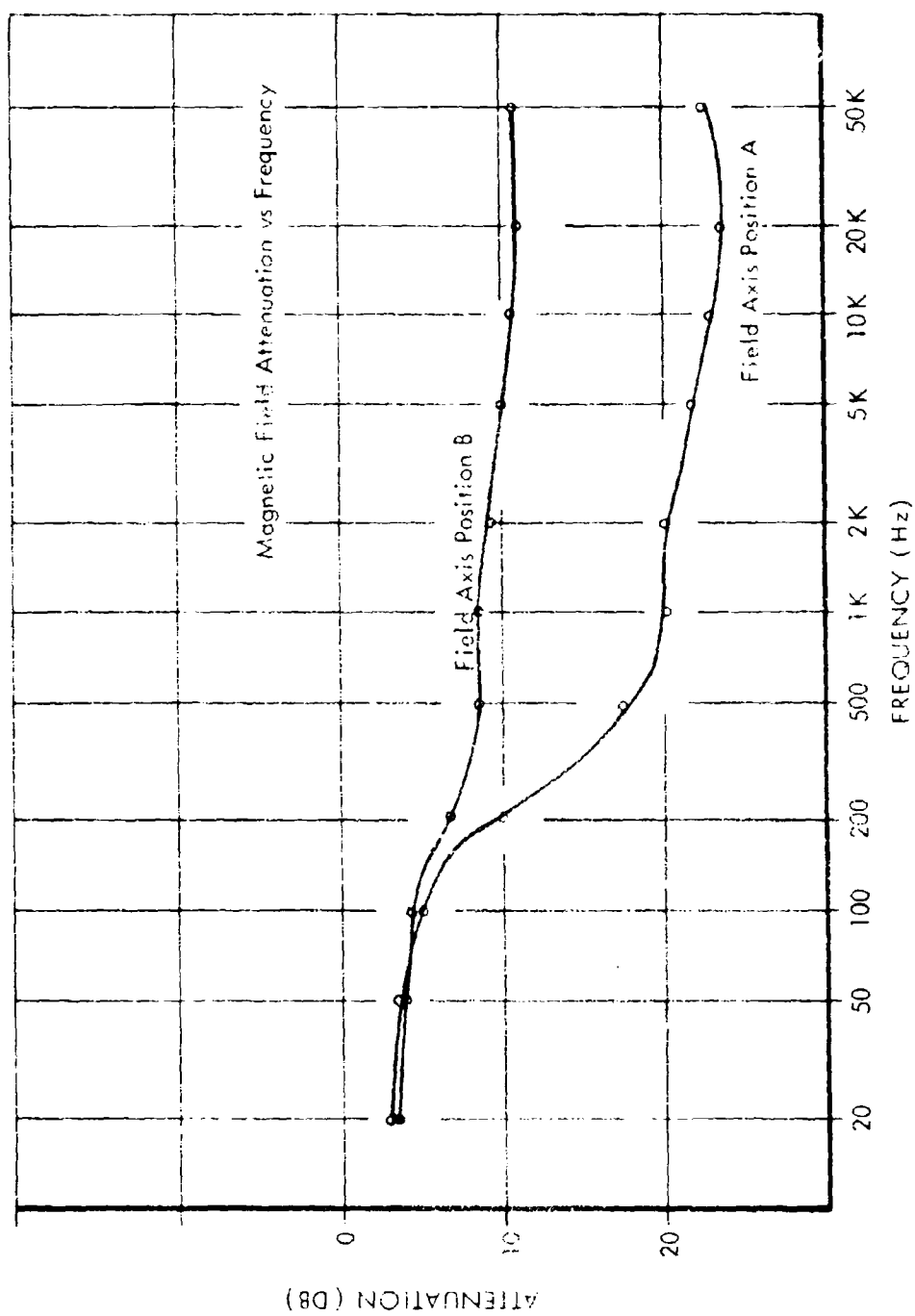


Fig. 19 SE of 1-Foot Cubed, Open-Ended Enclosure of 0.055-Inch Galvanized Steel;
All Seams Soldered

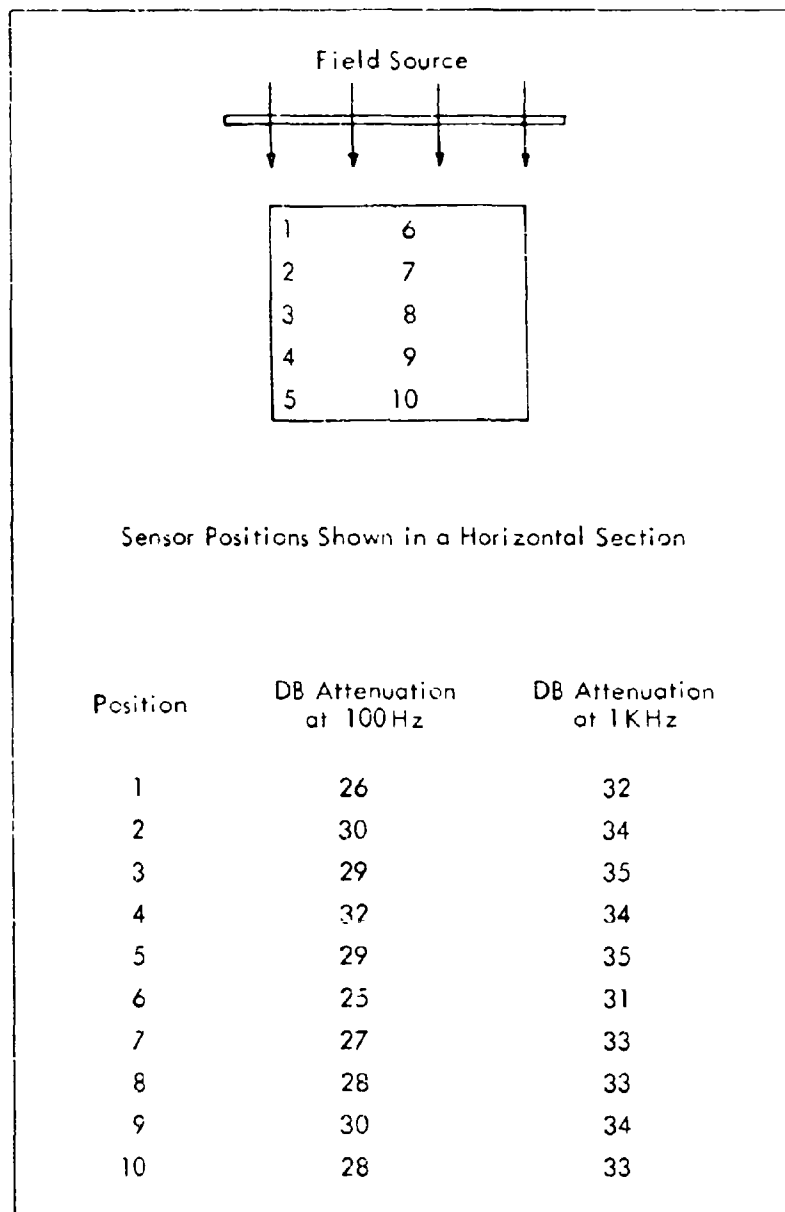


Fig. 20 Shielding Effectiveness at Various Positions within a
4-Foot Cubical, 3/8-Inch Annealed Wrought Iron Box

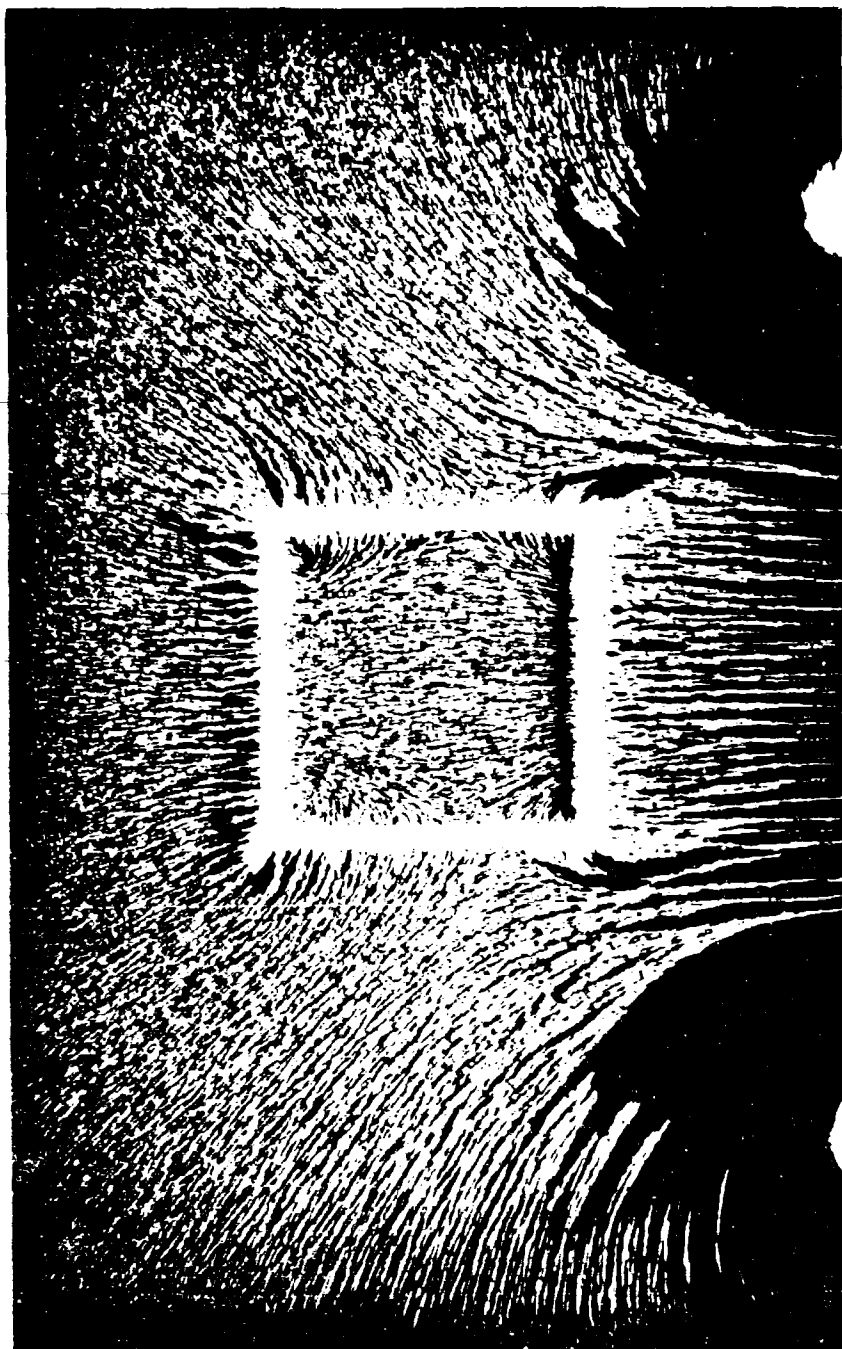


Fig. 21 Magnetic Field Shadowgraph Showing Field Distribution about a Square Cross-Section Barrier

Conducted Measurements:

Conducted measurements refer to those electrical measurements with the test apparatus in contact with the material being tested. These tests are designed to measure the electrical characteristics of a material. The values of the electrical parameters give insight into the electromagnetic shielding capabilities of the material.

The results of conducted measurements give such parameters as the dielectric constant, dielectric loss factor, magnetic permeability, magnetic loss factor and conductivity of materials.

Most building materials are in the class of nonconductors or dielectric materials. They have no appreciable magnetic qualities; therefore, the only characteristic influencing their value as a shield are the dielectric constant and the dielectric loss factor. In the case of a dielectric's electrical parameters, the higher values of dielectric constant (or relative permittivity) cause a smaller amount of energy absorption and therefore less shielding. Conversely, the materials having higher values of dielectric loss factor (or loss tangent) show the greatest amount of shielding because this loss factor is indicative of the power consumed in the medium. It will be seen, however, that neither of these values is of a sufficient magnitude in most dielectric materials to produce any significant shielding at frequencies below 100 MHz. Shielding will increase by a factor of one million for a given material as the frequency increases from 1 KHz to 1 GHz provided that the dielectric constant and dielectric loss factor do not change significantly over these frequencies, because SE is directly proportional to a change in the EM frequency.

A requirement of this contract is that conducted measurements be made for a number of common building materials over the frequency range of 10 Hz to 1 GHz. An attempt to correlate values of SE calculated from these conducted measurements with those obtained in the low frequency radiated measurements will also be shown.

The materials selected for the conducted measurement program were those which could be made homogeneous on a relatively small scale and which could be molded or machined to fit in a holder for bridge measurements. A number of concrete, plaster, brick, wooden and other materials which were adaptable to being made into samples were chosen. The procedures for making conducted measurements can not be carried out on reinforced concrete, aluminum windows, steel windows, and large scale structural masses, except that the characteristics of the materials may be measured and these are involved in calculating the SE of large-scale structural parts.

The largest group of measurements were made on dielectric building materials and were made with capacitance bridges or, as in the case of the VHF range, measurements were accomplished using slotted line techniques.

The frequency ranges covered and equipment used in making the conducted tests on the building material samples are given in Table I.

A General Radio Model 1690A dielectric sample holder was used to facilitate the measurement of the building material samples. Samples prepared were 2 inches in diameter and no more than 0.30 inches thick. Thin materials could be tested alone or stacked in laminated form to approximate a 1/4-inch thick sample.

The test setup for making bridge measurements is shown in Fig. 22. The procedure for determining dielectric constants and dissipation factors are as follows. With the test sample in the sample holder, the conductance (G_1) and capacitance (C_1) adjustments of the bridge are tuned for a null, and dial settings are recorded. The sample thickness (t_1) is also recorded. Next, the test sample is removed from the sample holder, and the bridge is again nulled by readjustment of the conductance knob to C_2 and the micrometer thickness adjustment to t_2 . These values are recorded. A reference chart for 2-inch diameter test samples, furnished with the sample holder, gives values of the geometric air capacitance of electrodes (C_{A1}) from t_1 and the geometric air capacitance of electrodes (C_{A2}) from t_2 . The capacitance of the test sample is calculated from the formula

$$C_s = C_{A2} + \Delta C_{A2} - \Delta C_{A1}, \quad (1)$$

where

C_s = equivalent series capacitance of the sample,

ΔC_{A1} = correction factor for setting t_1 (from chart), and

ΔC_{A2} = correction factor for setting t_2 (from chart).

Next, the dielectric constant, ϵ'_r , is calculated from

$$\epsilon'_r = \frac{C_s}{C_{A1}}. \quad (2)$$

TABLE I

Conducted Tests Equipment List

Frequency Range	Bridge	Detector	Signal Generator
10 Hz - 300K Hz	General Radio 716C and 1615A Capacitance Bridges	General Radio 1232A Tuned Amplifier and Null Detector or Empire Devices NF 105	Hewlett-Packard Model 650A
300K Hz - 50 MHz	General Radio Twin-T 821A RF Bridge	Empire Devices NF 105	Hewlett-Packard Model 608A
100 MHz - 1 GHz	General Radio 874 LBA Slotted Line	Empire Devices NF 105 or Hewlett-Packard Model 415B Standing Wave Indicator	Hewlett-Packard Model 612A

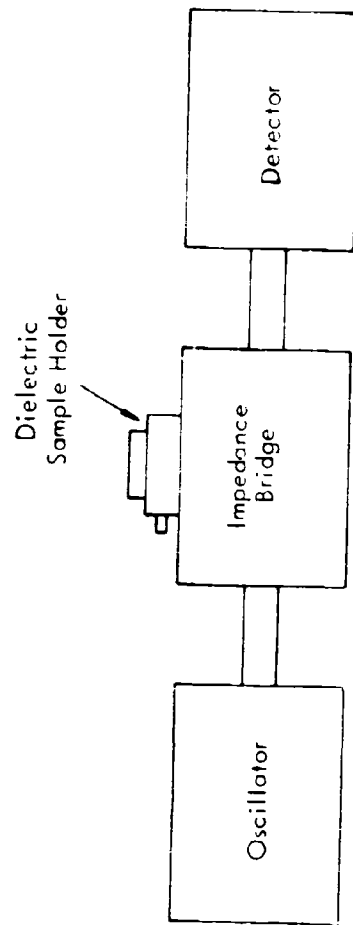


Fig. 22 Test Setup for Conducted Measurements

The dissipation factor, ϵ'' , is calculated by the equation

$$\epsilon'' = (D_1 - D_2) \frac{C_1}{C_2} \quad (3)$$

where

D_1 = conductance with test sample in holder,

D_2 = conductance with test sample removed from holder, and

C_1 = total capacity in circuit (this value does not change for the sample in or out of the holder because capacitor plate separation has compensated the change in dielectric constant).

Once the dielectric constant and dissipation factor are determined, the amount of shielding due to energy absorption in a medium may be calculated from the equation below.

$$\text{Attenuation} = 20 \log_{10} \exp \beta x$$

$$\text{where } \beta = \frac{\omega \epsilon'' \epsilon_0}{2} \sqrt{\frac{\mu_0}{\epsilon' \epsilon_0}} \quad , \text{ and} \quad (4)$$

x = thickness of material, meters.

In rationalized mks units, attenuation on a per meter thickness basis may be calculated using the values of

$$\epsilon_0 = 8.854 \times 10^{-12} \text{ farads/meter}$$

$$\mu_0 = 4\pi \times 10^{-7} \text{ henries/meter.}$$

Extracting the constants for the equation above, it may be simplified to

$$\beta = 1.048 \times 10^{-8} \frac{f \epsilon''}{\sqrt{\epsilon'}} \quad (5)$$

Then

$$\text{Attenuation} = 8.686 \mu \sigma, \text{ decibels,}$$

or

$$\text{Attenuation} = 9.102 \times 10^{-8} \frac{f \epsilon''}{\sqrt{\epsilon'}} , \text{ decibels.} \quad (6)$$

Removing the variables from the shielding equation shows that SE is a direct function of the frequency of the electromagnetic signal and dielectric loss factor. The SE is an inverse function of the square root of the dielectric constant. Furthermore, the frequency of the electromagnetic wave passing through a dielectric medium must be at least above 10 or 100 MHz before the SE increases above 1 db per meter thickness with the magnitude of dielectric constants and loss tangents that are normally encountered. The extremely small attenuation obtainable at frequencies below 50 KHz was verified in the radiated measurements when no measurable shielding could be recorded.

Generally speaking, materials such as concrete, stone, tile, glass, rock, brick, lumber, papers, plastics, asbestos and fiberglass will not offer significant shielding (less than 1 db attenuation) at frequencies below 1 MHz. This is assuming the thickness of the materials used is typical for standard building practices, such as brick and wooden walls much less than one meter thick.

The electrical parameters of materials are likely to vary by several orders of magnitude when exposed to large changes of moisture and the moisture content of many materials may be a function of the ambient temperature. An increase in moisture content was shown to increase the dielectric constant of most materials. Such an increase by itself would tend to make the material shield less than normal, but the increase in moisture content also causes an increase in the dielectric loss factor. This change increases the SE enough to more than offset any SE decrease caused by an elevated value of the dielectric constant because SE is directly proportional to the dielectric loss factor but inversely proportional to the square root of the dielectric constant. Materials which are most significantly affected by the high moisture environments are the concrete and masonry materials, lumber and other porous materials. Very dense materials which are impervious to water are least likely to show changes in electrical parameters in moist environments.

The conductive and magnetic materials are more difficult to evaluate for SE because of the importance played on the geometry. Magnetic field shielding which is due to the regeneration of fields in a conductive barrier is proportional to the conductivity of

the barrier. Thus, the factors involved are the conductance of the material and the material density. In the case of electromagnetic waves, the change in intrinsic impedance of one medium to the next will cause the reflection of an EM wave at the interface of the two mediums. The numerical evaluation of a solution to Maxwell's equations for transverse EM waves propagating through space and striking a shield will give a simplified equation for attenuation,

$$A = 3.338 \sqrt{f}, \text{ decibels mil thickness,} \quad (7)$$

which is based on copper.

According to J.R. Sodaro ("Shielding Nomograph," Electronics, Vol. 27, No. 2, May 1954, p. 190), other materials require a correction factor.

$$L = A \sqrt{\frac{1.72 \mu}{R}} \quad (8)$$

where R is the resistivity of the metal in micro-ohm-centimeters and μ is the relative permeability of the metal. For metals other than those classed as ferromagnetic metals, $\mu = 1$. This equation, however, is valid only for electromagnetic waves and would not hold true for magnetic field or near field phenomena.

Since the absolute shielding offered by a metal barrier is so dependent on configuration and distribution of material in the barrier, it is more useful to compare the relative merits of different materials in the same distribution. For example, the SE offered by a cubical enclosure of 18-mesh copper screen should be compared with enclosures of the same size, shape and mesh of aluminum screen and galvanized iron screen. Sodaro's equation indicates that an increase in relative permeability will increase shielding. This is true when considering EM plane waves, but it is not the case when considering magnetic field shielding since the presence of a high μ material can increase the field at a point if the point is at an induced magnetic pole. A high μ material surrounding a region can lessen the field intensity at that region. The merits of building materials used as shields are shown in the tables of conducted measurements in Part II of this report.

Magnetic Field Pattern Shadowgraphs:

It is difficult to predict the magnetic field distribution about an enclosure or barrier of a ferromagnetic substance. This problem arises from the fact that the magnetic field direction and distribution may not follow the behavior of a steady state field. Magnetic field propagation through a ferromagnetic substance could be slow enough to show a standing wave pattern if the barrier is large and the frequency of the magnetic field is high.

The classical method of making magnetic field patterns has been to place a permanent magnet beneath a thin, flat, nonmagnetic material and then to sprinkle iron filings on the flat cover. Other experiments have involved the use of magnetic materials suspended in a liquid in order to get a three dimensional pattern.

In an attempt to make a magnetic field pattern from low frequency alternating current fields, an apparatus was built to simulate the magnetic fields about a flat circular coil. A heavy wire (AWG No. 6) was wound as the secondary of a toroidal transformer. Three turns of this heavy wire formed the 6-inch diameter secondary coil (see Fig.23). By exciting the primary of the transformer with 60Hz line current supply, a magnetic field produced by about 2,000 ampere turns will be generated about the coil. Finely divided particles of iron are shaken on to a platform which forms a horizontal plane in the center of the coil. With the power on, these particles align along the field vector and present a picture of the field distribution in this plane. After the pattern is formed, the current is shut off and the particles are not disturbed. A photosensitive paper, previously placed on the platform and now under the particles, is exposed with a point source light. Development of the paper reveals the pattern of the field as a shadowgraph.

The shadowgraph presents a display of the direction of the magnetic fields and, with the presence of a model enclosure of a ferromagnetic material, the field distortion caused by the model can be seen. The absolute magnitude of the field intensity is not available from the shadowgraph although the relative strength of the field distribution is shown. In the areas of highest magnetic field strength, the particle rows are widely separated. Because of the presence of large magnetic forces, some areas may be completely void of particles. This is especially noticeable in the vicinity of the conducting coil. Areas of least field concentration show the particles in a nearly random distribution.

For the tests on this project, two frequencies were used. The first tests were made at 60Hz and the field generated was about 2,000 ampere turns. A second convenient power frequency of 400Hz, supplied by a motor generator, was used. The transformer

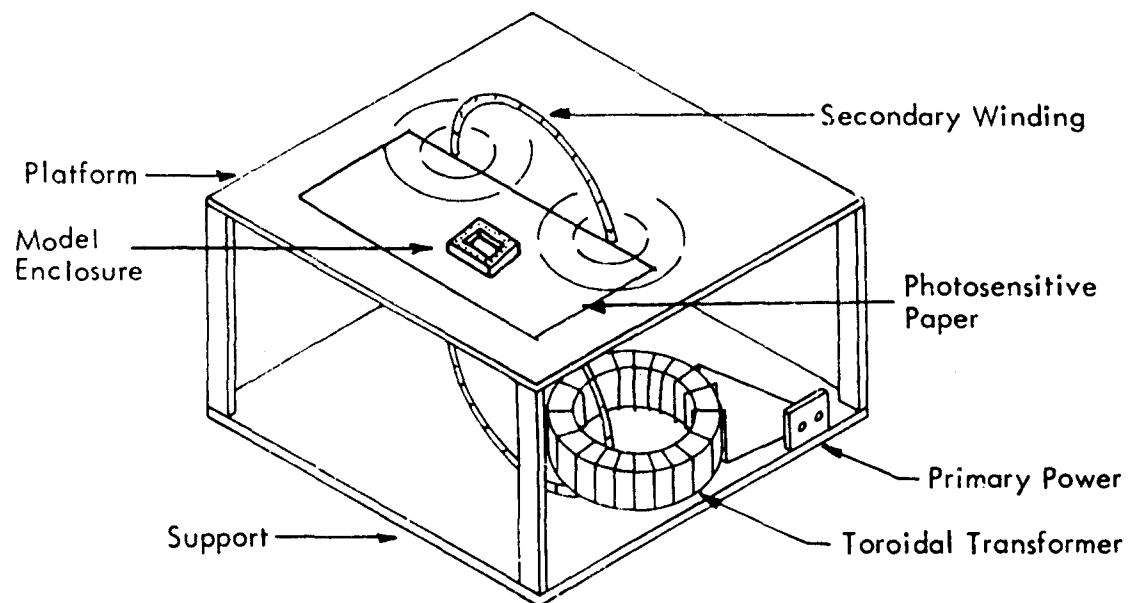


Fig. 23 Device for Graphical Illustration of
Magnetic Field Paths and Distortion

inductance caused an increase in reactance at the higher frequency and this factor, along with a reduced voltage supply, provided only about 600 ampere turns. This was still enough to produce magnetic field shadowgraphs within a small area about the coil. No attempt was made to produce magnetic field patterns at higher frequencies because special equipment would be required to supply the high power necessary for the magnetic field.

A variety of samples of powdered and granular magnetic materials were used to make the patterns. A number of magnetic material samples supplied by Engineering Experiment Station at Georgia Institute of Technology were tested for the quality of pattern which each makes. Particle size varied from the extremely fine (4 micron) carbonyl iron particles to the largest flat scaly variety of magnetic iron oxide called mill scale. The most satisfactory results came from samples of well graded spherical particles about 50 microns in diameter. These particles have freedom of movement and do not tend to stick to the surface of the paper as do the smaller particles. The large particles such as mill scale do not make smooth shadowgraphs and are difficult to move about in the magnetic fields.

The size graded 50 micron spherical particles are made of a material having a low coercive force. In this material, the magnetic domains can easily change with the alternating field; particles tend to align and form low reluctance paths. The magnetic force on a line of particles is much like the force tending to close a magnetic relay. Because of the ideal mobility and magnetic characteristics, the 50 micron spherical particles were used to make the magnetic shadowgraphs. Most satisfactory results were obtained with powdered iron manufactured by the American Photocopy Equipment Company and used as a toner carrier in their APECO electrostatic duplicators. A second choice material of similar particle size is Grade B-210 powdered iron manufactured by The Glidden Company, Metals Division, Baltimore, Maryland. These particles are rough shaped and therefore do not have the mobility of the APECO material.

To show the similarity of the calculated field about a circular coil and the measured field, the two were compared.

The field at a point in space around a circular coil immersed in a homogeneous isotropic medium has been calculated under the assumptions that the resulting field is symmetrical about the coil's axis and that the coil is constructed of a filament. From a practical point of view the dimensions of the coil's wires must be small compared to the diameter of the coil. Since the coil is symmetrical about the axis, only two coordinates are necessary; hence the formula is presented in terms of rectangular coordinates for the field in a plane.

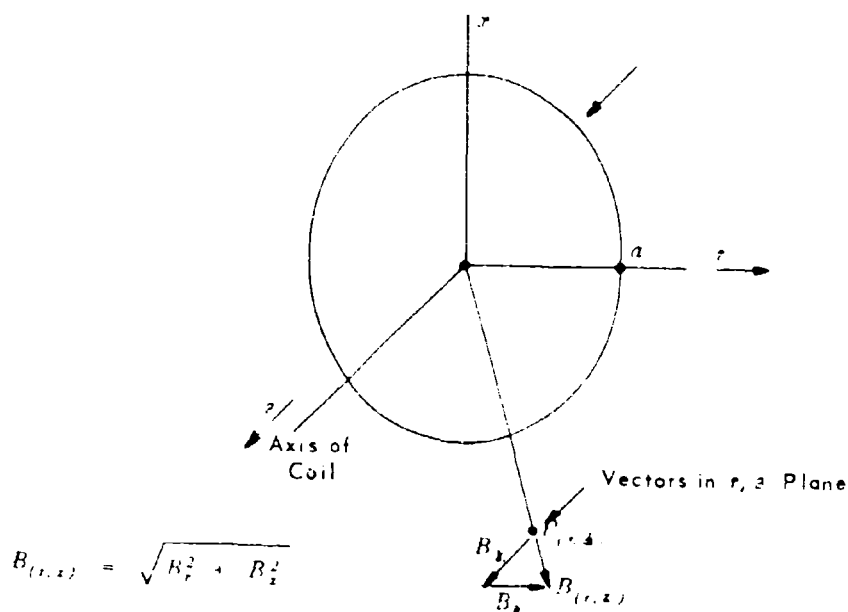


Fig. 24 Field Vector Diagram

The diagram, Fig. 24, explains the sense of the notation. Mathematical expressions for B_z and B_r in terms of r and z were used to calculate the component vectors B_r and B_z . The resultant vector $B_{(r,z)}$ was computed from

$$B_{(r,z)} = \sqrt{B_r^2 + B_z^2} \quad (9)$$

To generalize the results to any coil the coordinates r and z were expressed in tenths of a radius. The formulas (MKS System) used were:

$$B_z = \frac{NI}{2\pi a} \frac{1}{[(1+r)^2 + z^2]^{3/2}} \left[\int_0^{\pi/2} \frac{d\theta}{[1 - k^2 \sin^2 \theta]^{3/2}} + \frac{(1-r^2-z^2)}{(r-1)^2 + z^2} \cdot \int_0^{\pi/2} [1 - k^2 \sin^2 \theta]^{1/2} d\theta \right] \quad (10)$$

$$B_r = \frac{NI}{2\pi a} \left(\frac{3}{r} \right) \frac{1}{[(1+r)^2 + z^2]^{3/2}}$$

$$\left[- \int_0^{\pi/2} \frac{d\theta}{[1 - k^2 \sin^2 \theta]^4} + \frac{1 + r^2 + z^2}{(r-1)^2 + z^2} \int_0^{\pi/2} [1 - k^2 \sin^2 \theta]^4 d\theta \right] \quad (11)$$

$$k^2 = \frac{4r}{(r+1)^2 + z^2} \quad (12)$$

These equations reduce to

$$B_z = \frac{NI}{2a} \cdot g \quad (13)$$

$$B_r = \frac{NI}{2a} \cdot h \quad (14)$$

$$B_{(r,z)} = \frac{NI}{2a} \sqrt{g^2 + h^2} \quad (15)$$

where g and h are geometrical factors. By absorbing π into g and h at $(0,0)$

$$g = 1 \text{ and } h = 0 \text{ at } (0,0).$$

$B_{(r,z)} = \frac{NI}{2a} \sqrt{g^2 + h^2}$ holds for all coils and offers the advantages of not having to consider current magnitude, number of turns, or radius of a particular coil. Hence $\sqrt{g^2 + h^2}$ can be used to reduce computational labor for many different coils.

A graph was plotted of $\sqrt{g^2 + h^2}$ for various values of r and z .

Example:

Calculate the field at $z = 0.8$ radius and $r = 1.2$ radii

$$r = 1.2 \text{ and } z = 0.8.$$

A.) Evaluate the following integrals using tabulated elliptical integrals:

$$\int_0^{\pi/2} \frac{d\theta}{[1 - k^2 \sin^2 \theta]^{\frac{1}{2}}} \quad \text{and} \quad \int_0^{\pi/2} [1 - k^2 \sin^2 \theta]^{\frac{1}{2}} d\theta, \quad \text{for each } k^2.$$

$$\text{It was found that for } k^2 = \frac{4(1.2)}{(1.2 + 1)^2 + (0.8)^2} = 0.876 \quad (16)$$

$$\int_0^{\pi/2} \frac{d\theta}{[1 - k^2 \sin^2 \theta]^{\frac{1}{2}}} = 2.4773 \quad (17)$$

$$\int_0^{\pi/2} [1 - k^2 \sin^2 \theta]^{\frac{1}{2}} d\theta = 1.12385 \quad (18)$$

B.) Evaluating g

$$g = \frac{1}{\pi [(1 + 1.2)^2 + 0.8^2]^{\frac{1}{2}}} \left[2.477 + \frac{1 - (1.2)^2 - 0.8^2}{(1.2 - 1)^2 + 0.8^2} \cdot 1.124 \right] \quad (19)$$

$$g = 0.0941 \quad B_z = \frac{NI}{2a} (0.094). \quad (20)$$

C.) Evaluating λ

$$\lambda = \frac{1}{\pi [(1 + 1.2)^2 + 0.8^2]^{\frac{1}{2}}} - \frac{0.8}{1.2} \left[-2.477 + \frac{1 + (1.2)^2 + 0.8^2}{(1.2 - 1)^2 + 0.8^2} \cdot 1.124 \right] \quad (21)$$

$$\lambda = 0.237$$

$$B_z = \frac{NI}{2a} (0.237). \quad (22)$$

D.) Evaluating $B_{(r,z)}$

$$\sqrt{y^2 + h^2} = \sqrt{(0.094)^2 + (0.237)^2} = 0.255 \quad (23)$$

$$B_{(1.2,0.8)} = \frac{\mu I}{2a} (\sqrt{y^2 + h^2}) = \frac{\mu I}{2a} (0.255) \quad (24)$$

From the results of the tabulated calculations graphs were plotted. One of the graphs (Fig. 25) was plotted to show the vector direction only; the magnitude has been omitted. The graph of magnetic field vectors may be used as an overlay over the magnetic field shadowgraph of Fig. 26 showing the 60 Hz field generated about a circular loop. A photo comparison (Fig. 27) of the two figures shows good vector direction similarity. The calculated plot was drawn to a large scale and photographically reduced to the same size of the shadowgraph.

Slight irregularities may be found in the region of the coil. These are attributed to the following reasons: 1) The calculations were made under the assumption that the coil is constructed of a filament of dimensionless cross section rather than the heavy wire actually used. 2) The large magnetic forces in the region of the conductors pulls many of the iron particles toward the conductor and sometimes the paths indicated by the chain of particles is slightly distorted in these regions of the most intense magnetic field.

Shadowgraphs of magnetic field distribution were made about enclosures of several geometric patterns. The first patterns used extremely thin-walled models. These did not prove very useful because little could be seen about the field near the surface of the enclosure. Further experiments used models having half-inch thick walls. With these models, little could be seen of the interior distribution of fields. The best field patterns were made using a model having a wall thickness of about 1/8-inch thick. Shadowgraphs from these patterns clearly show the field distribution inside and outside the model enclosure. The field pattern of Figs. 28, 29, 30, 31, 32, 33, and 34 show the magnetic field distribution about some simple geometric shapes.

A series of shadowgraphs were made to show magnetic field behavior about various joints in ferromagnetic materials. First, a shadowgraph was made about a

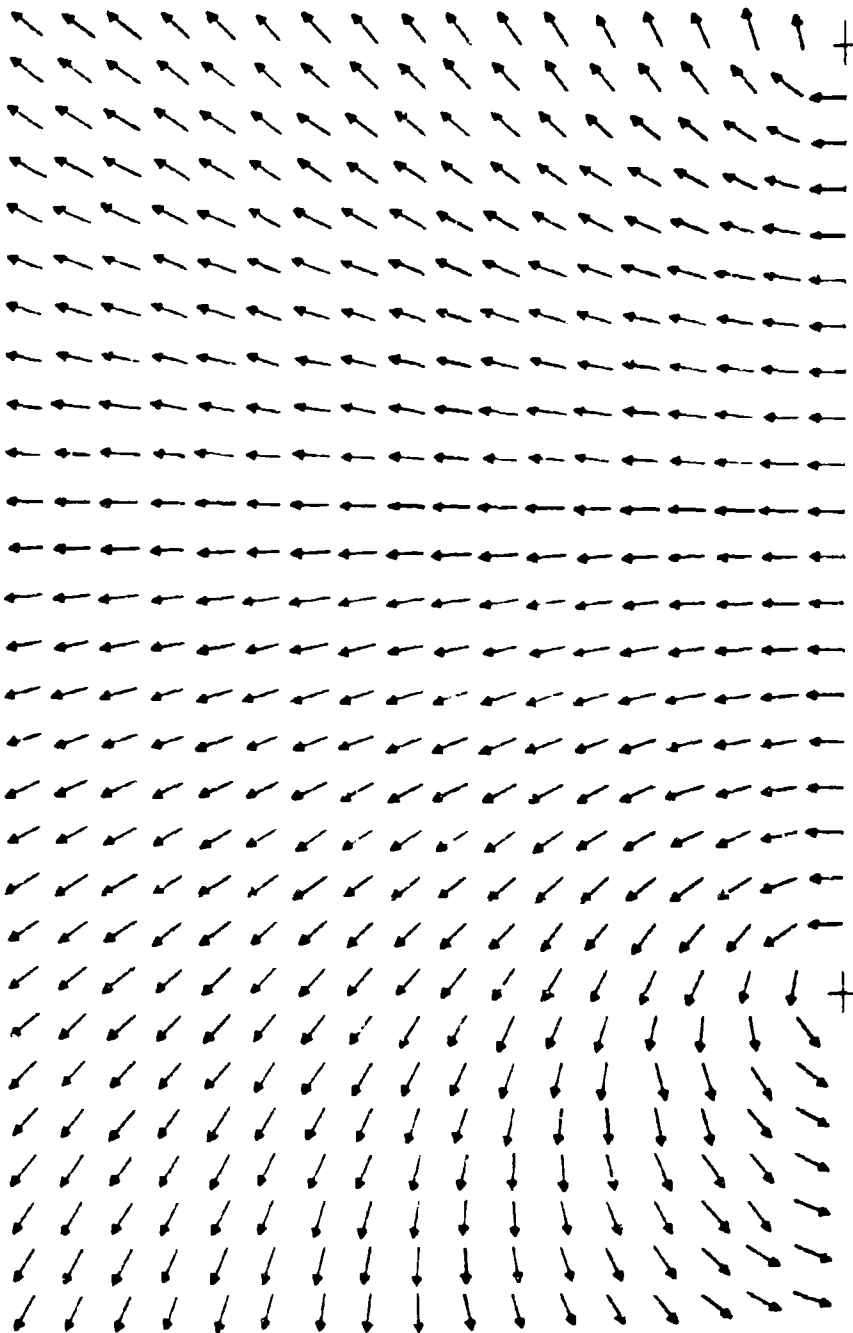


Fig. 25 Field Vectors Calculated by Elliptical Integrals

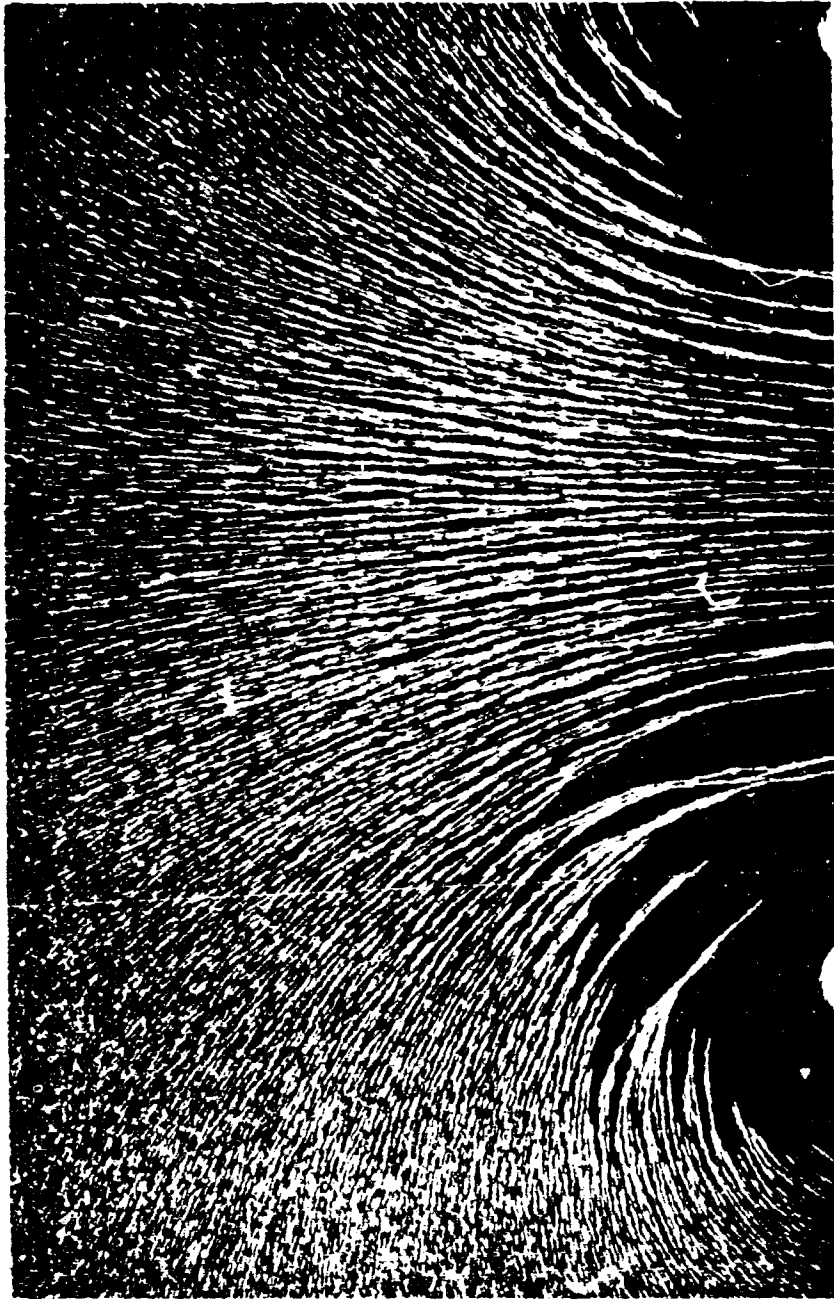


Fig. 26 Shadowgraph of the Magnetic Field Distribution
about the Center of a Circular Coil

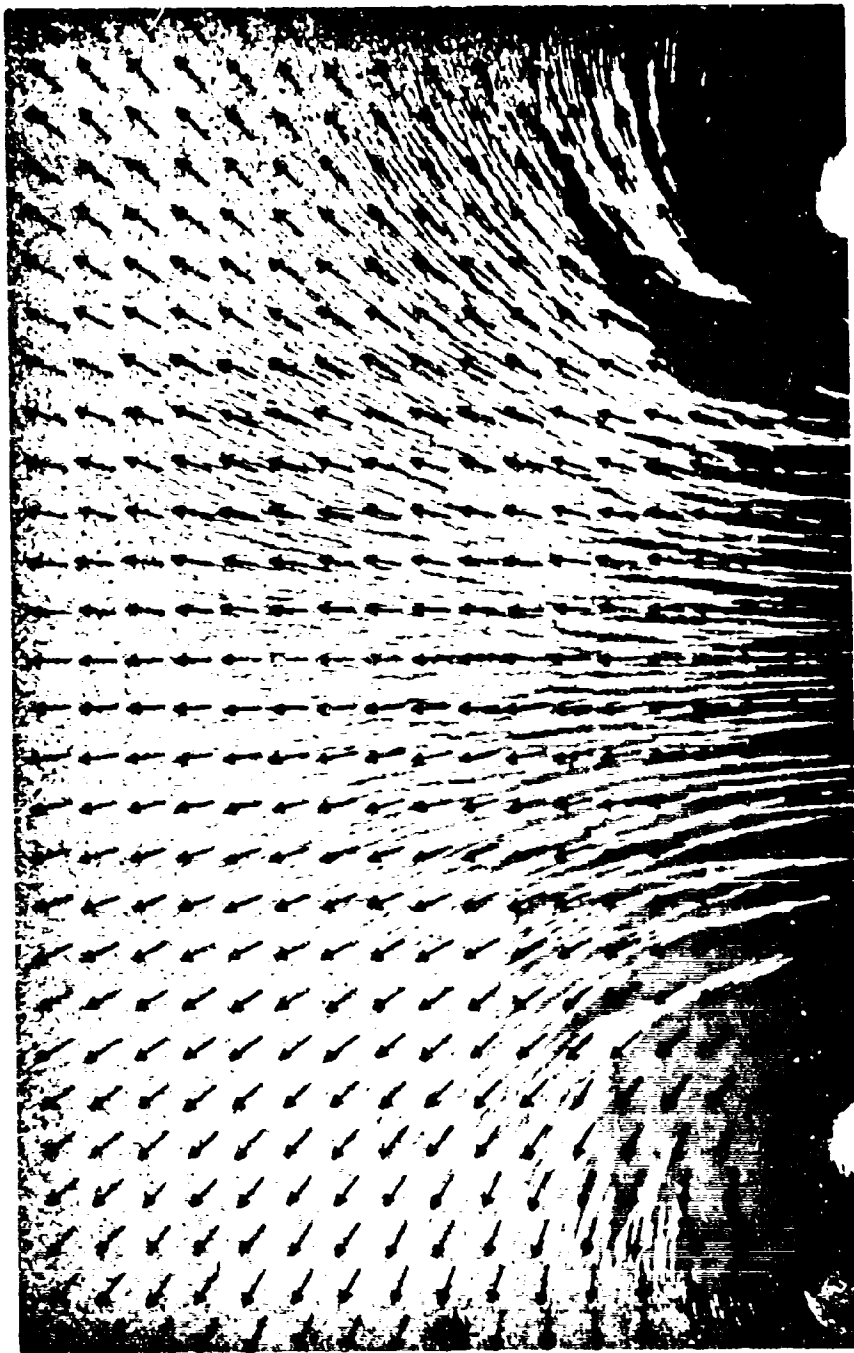


Fig. 27 Plot of Calculated Field Distribution Printed over
Magnetic Field Shadowgraph

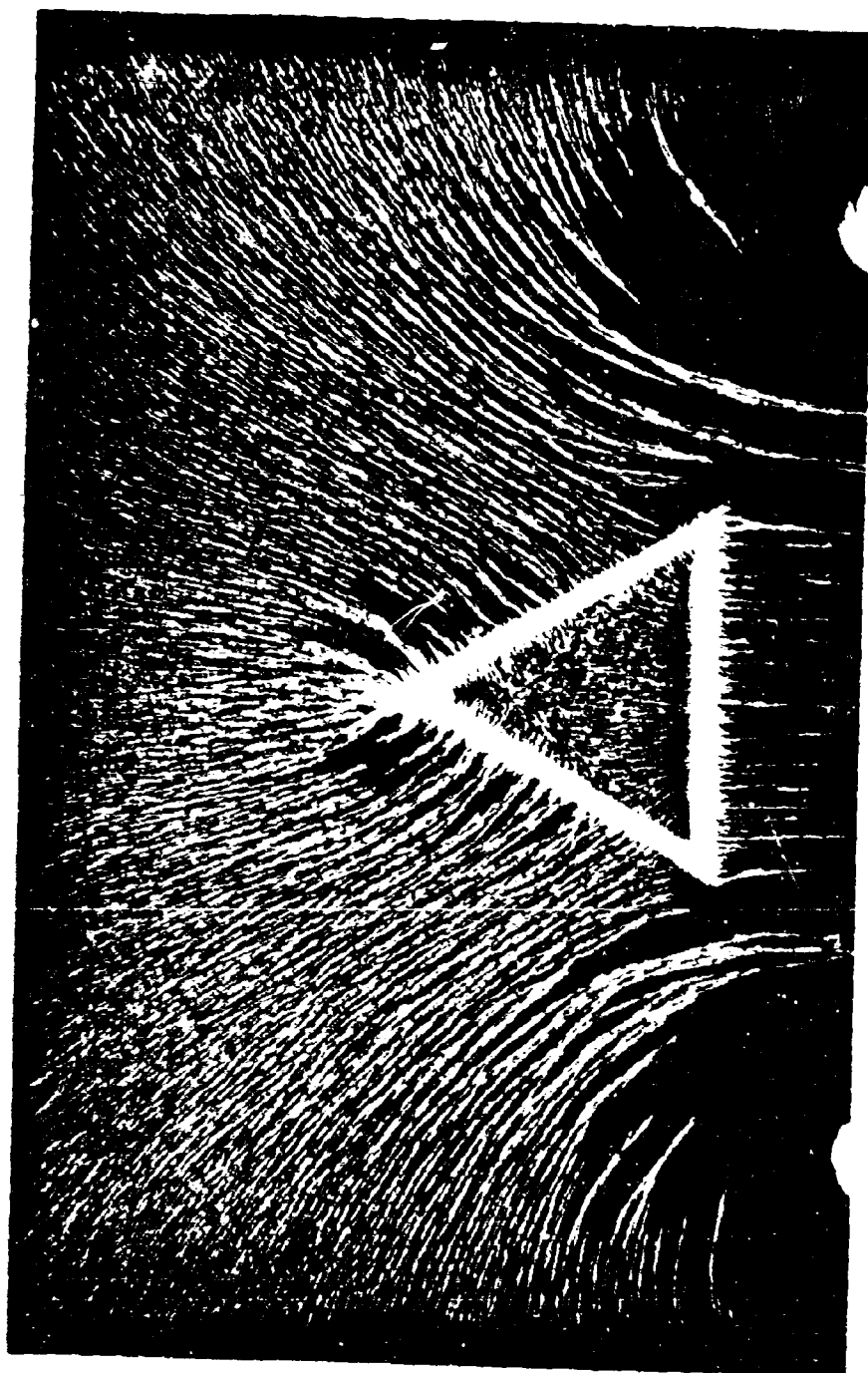


Fig. 28 60Hz Field Along Coil Axis

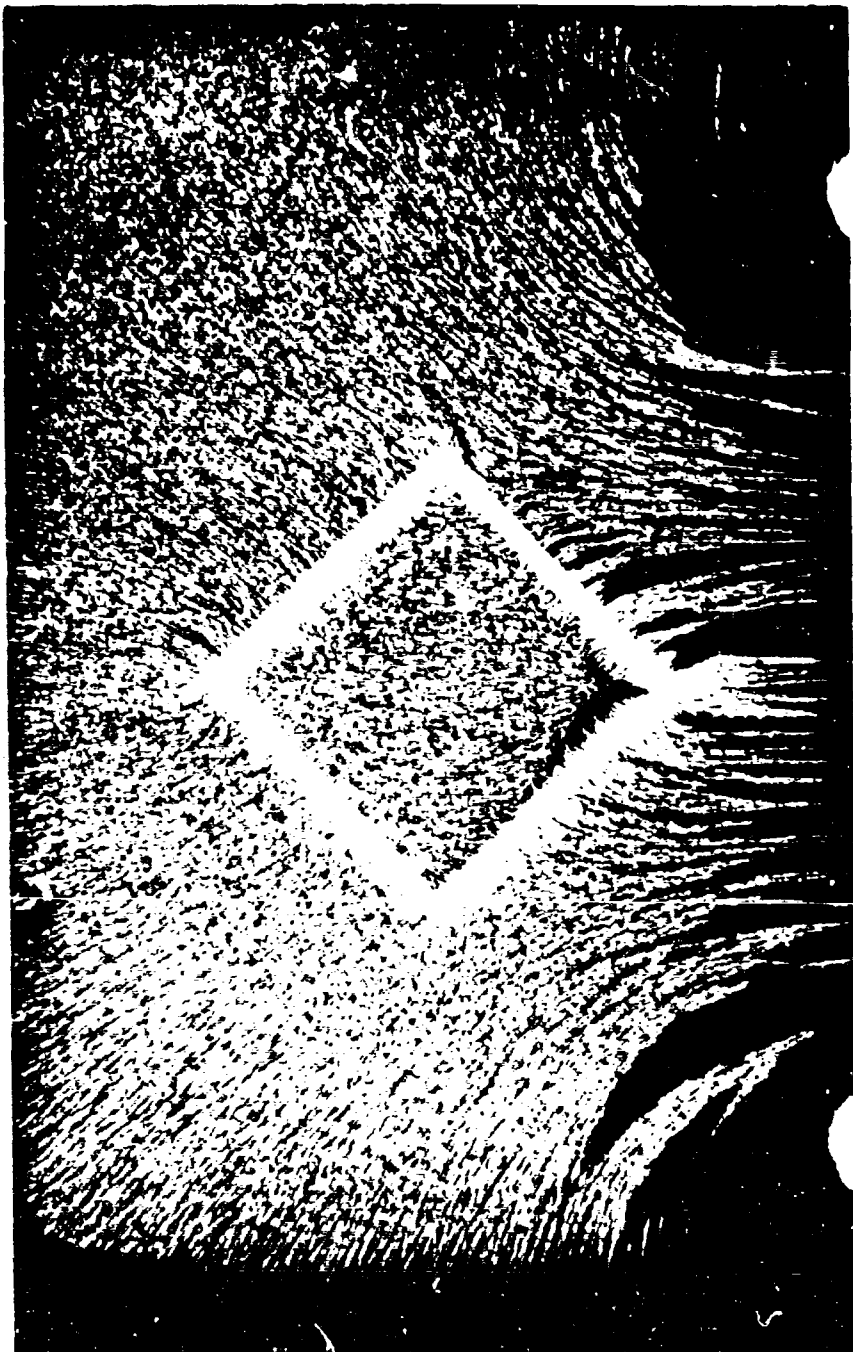


Fig. 29 60Hz Field Along Coil Axis

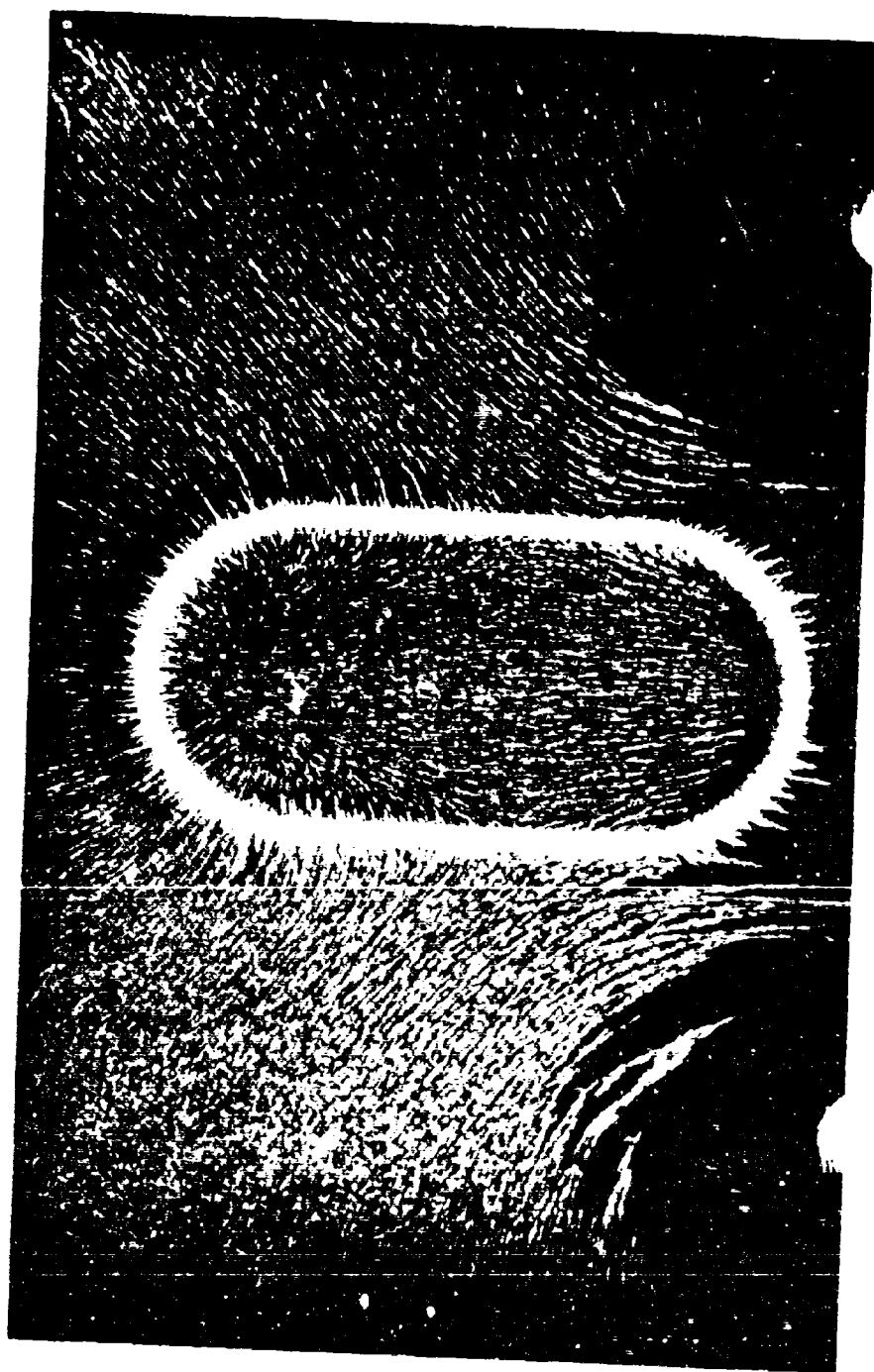


Fig. 30 60Hz Field Along Coil Axis

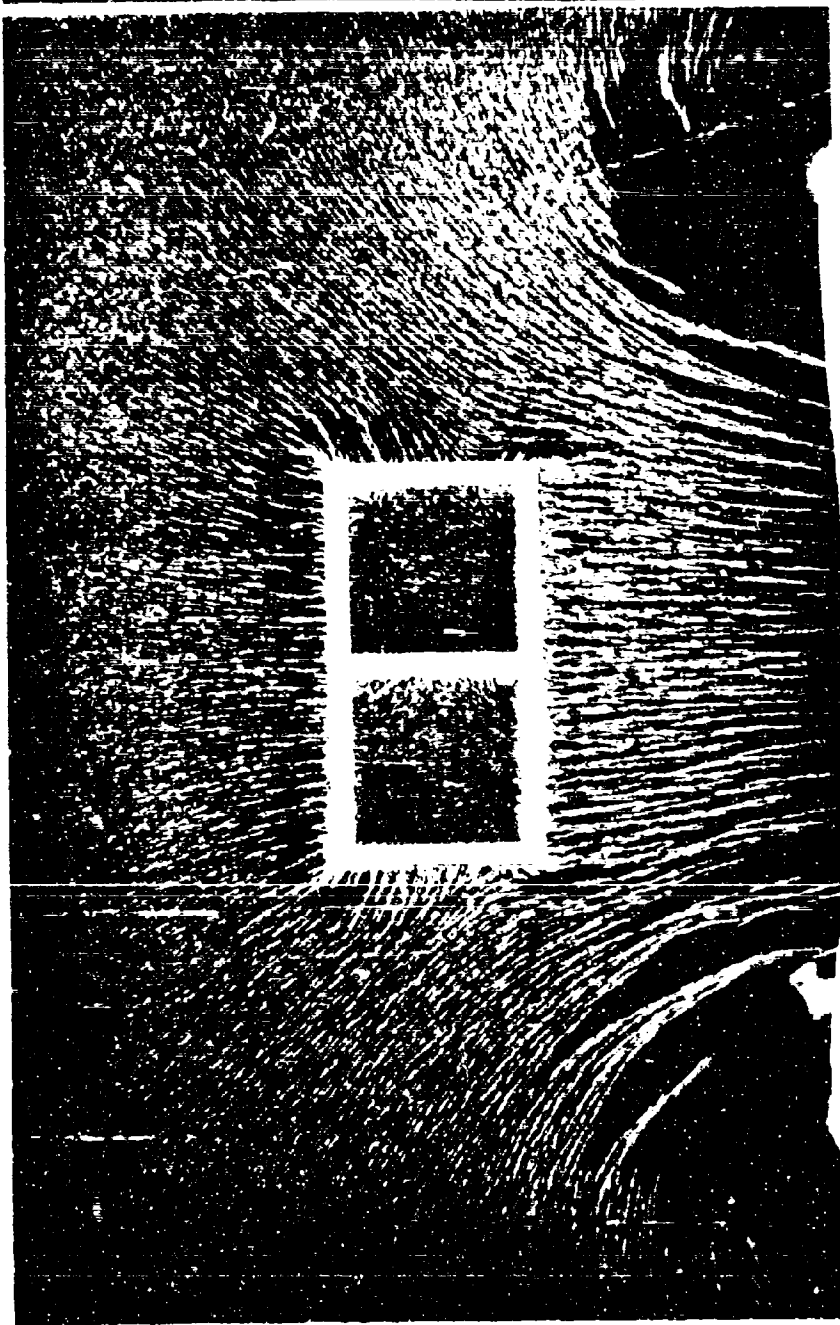


Fig. 31 60Hz Field Along Coil Axis

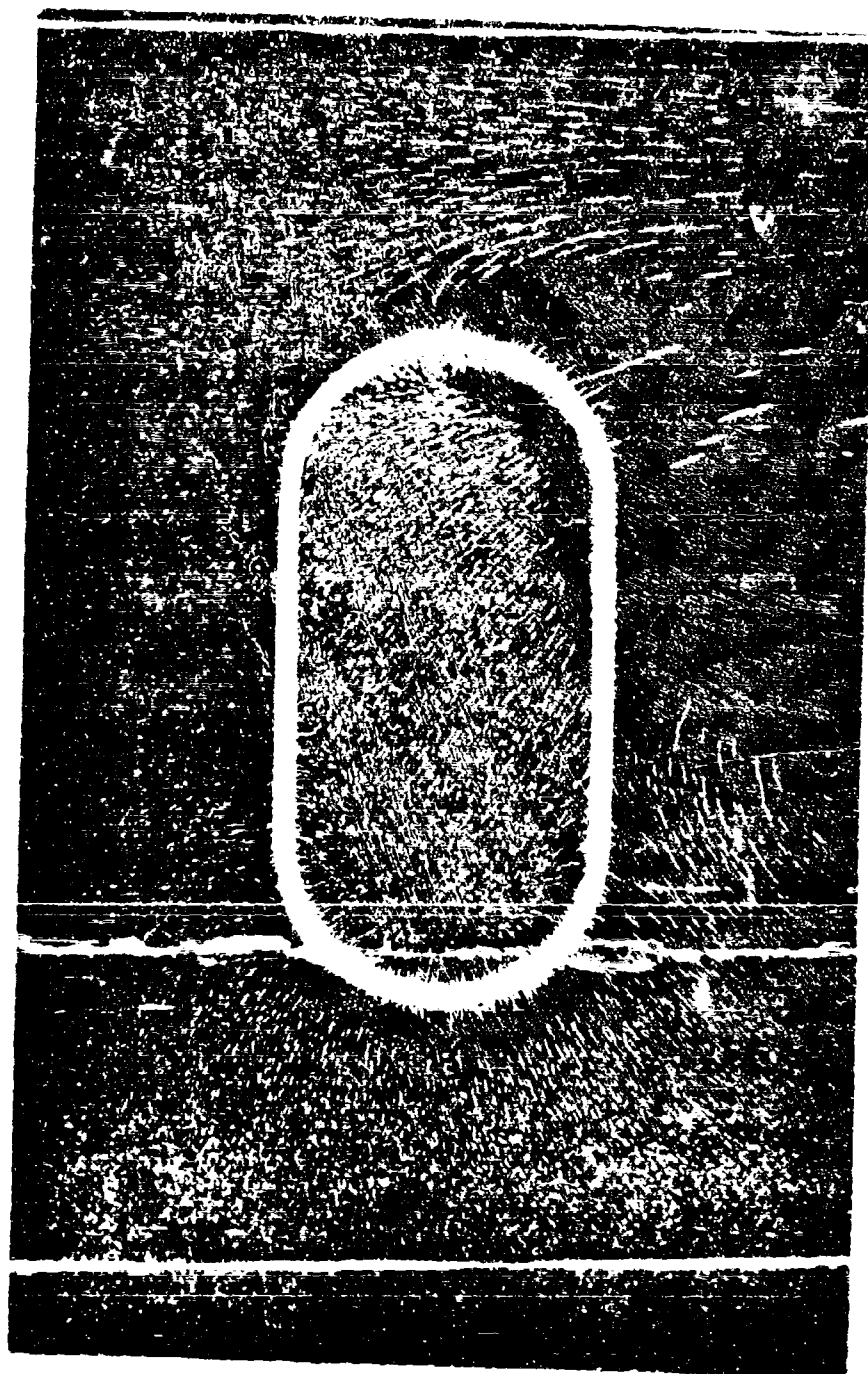


Fig. 32 60Hz Field at Edge of Coil

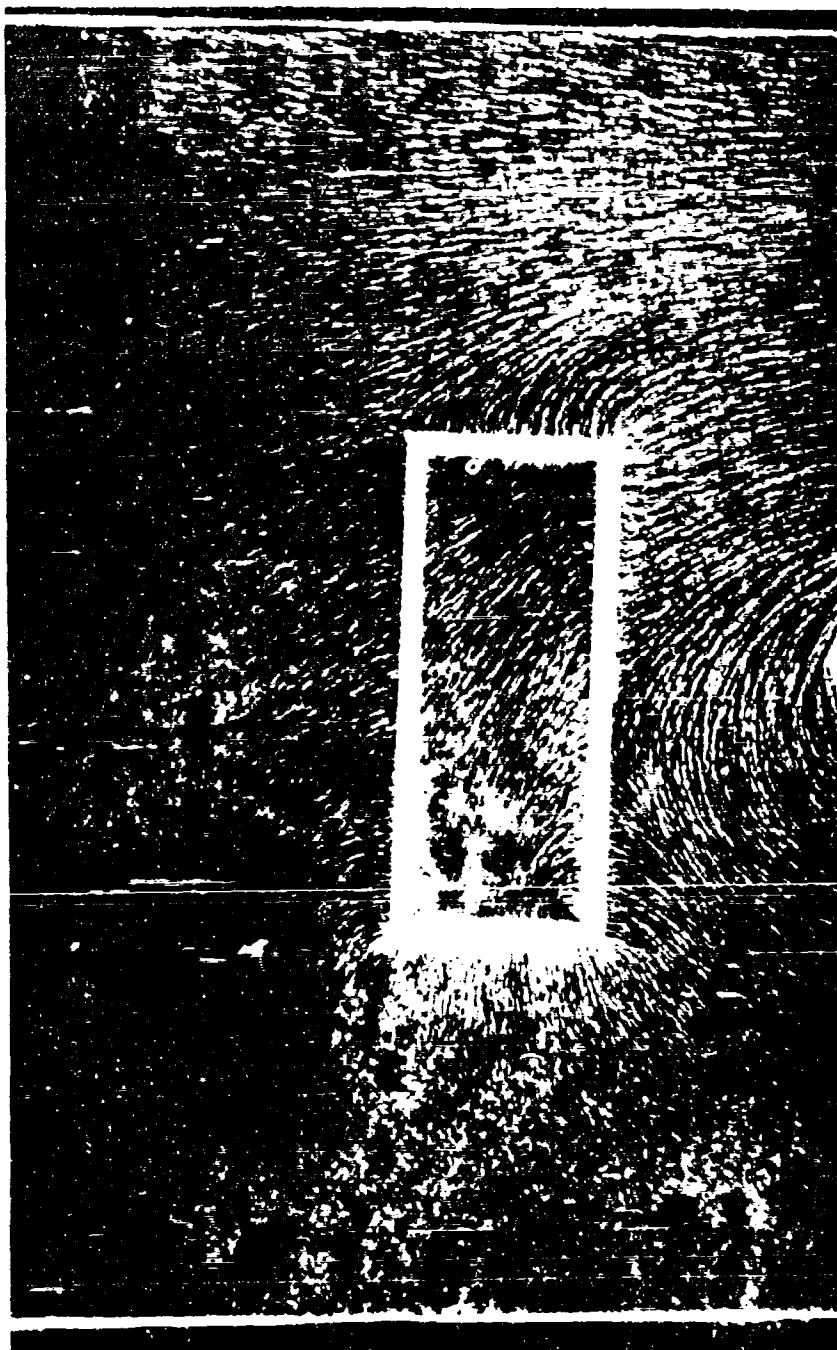


Fig. 33 400Hz Field at Edge of Coil

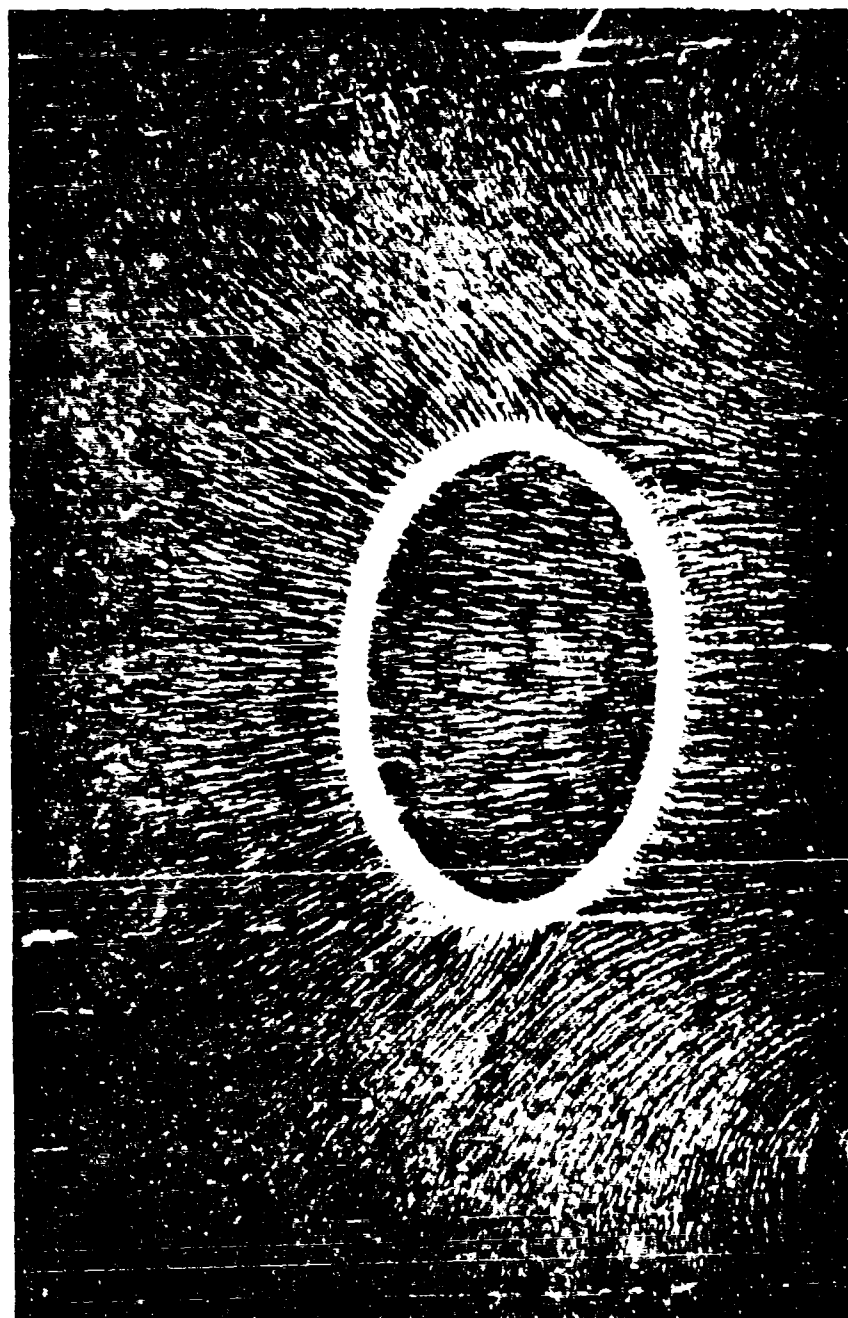


Fig. 34 400Hz Field Along Coil Axis

continuous circular enclosure (Fig. 35). Next, the enclosure was cut in half and the two sections butted together. As shown in Fig. 36, the shadowgraph of the fields about the butted halves shows considerable magnetic leakage across the high reluctance magnetic paths. The circular enclosure was again welded together. One side was welded with steel and the other side was brazed. The shadowgraph of the rejoined halves, Fig. 37, shows good magnetic continuity through the steel welded joint, but poor magnetic continuity through the brazed joint. This demonstrates the need for magnetic continuity when materials are joined in a shielding enclosure for low frequency magnetic fields. If only frequencies above 100 KHz are of interest in shielding problems, or if electric fields are the only concern, then the conductive rather than magnetic continuity of joined metal sections would be important.

The use of magnetic field shadowgraphs is helpful in analyzing the behavior of magnetic fields about ferromagnetic objects or enclosures. The patterns do not give an absolute intensity of the fields at a certain point from a source, but they can act as a relative field strength indicator for various points about a magnetic field source. The most important use of the magnetic shadowgraphs is their ability to show the vector direction of a magnetic field in the vicinity of a ferromagnetic object or barrier. Further development of equipment will aid in showing the behaviors of magnetic fields at much higher frequencies. Present limitations are the generation of high frequency fields of very high intensity.

Effects of Geometry and Construction Methods:

Having knowledge of the shielding properties of building materials only partially solves the problem of constructing a sound economical enclosure. Proper construction practices and good design can greatly influence the SE of an enclosure.

An enclosure that is to keep low frequency magnetic fields from either entering or exiting must be constructed of a ferromagnetic material. Unless a superconductive shield is considered, the most conductive materials available do not lend themselves to significant magnetic field shielding at frequencies below 100 Hz. Since shielding by a material of high magnetic permeability is a function of the total mass of material, this type of shield must be bulkier than shields for high frequencies. The ferromagnetic material may be an effective shield even with large openings in the barrier. For example, an enclosure of a heavy gauge expanded steel which has openings 4 inches long but which weighs 4 pounds per square foot makes a better magnetic shield than a light gauge

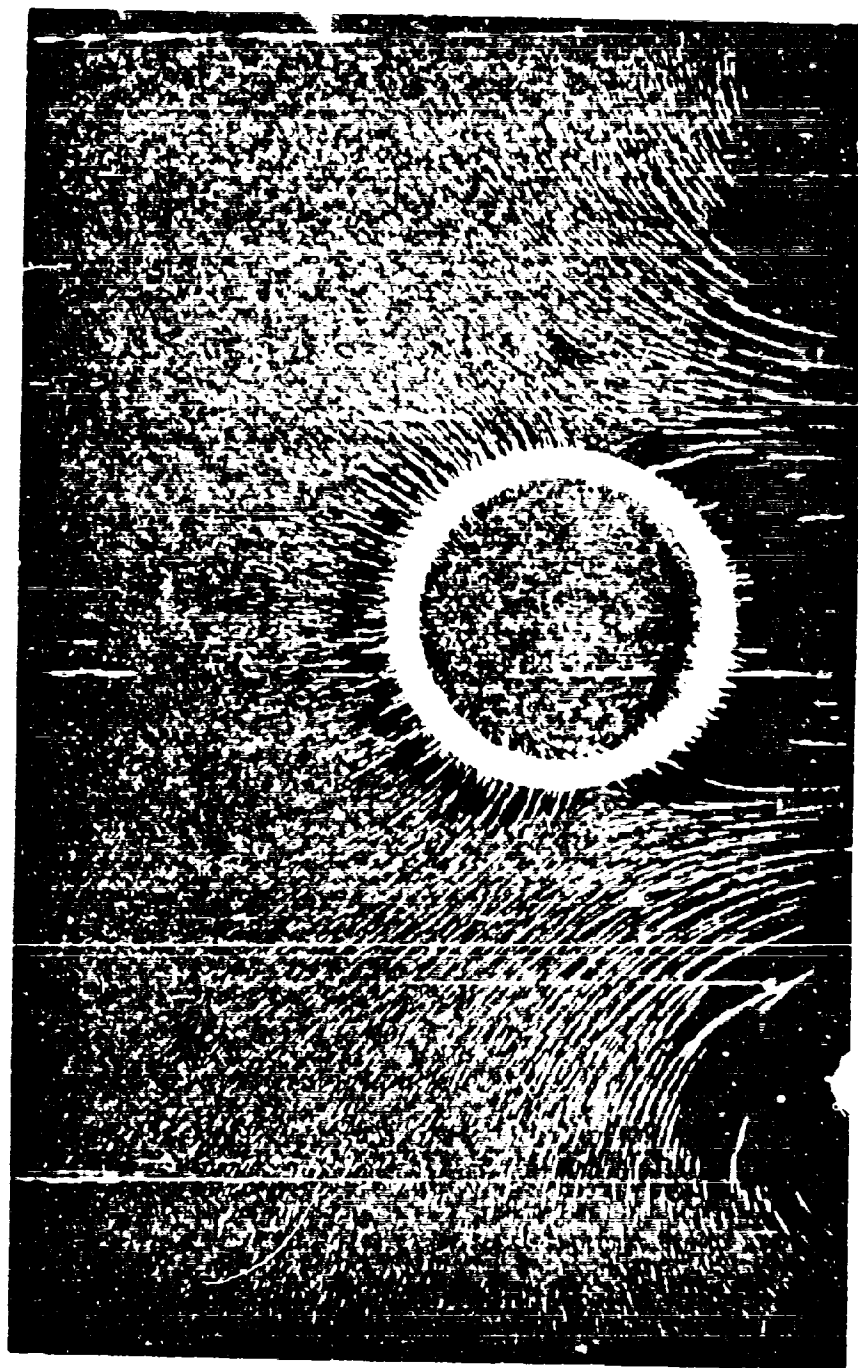


Fig. 35. Shadowgraph of 60 Hz Field Distribution about a Circular Barrier

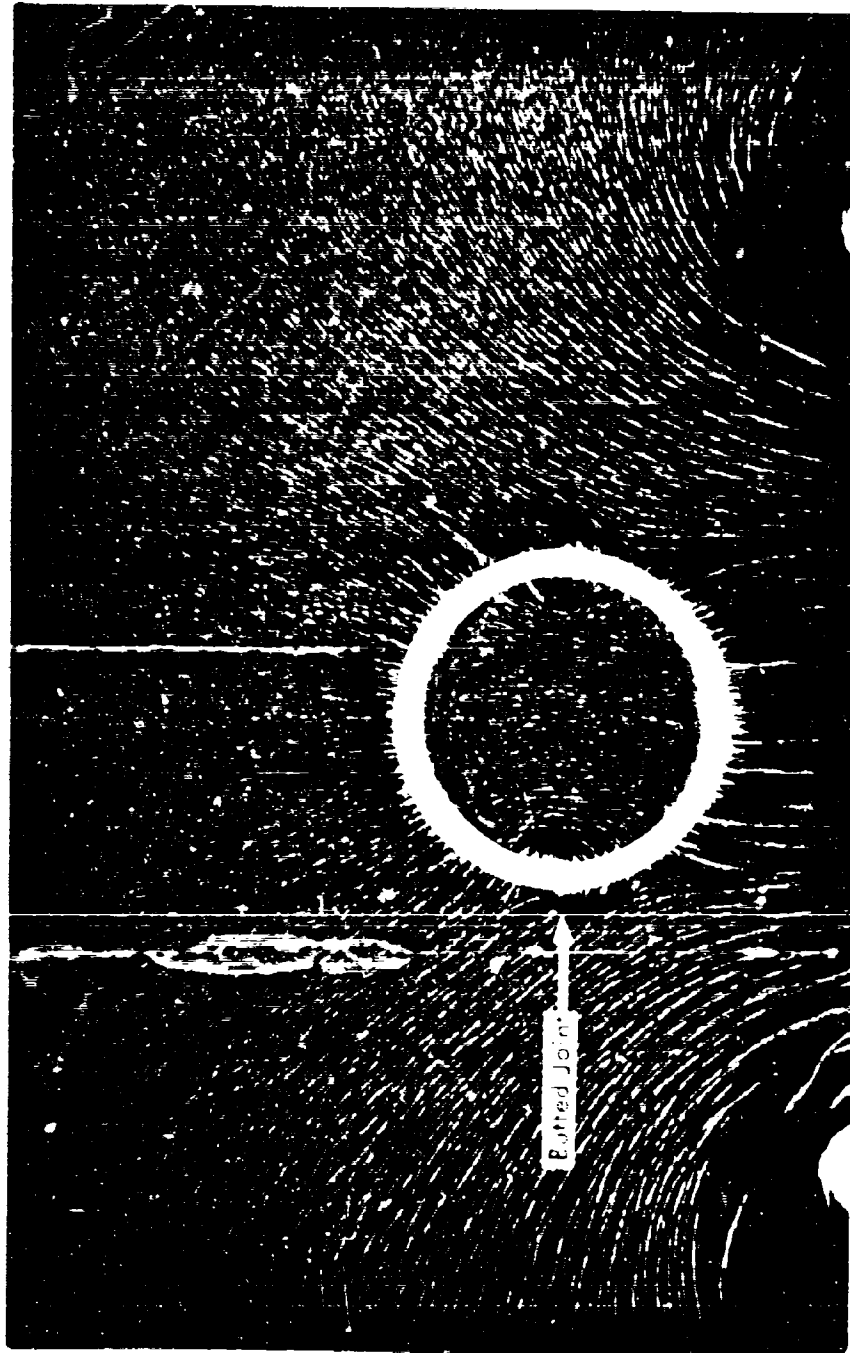


Fig. 36 Shadowgraph of 60 Hz Field Distribution about a Circular
Barrier Cut in Half and Pinned Together

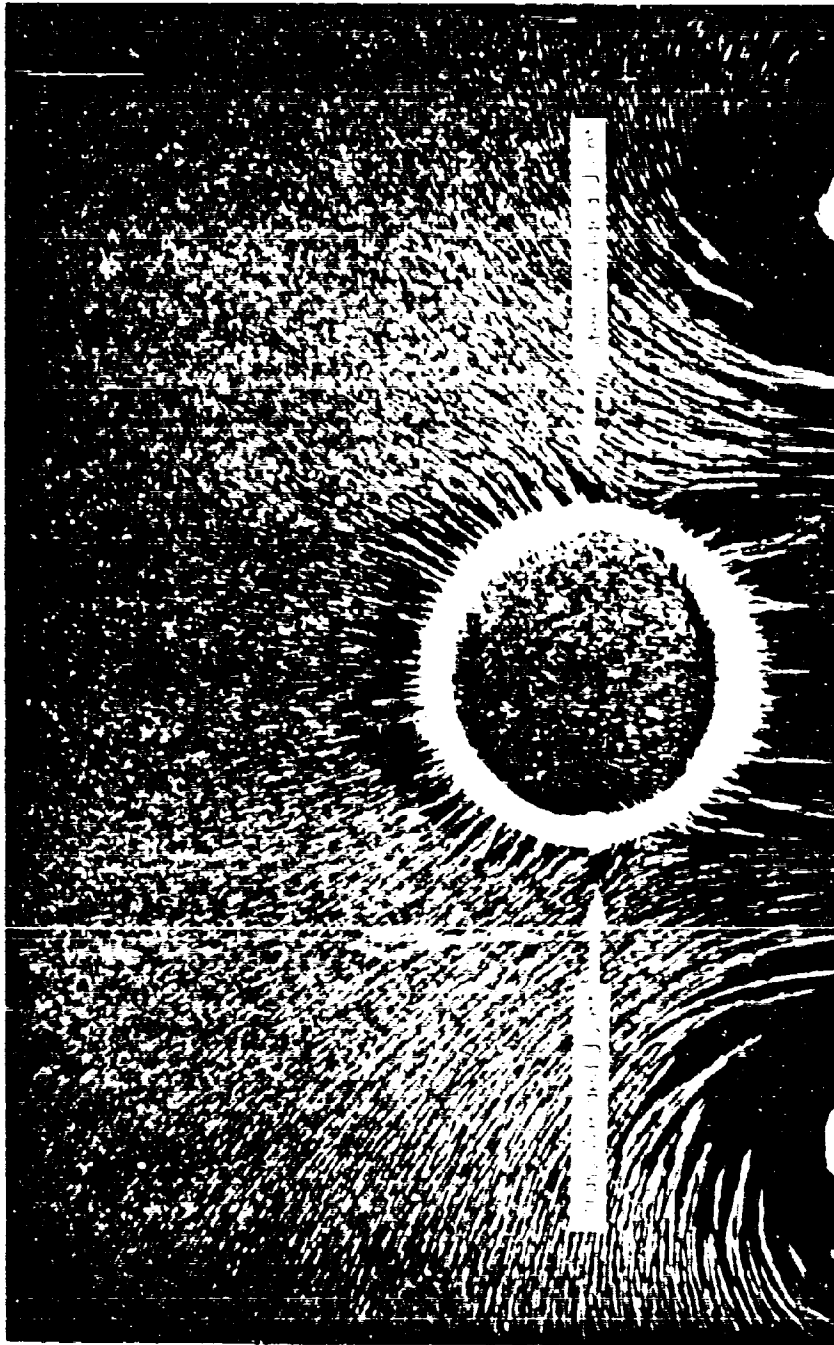


Fig. 37 Shadowgraph of 60 Hz Field Distribution about Rejoined Halves of Circular Barrier, Showing Steel Vault and Brazing Joint.

expanded steel having openings only $3/4$ inch long and weighing about $1/2$ pound per square foot, see Fig. 38. If the enclosure were also required to shield electromagnetic signals in the UHF region of the spectrum, light weight materials would provide more shielding than the heavy material because of the wave guide effect caused by the openings in the material. The large opening material "leaks" more UHF signals and has a lower cutoff frequency than the material having smaller openings. Tests on large enclosures of a material offer more shielding against low frequency magnetic fields than a small enclosure. The variations in SE at frequencies below 1 KHz are most likely due to the presence of more ferromagnetic material in the larger enclosure. At higher frequencies (above 1 KHz), a large enclosure may show less apparent shielding than a small enclosure. This could be explained two ways. First, the path of the loop for induced currents is larger on a larger enclosure. This path must have a higher resistance than a small path thus causing less field cancellation by the Lenz's Law effect. Secondly, if the separation between two parallel, conductive walls in a room is some multiple of a half wavelength of an electromagnetic wave, the intensity of a signal of this frequency could show up stronger inside the enclosure because of a cavity resonance reinforcement. This could make the signal inside the shield stronger than the signal outside the "shielded" area. Because signal leakage through openings, holes, etc., is so prevalent at UHF, the construction of an efficient shield to block passage of these waves must be restricted to solid materials. The popular screen rooms made of copper wire screen become poor EM shields at frequencies above 1 GHz. When it is necessary to have a window or air passage in a high frequency shield, elaborate traps must be built which will allow a flow of air but block passage of electromagnetic waves.

Nearly all cases of shielding are best accomplished by the use of several layers of a shielding material rather than one larger layer. Some manufacturers of magnetic shields sandwich layers of ferromagnetic materials having different magnetic characteristics. Outer layers of the barrier are made of a medium permeability material which will take a large magnetizing force before saturating. The inner layers are made of materials having very high permeabilities but which saturate much more readily. The combined materials in an enclosure form a barrier which lessens the penetration of magnetic fields in an efficient manner.

The use of multilayered materials in a shield was also shown to be better than a thicker, single layered enclosure. Two and three layers of aluminum foil make a better shield if the layers are separated by a nonconductive medium. Other tests showed that

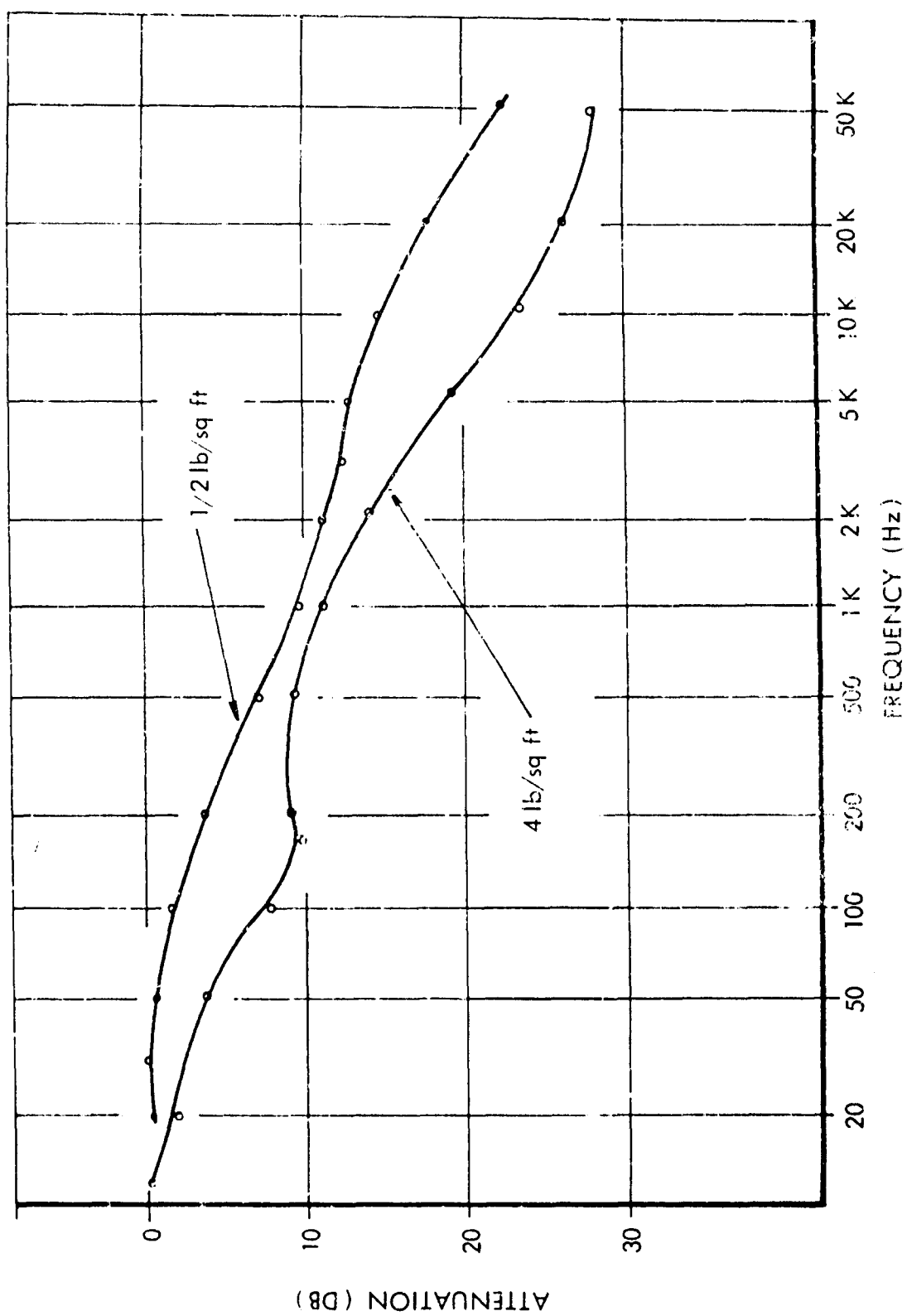


Fig. 38 Magnetic Field SE of Two Sizes Expanded Steel

doubling the thickness of a material did not double the shielding effectiveness of an enclosure. Since alternating currents by nature tend to flow on the surface of an electrical conductor, a barrier of several conductive layers will have less impedance to induced currents than a barrier of a single thick conductive layer. Much of the shielding of low frequency magnetic fields is generated by induced currents in conductive shields; therefore, the multilayered barriers offer more shielding than a single layered barrier.

When electromagnetic plane waves travel through a shielding barrier, the reflection at the surface of the barrier is associated with the change in intrinsic impedance across the barrier. The greatest amount of shielding will occur when an EM wave traverses several changes of intrinsic impedance. Again, a multilayered configuration offers the best shielding.

The effectiveness of shields for low frequency magnetic fields may be significantly influenced by the shape of the enclosure. If the direction of the interfering signal is known, the best shields take the form of an ellipsoid or similar streamlined model. For protection from all directions, a spherical enclosure is the best design. However, the cost of making a spherical enclosure may not be considered worth its high price if it is compared with a slightly less effective but much less expensive enclosure having a cubical or other flat sided shape.

In cases where reinforcing steel or structural steel is used to the advantage of shielding, it is important that conductive and magnetic paths be complete around the entire enclosure. Little good is accomplished by having one wall in an enclosure of a good shielding material and the rest of the materials having poor shielding quality. This means that reinforcing steel set vertically in a wall must have horizontal members attached to form a lattice in order to effect any measurable SE. It is also necessary that the metal in one wall be attached to the metal in adjacent walls, roof and floor.

As discussed in the section on radiated measurements, much apparent shielding is brought about by the regeneration of magnetic fields produced by an incident, time varying field that impinges on a conductive plane perpendicular to the incident field. If the loops for regenerated currents and fields do not exist in the walls, floors and ceilings of an enclosure, there will be no closed loops in which currents may be developed for a field regeneration type of shielding, nor will there be the proper magnetic paths to shunt low frequency magnetic fields around an enclosure.

This study has been concentrated on the investigation of the SE of building materials. The accentuation was on finding the most efficient shields among "standard" materials rather than some of the more elaborate and certainly very expensive types of shielding materials. The cost of installing a shielded room which greatly attenuates low frequency magnetic fields is often prohibitively high if the area to be shielded is larger than a few cubic feet. The price of installation for the exotic material shield can easily cost over \$100 per square foot of floor space. Sometimes a minimal amount of shielding may be satisfactory in preventing degrading interference. Metallic materials, ferromagnetic and conductive, without question have the best shielding properties for magnetic, electric, and electromagnetic fields. A structure of corrugated, galvanized steel can be made into a useful shield if all sheets of the material are carefully bonded, and if joints between adjacent walls and the roof are also electrically bonded.

During the measurement progress it was found that expanded steel materials provided the proper magnetic and electrical continuity for a good shield. This material also is well adapted for use in reinforced concrete walls, floors and roof as a substitute for reinforcing steel. The expanded steel has an advantage over reinforcing bar steel in that the expanded metal does not require welding at each cross point to make a reasonably good shield. The necessity remains, however, for welding all sheets to adjacent ones and to weld corner seams where wall, roofs and floors join.

If the substitution of bar type reinforcing steel is not economically feasible, a smaller expanded steel called plaster lath can be used for shielding. This thinner material has less SE against magnetic fields below 1 KHz, but since the plaster lath has smaller openings in the material, it will shield to a higher frequency than the heavier expanded steel.

Material Selection for Shielding:

The materials from which structures are built are primarily determined by availability at the site of construction. The lumber materials used in the northwestern part of the United States are not the same as those used in the southeastern United States. Most probably both of these are considerably different from the wooden materials used in the Far East and Pacific. There are some materials such as concrete, corrugated iron, and asbestos shingles which (because of modern logistic advances), are available practically anywhere in the world.

Whatever materials are available, the choice must be made as to which will be used. The choice of materials must be made giving consideration to the type of shielding which is necessary at a particular location. If a building is to house communication equipment and this building is near a powerful radar installation, the interfering frequency of paramount importance may be expected in the radar frequency ranges. Therefore, the shielding should be one which protects against very high frequency electromagnetic waves rather than low frequency magnetic fields. Conversely, a shield to protect from low frequency magnetic fields should have a large mass of material having a high magnetic permeability rather than being a thin, highly conductive material.

As has been previously discussed, the type and frequency of the fields and waves causing interference define the material characteristics required for an optimum shield. The high magnetic permeability of ferrous materials make them the best kind to use to shunt magnetic fields away from a desired area. When the shields must protect an area from high and low frequencies, it is necessary to combine both types of materials to effect a satisfactory shield.

When analyzing the type of shielding necessary in a certain installation, the properties of materials which vary the shielding characteristic should also be studied. The three main characteristics are: 1) the magnetic permeability, 2) the electrical permittivity, and 3) the electrical conductivity of the material.

Ferromagnetic materials can be divided into two main categories: First, there are those materials which have medium permeability, but which do not saturate until a high magnetic induction level is reached. This type of shielding is best for locations of high level magnetic fields. A second type of ferromagnetic material is one which saturates at a relatively low level of magnetic induction, but which has an extremely high magnetic permeability. This type of material makes the best magnetic shield in an environment where high levels of magnetic shielding are required, but where the magnetic field intensities are well below the saturation level of the material. Since both favorable characteristics do not occur in the same material, the combination of materials can be used effectively to provide a good shield. The Perfection Mica Company is one organization which claims to make an effective magnetic shield by using prefabricated panels containing alternate layers of "Netic" and "CoNetic" which have the desirable characterization previously described.

Dielectric materials exhibit a characteristic called electrical permittivity. The relative permittivity (compared with the permittivity of a vacuum) can effect the energy absorption of a wave traveling through the medium. A high permittivity allows the greatest penetration of EM energy, but an associated characteristic called the dielectric loss factor or loss tangent influences the shielding in an opposite manner, that is, the greater the loss tangent, the more EM energy is absorbed as it travels through a dielectric medium. In general, the shielding caused by energy absorption in a dielectric medium is very small. The shielding is a direct function of frequency and does not become significant until the frequency of an EM wave goes above several hundred megacycles.

The third characteristic, electrical conductance or its reciprocal, resistance, is very far reaching in determining shielding at frequencies above several hundred cycles. Lenz's Law states that a time varying magnetic field which intersects a conductive medium induces a voltage in that medium which causes a current to flow in a direction that will generate a magnetic field tending to cancel the incident field. If the conductive medium were a super conductor, the field cancellation would be complete at any frequency. However, nearly all materials have considerable resistance and so shielding does not become significant until the frequency rises above several hundred cycles per second. The voltage induced is a function of frequency and therefore higher frequencies of the same magnetic intensity induce higher voltages in a conductor.

When the frequencies increase enough to be considered electric waves, shielding is effected because electrical fields are greatly reduced in conductive mediums. The permittivity of an electrical conductor is not defined and, therefore, the SE in a conductive nonmagnetic medium is difficult to predict other than for those losses which are caused by pure resistance.

From the measurements made on dielectric materials, it may be concluded that no ordinary dielectric material causes any significant shielding at frequencies below 100 MHz. Certain dielectrics which have ferromagnetic properties may perform as magnetic field shields. These materials (ferrites) are not considered as building materials. Their effectiveness as a shield is usually confined to UHF and microwave frequencies because of their useful property of absorbing high frequency radiation rather than reflecting it as does a conductive shield.

Some environmental effects on shielding characteristics are not pronounced. Very little change occurs in the electrical characteristics when materials are exposed to the

temperature ranges normally encountered. Magnetic materials can lose their magnetic characteristics when exposed to elevated temperatures. For some materials, the high temperature limit (the Curie Point) can be reached without difficulty in hot climates. Although such sensitive materials are a minority group, the ambient temperatures a shield will reach should be carefully considered if temperature sensitive materials are used.

Moisture content of a dielectric material will cause a change in its shielding characteristics. An increase in moisture content nearly always causes an increase in both dielectric constant and dielectric loss factor. As previously stated, the increase in dielectric constant tends to decrease the shielding effectiveness of a material, but the increase in SE due to the increased dielectric loss factors usually overshadow the decrease in SE due to increased dielectric constant. Those materials which show the greatest change in electrical characteristics in moist environments are most frequently those materials which are very porous. Cement, mortar, and bricks show more change with moisture variations than denser materials which are more impervious to water. Similarly, porous lightweight wooden materials are more affected by increased moisture than a dense, less porous wood. As could be expected, plastics and other materials that are virtually nonporous show little or no change when exposed to a high moisture environment.

The analysis of moisture sensitivity also gives insight to the effect that aging has on some materials. Although insufficient time was available to show the effect of aging on the electrical parameters of materials, it may be assumed that those materials which increase porosity with age are more likely to be effected by changes in environmental moisture. Conversely, those materials which change their structure minimally with age will show the least change in electrical characteristics, especially in varying moisture environments.

PART II
HANDBOOK OF SHIELDING

LIST OF ILLUSTRATIONS

PART II

Fig. No.		Page
1	SE of 2-Foot Cubical Enclosure of Single-Layered 16 x 18 Mesh Copper Screen with Edges Lapped and Stapled; Field Orientation Shown	79
2	SE of a 2 1/2 ft x 2 ft x 1 1/2 ft Three-Layer 16 x 18 Mesh Copper Screen Enclosure, Each Layer Separated by 1-Inch Space; All Seams Soldered	80
3	Curves of SE of Two 1-Foot Square Copper Sheets (see Fig. 18, pg. 96, for Composite Data Presentation)	81
4	SE of 3 x 8-Foot Copper Sheets	82
5	SE of a 1-Foot Cubed .026-Inch Wall Copper Box, Seams Soldered	83
6	SE of 2-Foot Cubical Enclosure of Single-Layered 18 x 16 Mesh Aluminum Wire Screen, Seams Lapped and Stapled	84
7	SE of 0.002-Inch Aluminum Foil, Lapped and Stapled to Inside and Outside Surfaces of a 2-Foot Cubed, 3/4-Inch Plywood Enclosure	85
8	SE of One Layer of 0.002-Inch Aluminum Foil in a 2-Foot Cubed Configuration with Seams Lapped and Stapled	86
9	Comparison of SE of Two Configurations of .0014-Inch Aluminum Foil Lapped and Stapled to the Surfaces of a 2-Foot Cubed, 3/4-Inch Plywood Enclosure	87
10	Comparison of SE for Adjacent Layers of .0014-Inch Aluminum Foil, Seams Lapped and Stapled, Lining a 2-Foot Cubical Enclosure	88
11	SE of a 2-Foot Cubed Enclosure of Three Adjacent Layers of .0014-Inch Aluminum Foil, Seams Lapped and Stapled; Field Orientation Shown	89
12	Curves of SE of Two 1-Foot Square Aluminum Sheets (see Fig. 18, pg. 96, for Composite Data Presentation)	90

Fig. No.		Page
13	SE of Plate Glass Door Bordered by an Aluminum Framework	91
14	Curves of SE of Two 1-Foot Square Brass Sheets (see Fig. 18, pg. 96, for Composite Data Presentation)	92
15	SE of a 1-Foot Cubed Brass Enclosure Having a 0.025-Inch Wall Thickness with Soldered Seams; Field Orientation Shown	93
16	SE of a 1-Foot Cubed Brass Enclosure Having a 0.064-Inch Wall Thickness with Soldered Seams; Field Orientation Shown	94
17	Curves of SE of Two 1-Foot Square Monel Sheets (see Fig. 18, pg. 96, for Composite Data Presentation)	95
18	A Composite Data Presentation of SE of 1-Foot Square Sheets of Various Materials	96
19	SE of 3 x 8-Foot Monel Sheets	97
20	SE of a 1-Foot Cubed Monel Enclosure having a 0.026-Inch Wall Thickness with Soldered Seams	98
21	SE of a 4-Foot Cubed Wrought Iron Enclosure Having a 1/4-Inch Wall Thickness with Seams Welded and Annealed	99
22	Sensor and Exciter Coil Orientation for SE Measurements Made on a Steel Tank Having a 1/2-Inch Wall Thickness	100
23	SE of a Steel Tank with 1/2-Inch Thick Walls (Position 1 of Fig. 22)	101
24	SE of a Steel Tank with 1/2-Inch Thick Walls (Position 2 of Fig. 22)	102
25	SE of a 2-Foot Cubed, Mild Steel Sheet Enclosure Having a 0.053-Inch Wall Thickness with Welded Seams	103
26	SE of a 1-Foot Cubed, 18 Gauge Galvanized Steel Enclosure; All Seams Soldered	104
27	Measurement Configuration Through Window and Wall of Galvanized Iron Building	105
28	SE of a Corrugated Galvanized Iron Wall, See Test Configuration in Fig. 27	106

Fig. No.		Page
29	SE of a 35" x 42" Steel and Glass Window in a Corrugated Iron Wall; See Test Configuration in Fig. 27	107
30	SE of One Layer of 18 x 14 Mesh Galvanized Iron Wire Screen in a 2-Foot Cubed Configuration, Screen Edges Lapped and Stapled	108
31	SE of a 1/4-Inch Mesh, 0.025-Inch Galvanized Iron Wire Hardware Cloth in a 2-Foot Cubed Enclosure with Edges Lapped and Stapled	109
32	SE of a 1/2-Inch Mesh, 0.040-Inch Galvanized Iron Wire Hardware Cloth in a 2-Foot Cubed Enclosure with Edges Lapped and Stapled	110
33	SE of a 2-Foot Cubed Enclosure of 6" x 6" x No. 10 Reinforcing Steel Wire Mesh with Edges Wired Together Using Iron Wire	111
34	SE of a 2-Foot Cubed Enclosure of 6" x 6" x No. 6 Reinforcing Steel Wire Mesh with Edges Wired Together Using Iron Wire	112
35	SE of a 9-Inch Reinforced Concrete Wall; at Least One Near-Midsection Cross-Member per Vertical Section with Rods Bent and Tied with Iron Wire at Each Juncture	113
36	SE of a 2-Foot Cubed Cage Enclosure of 3/8-Inch Reinforcing Steel Rods Spaced on 6-Inch Centers Both Ways with Steel Welded Cross Points and Corners	114
37	A Section of Expanded Metal Showing Measured Dimensions	115
38	SE of a 4 x 8-Foot Sheet of 1/2-Inch Safety Mesh Expanded Steel	116
39	SE of a 4 x 8-Foot Sheet of 15/16-Inch Safety Mesh Expanded Steel	117
40	SE of a 4 x 8-Foot Sheet of 1 3/8-Inch Safety Mesh Expanded Steel	118
41	SE of a 2-Foot Cubed, Plaster Lath Expanded Steel Enclosure Having Lapped and Wired Seams	119

Fig. No.		Page
42	SE of a Two-Foot Cubical Enclosure of 15/16-Inch Flattened Steel Mesh with Edges Steel Welded	120
43	SE of a Two-Foot Cubical Enclosure of 1 1/4-Inch Safety Mesh with Edges Steel Welded	121
44	SE of a Combination of a High Permeability Material and a Highly Conductive Material in a 2-Foot Cubed Configuration with Field Orientation Shown	122
45	SE Variations Caused by Removing One Side of a 1-Foot Cubed Sheet Copper Enclosure (Soldered Seams) Having a 0.026-Inch Wall Thickness	123
46	SE Variations Caused by Removing One Side of a 1-Foot Cubed Sheet Brass Enclosure (Soldered Seams) Having a .025-Inch Wall Thickness	124
47	SE Variations Caused by Removing One Side of a 1-Foot Cubed, 18 Gauge Galvanized Sheet Steel Enclosure; Seams Soldered	125
48	A Composite Data Presentation of Magnetic Field SE of 1-Foot Cubed Enclosures of Various Materials.	126

LIST OF TABLES

PART II

	Page
Table of Relative Resistivities of Several Metallic Building Materials	
Using Copper as a Standard	124
Tables of Results of Conducted Measurements:	
Masonry:	
Brick, Clay - Dry	125
Brick, Clay - Moist	126
Concrete (94 lb sack):	
Dry: 5 gal. water; portland cement aggregate ratio: 1/0	127
Moist: 5 gal. water; portland cement aggregate ratio: 1/0.	128
Dry: 6.5 gal. water; portland cement aggregate ratio: 1/0	129
Moist: 6.5 gal. water; portland cement aggregate ratio: 1/0	130
Dry: 8 gal. water; portland cement aggregate ratio: 1/0	131
Moist: 8 gal. water; portland cement aggregate ratio: 1/0.	132
Concrete Block (Featherlite) - Dry	133
Concrete Block (Featherlite) - Moist	134
Limestone, Natural Slab - Dry	135
Limestone, Natural Slab - Moist	136
Mortar (94 lb sack):	
Dry: 6.5 gal. water; portland cement aggregate ratio: 1/1	137
Moist: 6.5 gal. water; portland cement aggregate ratio: 1/1	138
Moist: 6.5 gal. water; portland cement aggregate ratio: 1/3	139
Moist: 9.8 gal. water; portland cement aggregate ratio: 1/3	140
Plaster of Paris - Dry	141
Plaster of Paris - Moist	142
Synthetics:	
Acrylic Plastic (Hysol)	143
Acrylic Plastic (Lucite)	144
Formica	145
Fiberboard - Masonite	146
Phenolic - Linen	147

	Page
Synthetics (continued):	
Phenolic - Paper	148
Vinyl Asbestos Tile	149
Woods:	
Balsawood	150
Birch	151
Cedar	152
Douglas Fir	153
Mahogany	154
Mahogany Paneling	155
Mahogany Trim	156
Oak Flooring	157
Pine - Yellow	158
Plywood - Fir	159
Miscellaneous Materials:	
Asbestos Shingle	160
Beeswax - Dark	161
Beeswax - Light	162
Cardboard	163
Glass	164
Pasteboard, Corrugated - Dry	165
Pasteboard, Corrugated - Moist	166
Tar Paper	167

HANDBOOK OF SHIELDING

PART II

Introduction:

This handbook of shielding has been compiled to assist building design architects and engineers. The handbook section is divided into three main groups. The radiated measurement section contains a group of graphs which show the measured magnetic field attenuation for a variety of building materials. This selection of materials is a cross-section of those which have shown measurable shielding characteristics for magnetic fields in the 10 Hz to 50 KHz range. Since the geometry of a building can measurably influence its shielding characteristics, the values of shielding for any material shown in the graphs should be used only as a guide, as the same material in different configurations will show different degrees of shielding. Those materials classed as dielectrics which do not show a measurable shielding effectiveness in the 10 Hz to 50 KHz range were not graphed.

The graphs presented in this section are plots of shielding effectiveness (magnetic field attenuation) versus frequency. Those graphs that describe the material as being in "sheets" do not show as much shielding as would have been obtained by measuring SE of enclosures of the same material, but the graphs do give an indication of the relative merits of several thicknesses of material. The accuracy of the measured SE falls off as the curves flatten out at the high frequency end of the curves.

The data from radiated measurements has been grouped by the type of material measured. Under each type of material, curves are presented for different structural forms such as solid sheet, screens, frames, etc.

In some cases, a diagram explaining the measurement configuration has been included immediately ahead of the data which it concerns. The attenuation curves for the various metals strongly indicates that the rate of increase of shielding with frequency is proportionate to the electrical conductivity of the material. In cases where ferrous materials exhibit shielding at low frequencies, the shielding is nearly always proportional to the volume of the material in the shield.

Conducted measurements are compiled immediately following the radiated measurement graphs. The first table lists the resistivities of conductive materials compared with copper as a standard of 1.00. The electrical conductivity or its reciprocal,

resistivity of a nonmagnetic building material gives more indication of its shielding ability for low frequency fields than any other parameter.

The tables of results of conducted measurements on dielectric materials show the dielectric constant, dielectric loss factor, and the calculated SE caused by absorption of electromagnetic energy within the substance. The dielectric material conducted tests are presented for a variety of the most common building materials. Calculations of the SE have been made for 4 frequencies in each table. These frequencies are 100 Hz, 1 KHz, 1 MHz, and 1 GHz. It can be seen from these tables that very little shielding is offered by dielectric materials at frequencies below 1 GHz.

Although the SE produced by dielectric materials is slight, the tables can be helpful in showing the best dielectric shielding materials for frequencies above 1 GHz.

Several of the dielectric measurements at 10 Hz and 50 Hz have been omitted. These measurements resulted in very broad nulls on the capacitor bridge because of the very high output impedance to the null indicator at these frequencies. The use of a field effect transistor source follower amplifier helped overcome the bridge loading in some cases, but with high dielectric factors and loss tangents the instrumentation capability was limited. The double dash (--) in the columns of some of the Results of Conducted Measurements indicate those measurements which resulted in broad nulls.

Samples listed as moist were exposed to a saturated atmosphere for 1 day prior to measurement. Dried samples were baked at 140°F for approximately 20 hours prior to measurement. Due to their hygroscopic nature, some of the conducted test samples began to absorb moisture rapidly after they were placed in the sample holder. The parameters of oven-dried samples were not measured above 100 MHz for two reasons. First, the samples absorb water vapor from the atmosphere quite rapidly. At the higher frequencies, the change in moisture content was rapid enough to make bridge balancing difficult because of the changing parameters. Also, it was found that a material's electrical parameters under real life conditions are equivalent to those of the material exposed to moisture. The higher moisture content usually gives the best shielding so the parameters of the dried samples were not measured above 100 MHz.

All samples of cement, mortar, and concrete which were used in conducted measurements are described by a cement-aggregate ratio. A 1/0 ratio means that only portland cement was used. A 1/1 ratio means that one part portland cement was mixed with one part sand. Although most concrete mixes are typically 1/2/3 where the third number

represents the quantity of heavy aggregate, this type could not be used in making the small samples for conducted measurements. Portland cement without aggregate is rarely used in construction, but pure cement samples were prepared to show the electrical characteristics of the hardened cement alone without influence of the aggregate.

Beeswax (both light and dark) are not considered to be building materials. They are, however, often used with paper and tar materials to create a moisture barrier. For this reason, these materials were included in the conducted measurements.

Section 1

GENERAL CONCLUSIONS

The following list of conclusions is the result of the measurement study on the SE of building materials.

1. Low frequency magnetic fields are the most difficult and most expensive to shield.
2. Shielding of low frequency magnetic fields below 1 KHz is a phenomenon dependent on the volume and magnetic permeability of material. Shielding of low frequency magnetic fields is accomplished by distortion of field lines away from the interior of an enclosure. This type of shielding is in contrast to that caused by field regeneration in a conductive medium, or wave absorption within the medium.
3. Streamlining a magnetic shield along the incident field path decreases the field concentration at the interior of the shield.
4. Magnetic field frequencies above 1 KHz can effectively be impeded by a barrier or enclosure having a high electrical conductivity.
5. The presence of conductive loops in a plane perpendicular to the field direction will produce the best shielding for frequencies above 1 KHz.
6. The use of reinforcing steel in concrete structures will not offer much shielding unless the bars are interconnected into a lattice network.
7. The combination of a good shielding material and a poor shielding material do not give much more shielding than the good material alone. For example, the SE of reinforced concrete at frequencies below 1 GHz is only a little better than the SE of the reinforcing steel alone.
8. A combination of materials in a shield for magnetic fields from 10Hz to 50 KHz never showed any greater shielding properties than the sum of the SE of the individual materials.
9. Good magnetic continuity between reinforcing lattice members is required for effective shielding below 1 KHz.

10. Low resistance electrical paths are necessary between interconnecting members of reinforcing rods for effective shielding above 1 KHz because most shielding above 1 KHz is accomplished by field regeneration.

11. A complete enclosure makes a better shield than an enclosure which is open on one side or more (see Figs. 45, 46 and 47 of the following Section).

12. Several layers of thin conductive material which are separated by nonconductive layers make a better shield than a single layer heavier material.

13. Screen wire and hardware cloth enclosures make reasonably good shields above 10 KHz but will begin to lose their shielding qualities in the ultra high frequency range. This loss of shielding effectiveness is caused by leakage through openings in the mesh. Leakage is higher for the larger opening mesh at any given frequency.

14. At an increase in structural cost, expanded steel sheets may be substituted for reinforcing steel rods in concrete. This form of steel, although costlier than steel rods, is a more effective shield for low frequency magnetic fields. Expanded steel sheets require less interconnecting welding than would be required in using steel rods.

15. Lighter weight steel lath may be used in a plaster wall or on the surface of walls, ceilings and floors to enhance the shielding characteristics of a structure. The thinner material lacks sufficient mass to be a good shield at frequencies below 1000 Hz, but the thin material is quite efficient at higher frequencies.

16. The presence of metal fixtures as furniture in an enclosure can cause apparent shielding which is not homogeneous throughout the enclosure. This can give misleading results when measuring shielding effectiveness of a building or room.

17. Radiated measurements on ferromagnetic enclosures show a greater SE of the enclosure when the field source is inside and the sensor outside than with the source outside and sensor inside. A field source which is fully enclosed completes a magnetic loop much like a transformer core. This closed magnetic path confines the fields to the enclosure walls and the interior of the enclosure. The more complicated geometry which exists when the field source is outside of the enclosure does not restrict the magnetic field to a closed ferromagnetic circuit; therefore, less shielding is effected in the latter case.

18. Radiated measurements on plane surface barriers (single walls) of conductive materials indicate greater shielding properties against time varying magnetic fields when the source or the sensor is close to the conductive barrier (see Fig. 10 of Part I, pg. 16).

19. Materials which have a high electrical conductivity are good shields at frequencies above 1 KHz.

20. The materials with the lowest resistance are the best shields. Copper and aluminum are better than stainless steel and Monel.

21. Dielectric materials offer no significant shielding at frequencies below 100 MHz.

22. The best shielding in dielectric materials is produced by a high dielectric loss factor and a low dielectric constant.

23. Porous materials such as unglazed ceramics and lightweight wooden materials are most likely to change their shielding characteristic with environmental changes in moisture.

Section 2

GRAPHED RESULTS OF RADIATED MEASUREMENTS

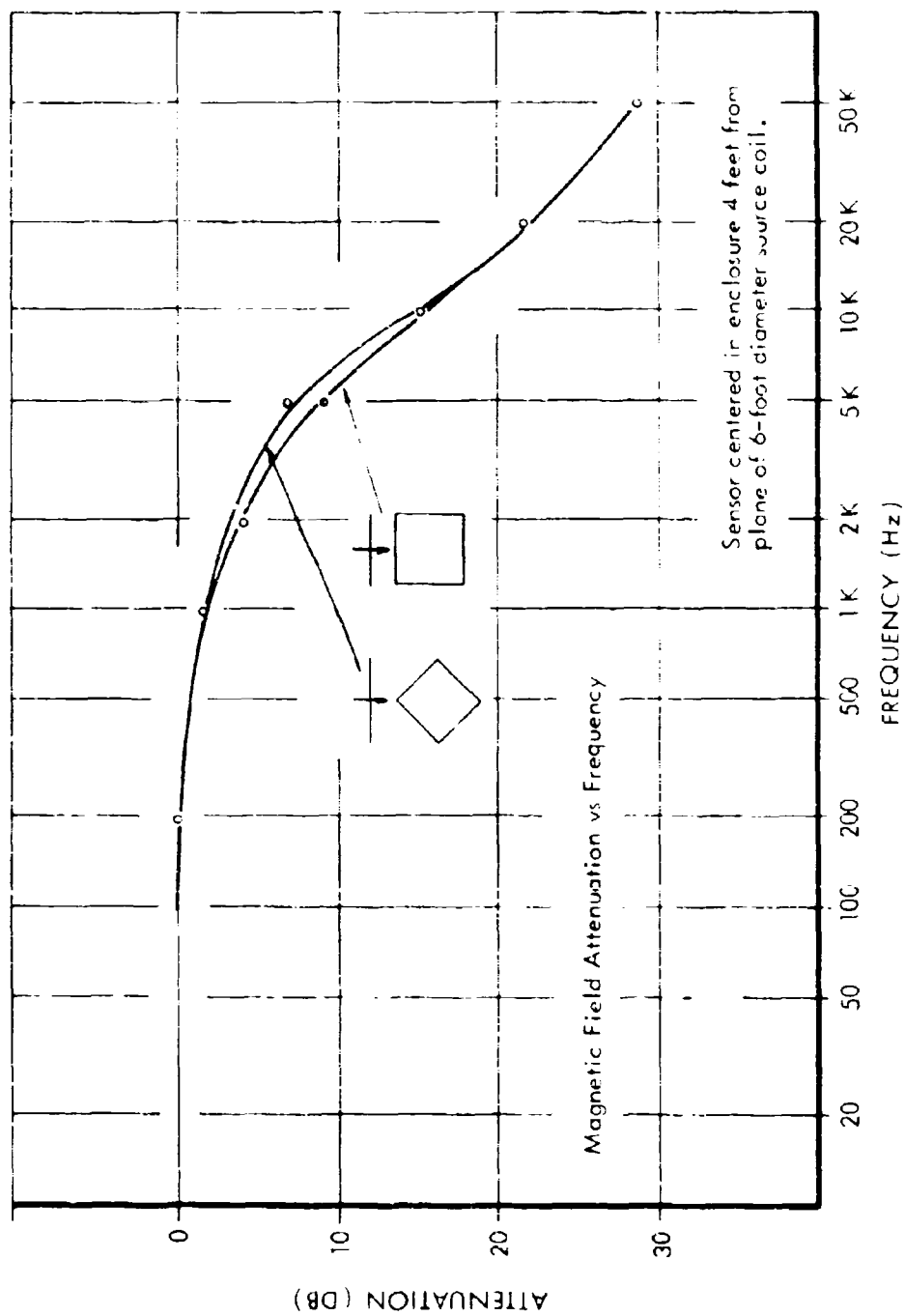


Fig. 1 SE of 2-Foot Cubical Enclosure of Single-Layered 16 x 18 Mesh Copper Screen
with Edges Lapped and Stapled; Field Orientation Shown

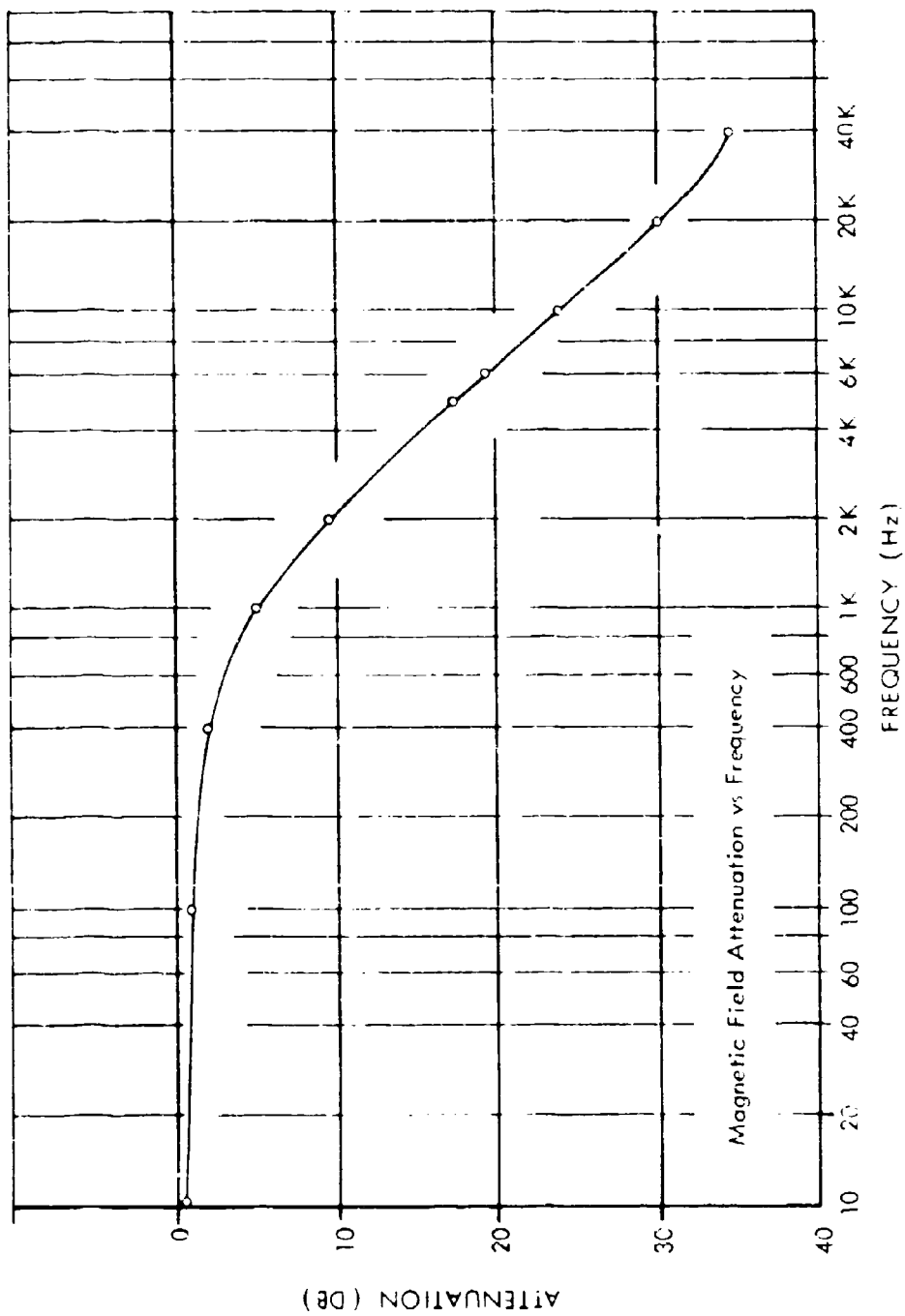


Fig. 2 SE of a 2 1/2 ft x 2 ft x 1 1/2 ft Three-Layer 16 x 18 Mesh Copper Screen Enclosure,
Each Layer Separated by 1-Inch Space; All Seams Soldered

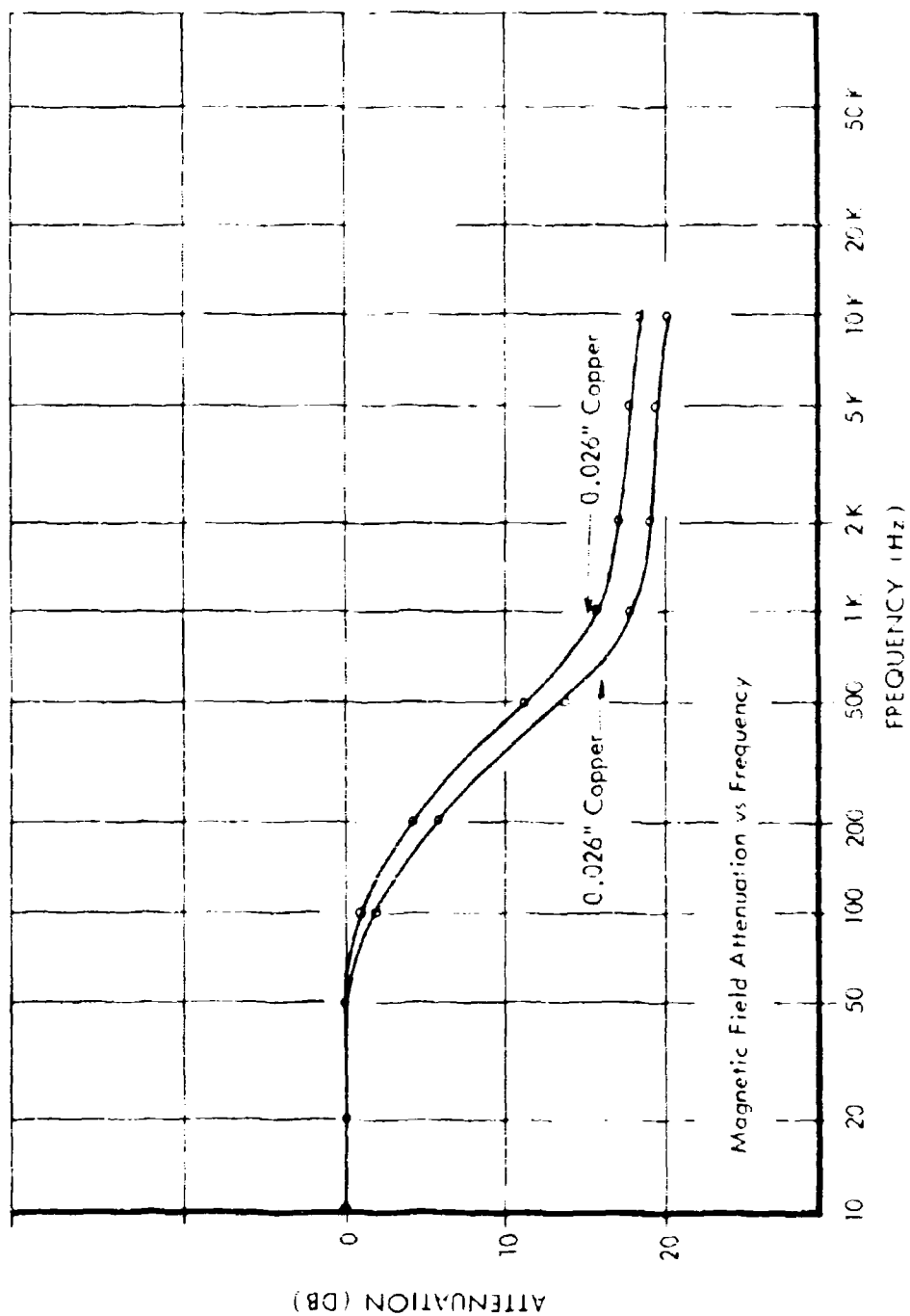


Fig. 3 Curves of SE of Two 1-Foot Square Copper Sheets
(see Fig. 18, pg. 96, for Composite Data Presentation)

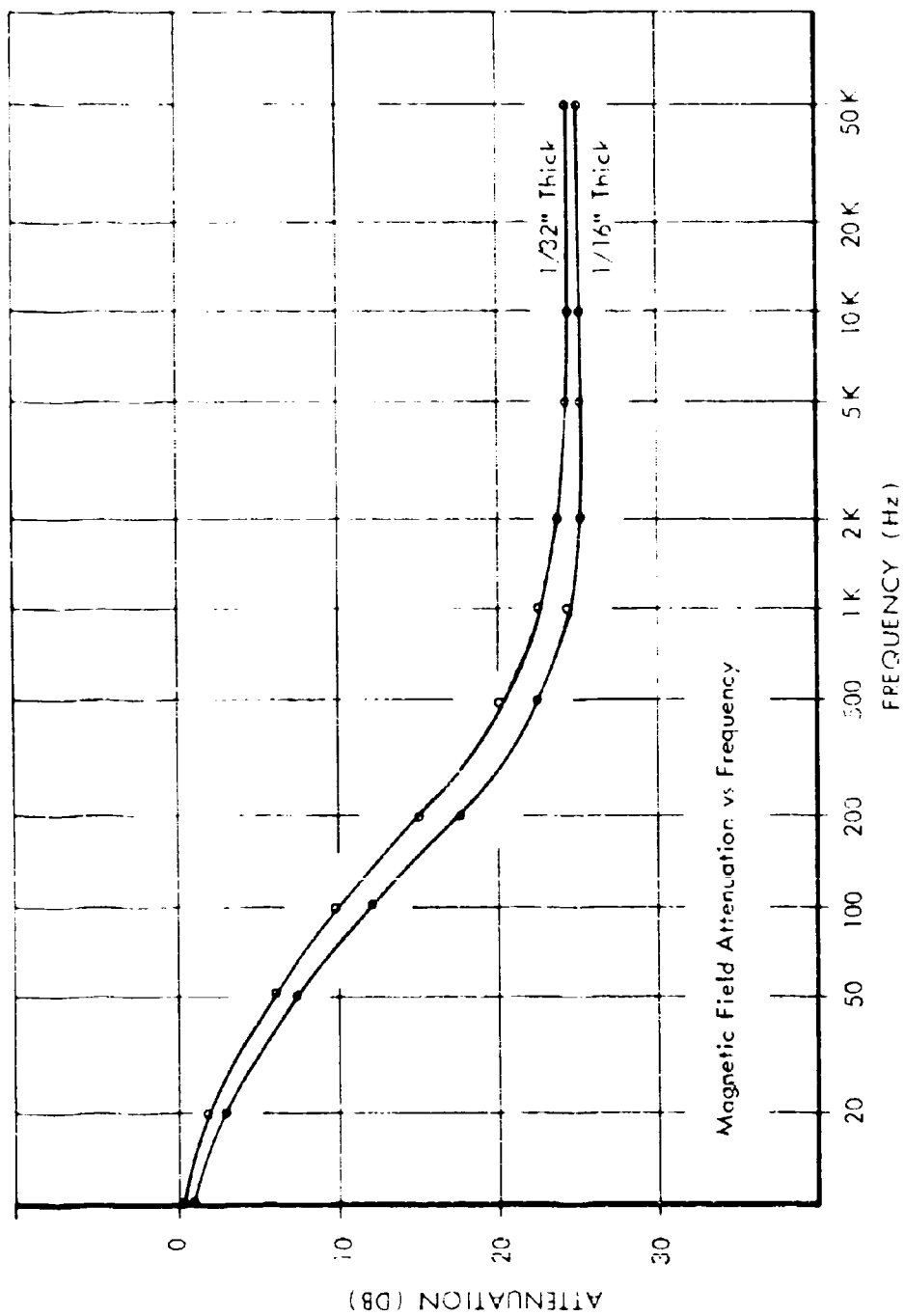


Fig. 4 SE of 3 x 8-Foot Copper Sheets

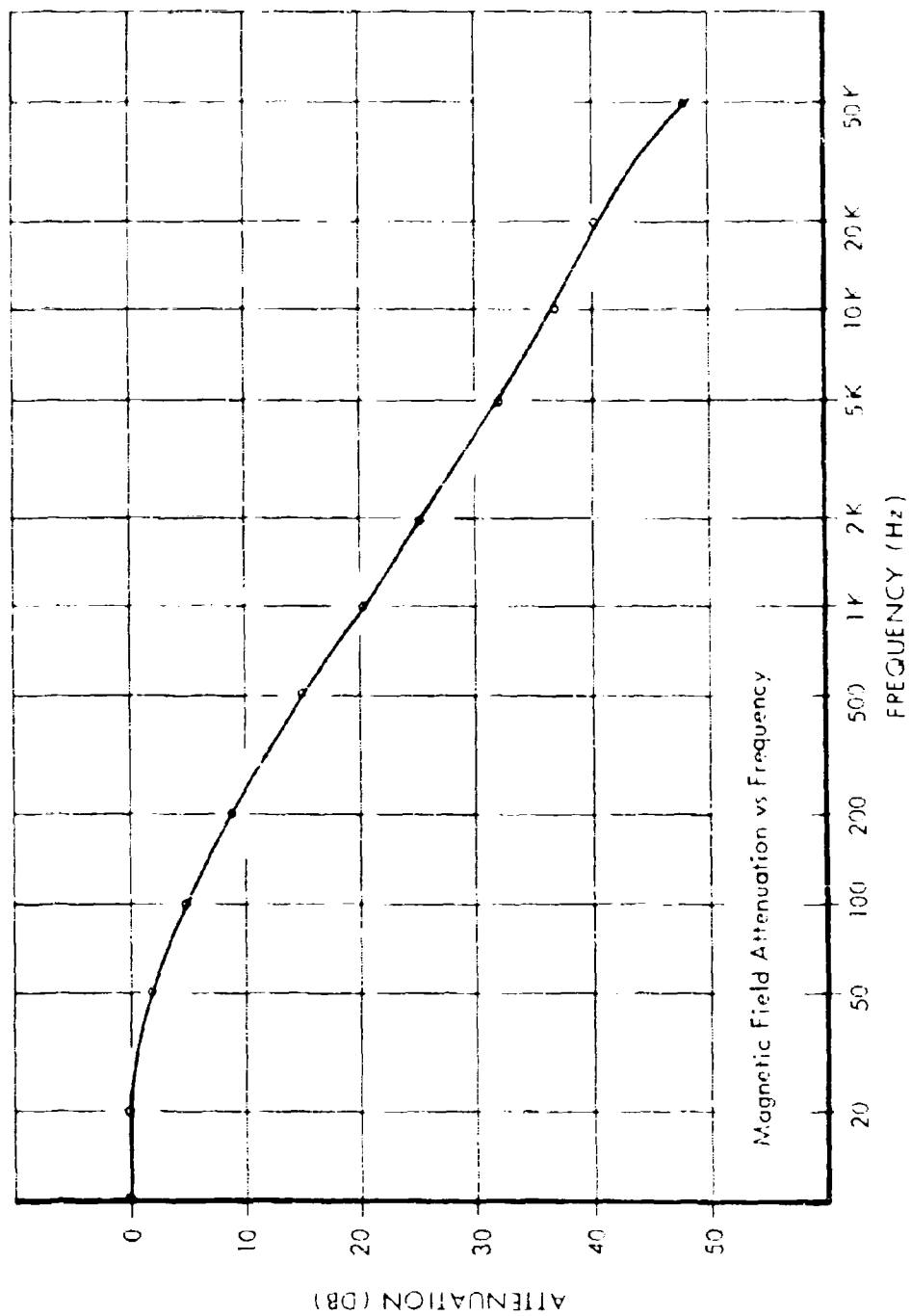


Fig. 5 SE of a 1-Foot Cubed .026-Inch Wall Copper Box, Seams Soldered

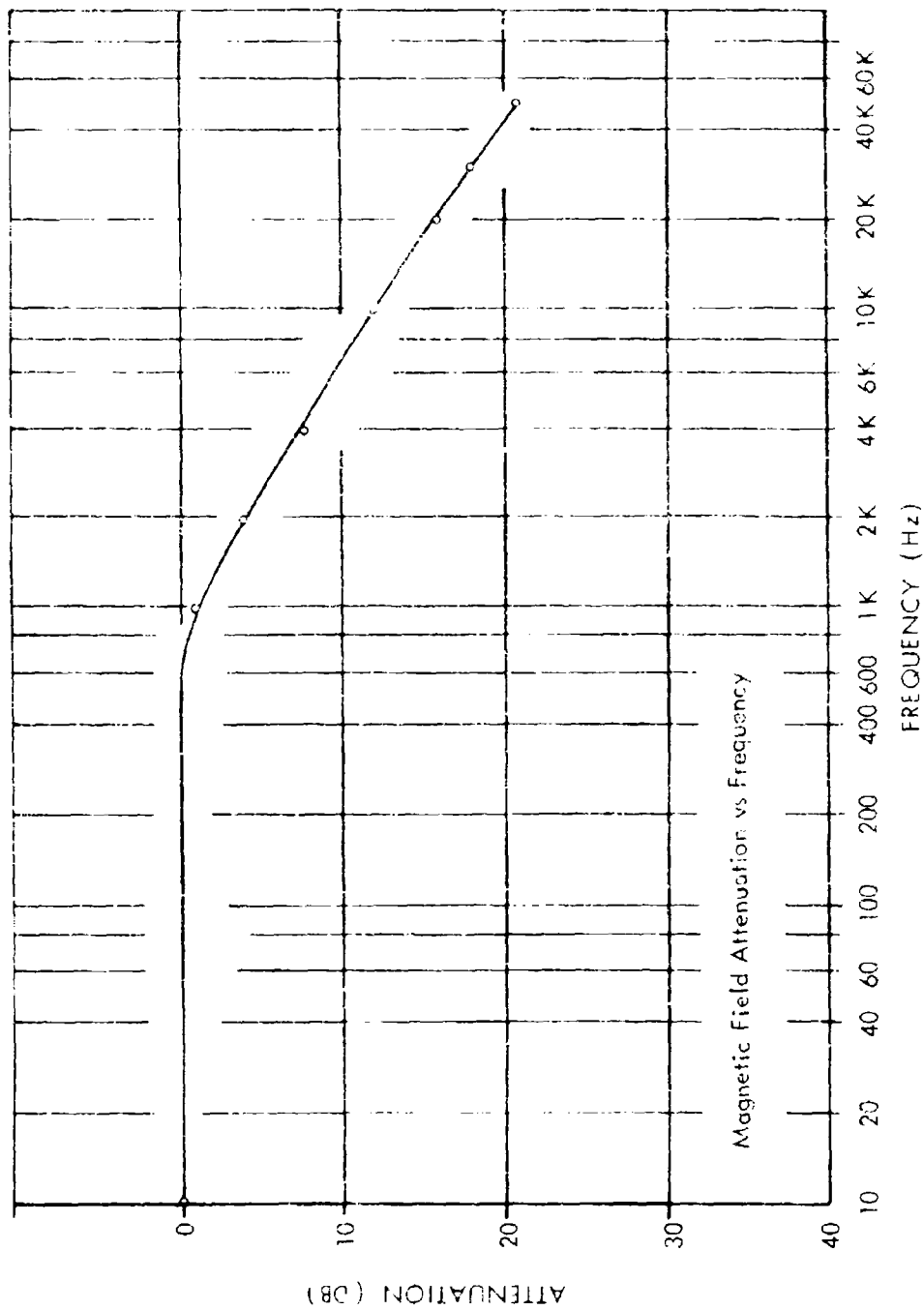


Fig. 6 SE of 2-Foot Cubical Enclosure of Single-Layered 18 x 16 Mesh:
Aluminum Wire Screen, Seams Lapped and Stapled

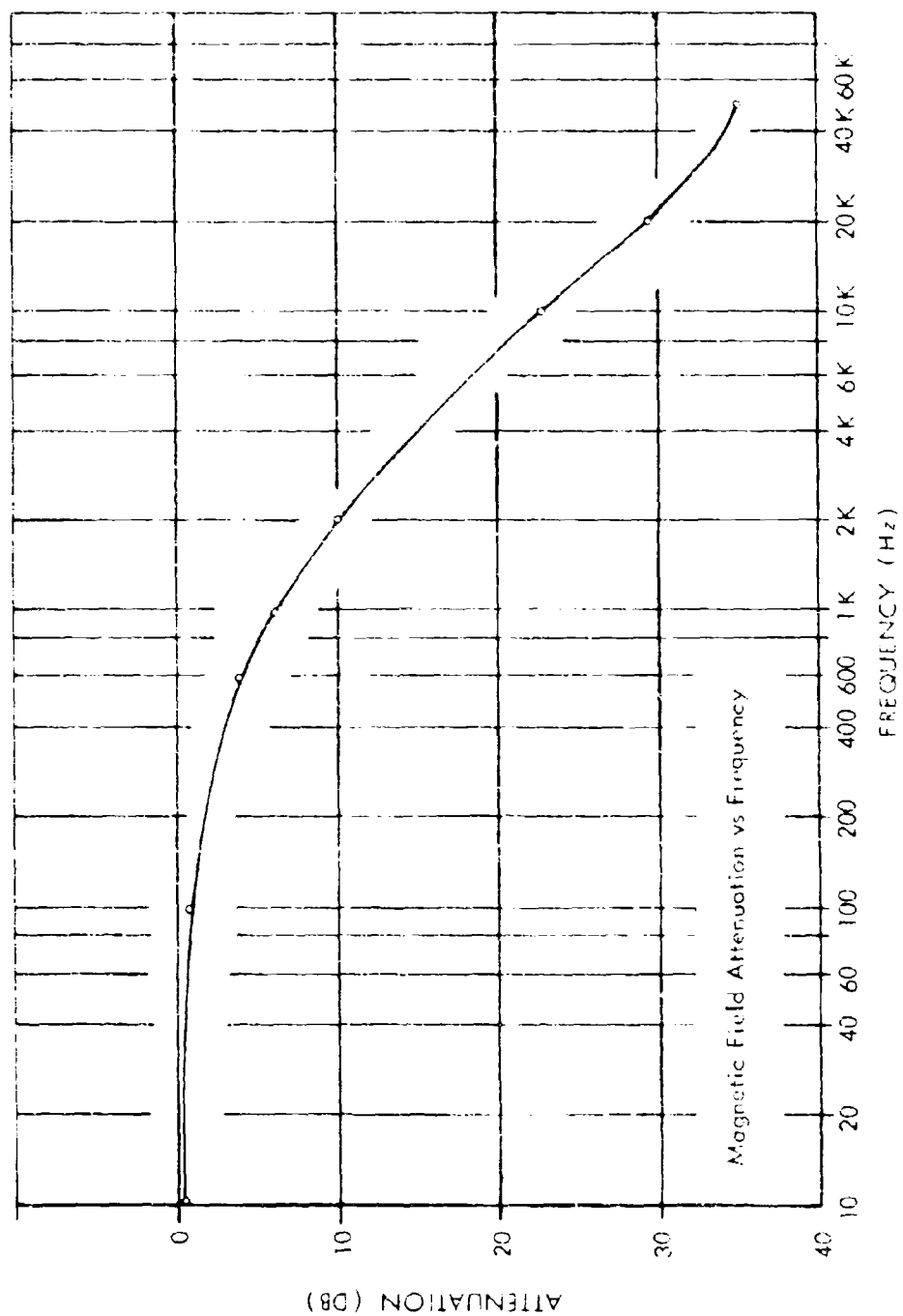


Fig. 7 SE of 0.002-Inch Aluminum Foil, Lapped and Stapled to Inside and Outside Surfaces
of a 2-Foot Cubed, 3/4-Inch Plywood Enclosure

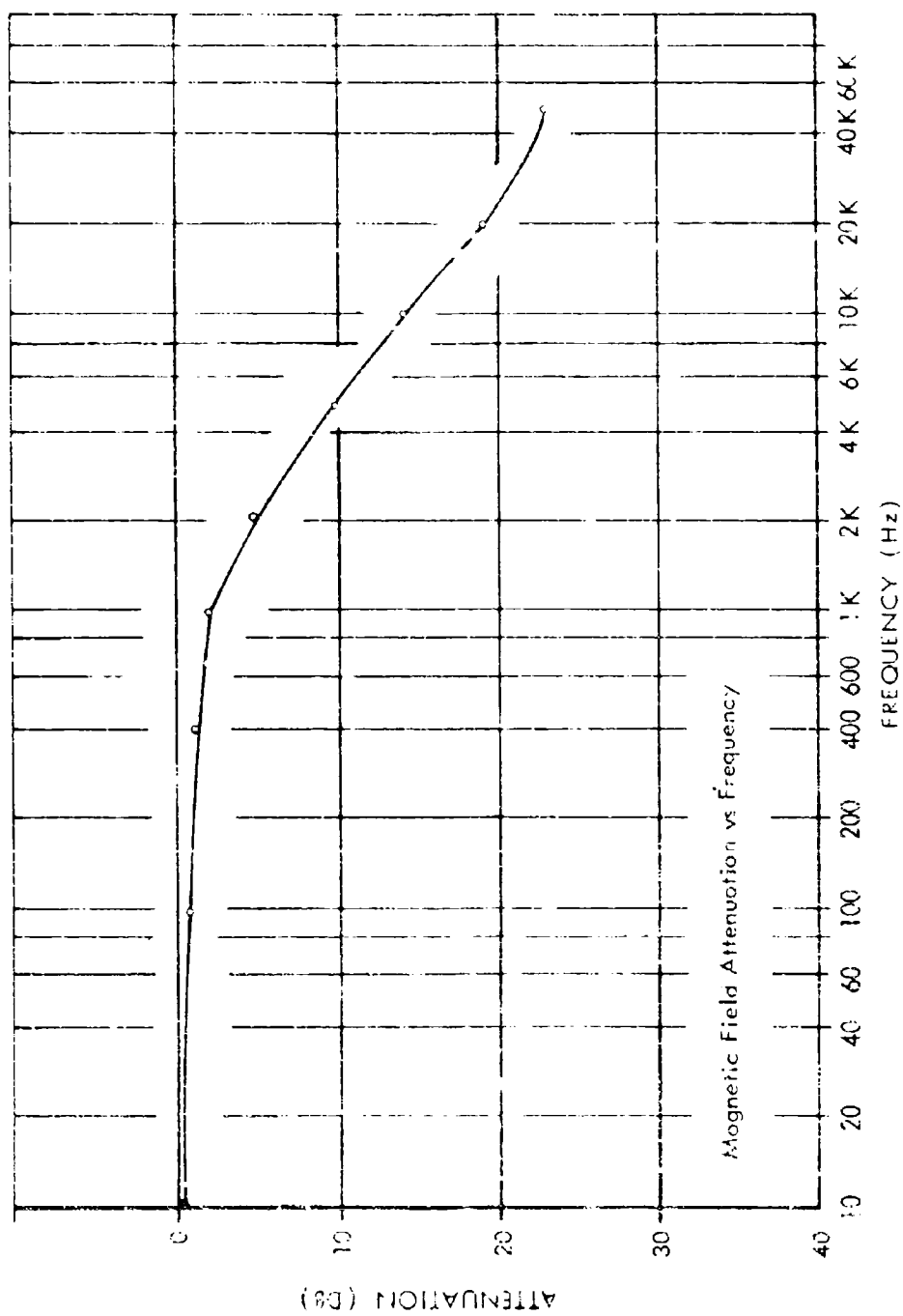


Fig. 8 SE of One Layer of 0.002-Inch Aluminum Foil in a 2-Foot Cubed Configuration
with Seams Lapped and Stapled

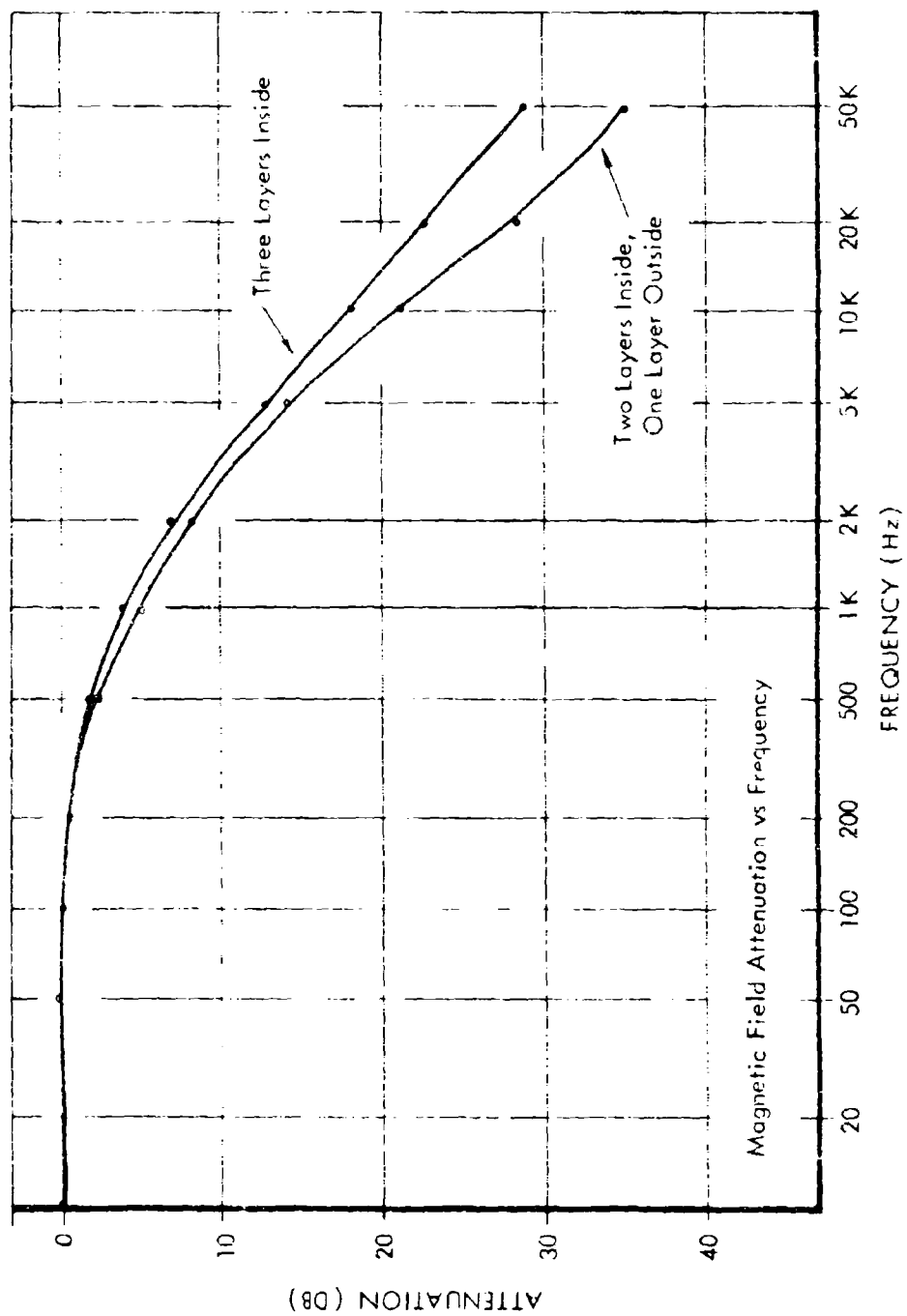


Fig. 9 Comparison of SE of Two Configurations of .0014-Inch Aluminum Foil Lapped and Stapled to the Surfaces of a 2-Foot Cubed, 3/4-Inch Plywood Enclosure

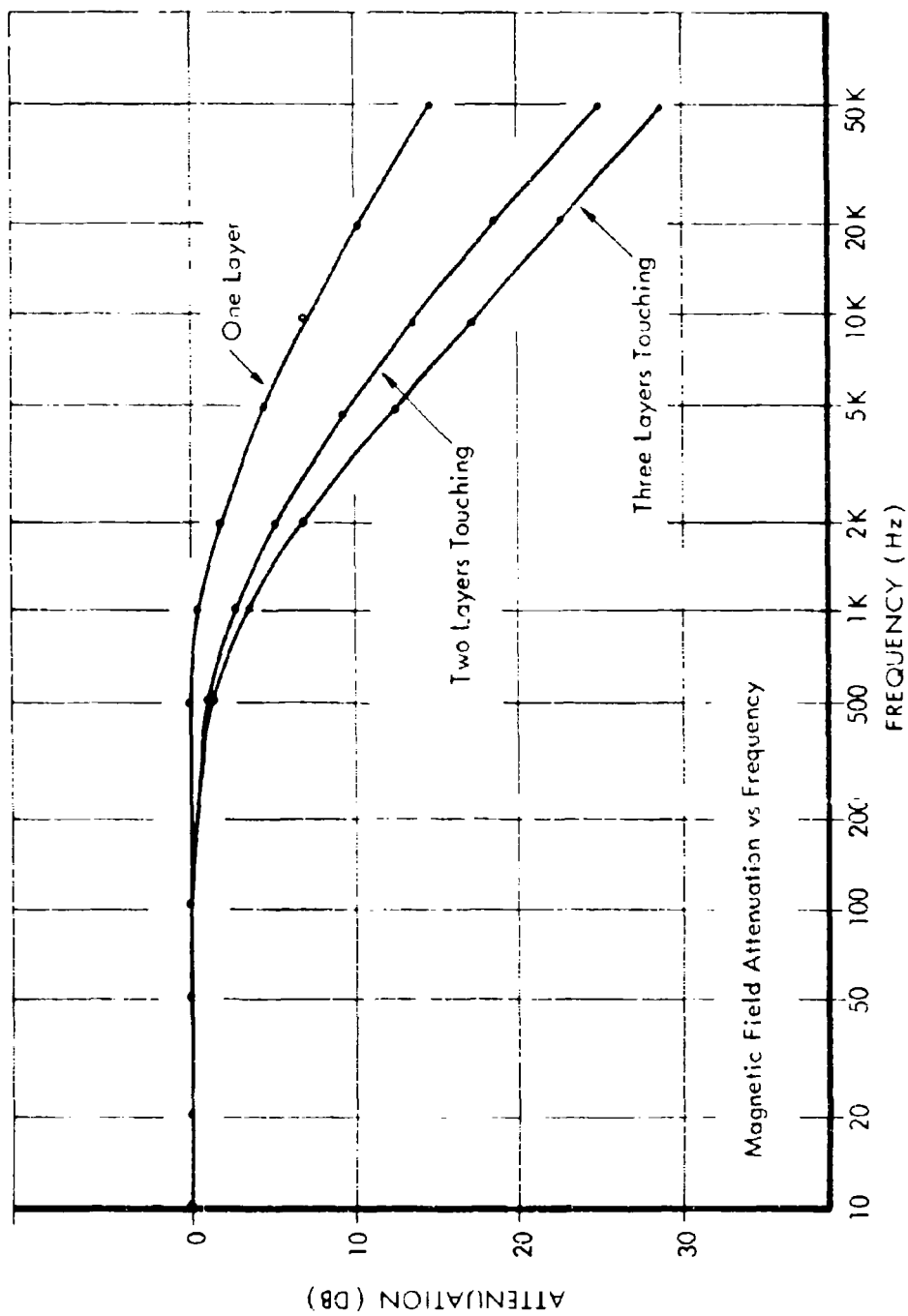


Fig. 10 Comparison of SE for Adjacent Layers of .0014-Inch Aluminum Foil, Seams Lapped and Stapled, Lining a 2-Foot Cubical Enclosure

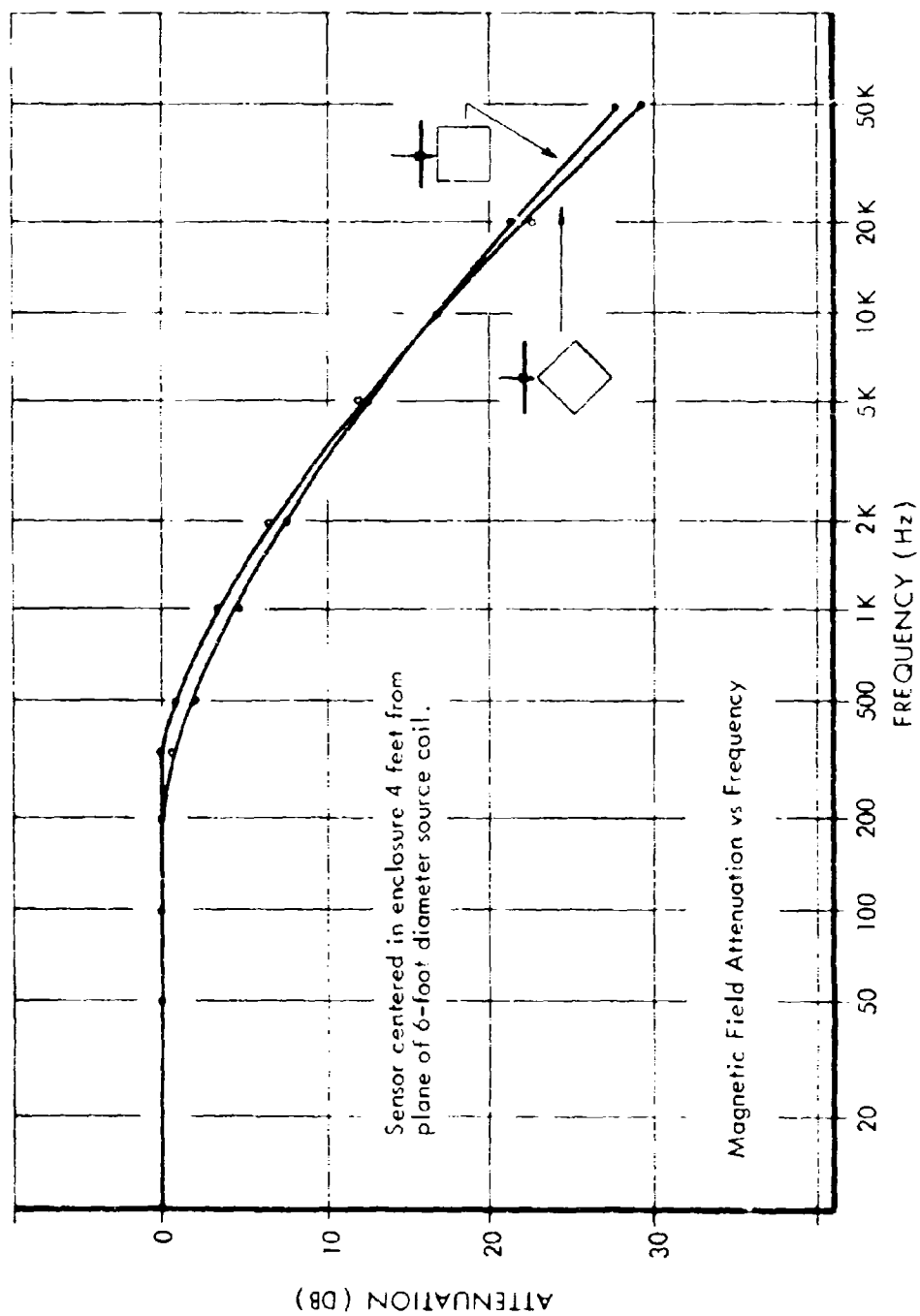


Fig. 11 SE of a 2-Foot Cubed Enclosure of Three Adjacent Layers of .0014-Inch Aluminum Foil, Seams Lapped and Stapled; Field Orientation Shown

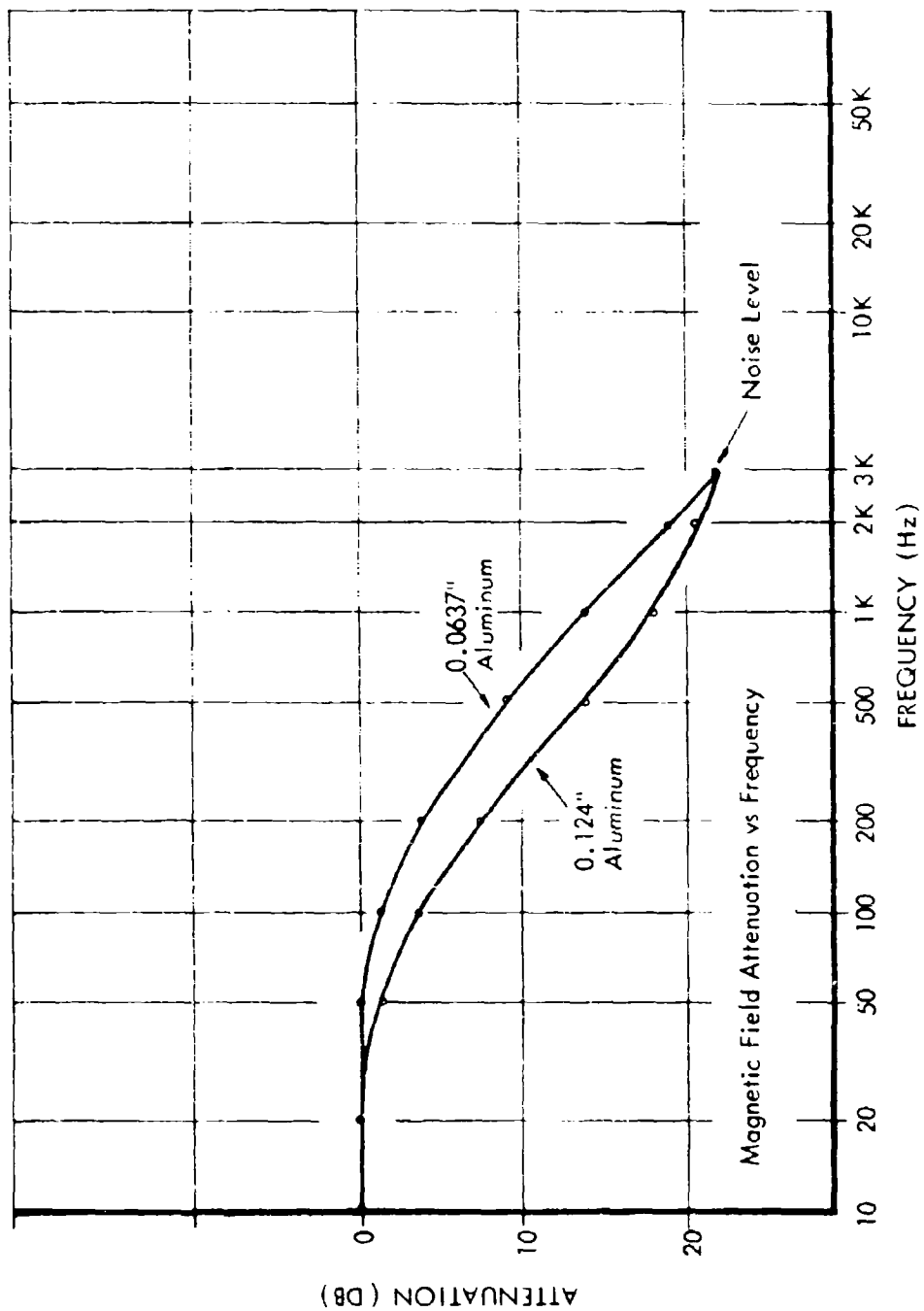


Fig. 12 Curves of SE of Two 1-Foot Square Aluminum Sheets
(see Fig. 18, pg. 95, for Composite Data Presentation)

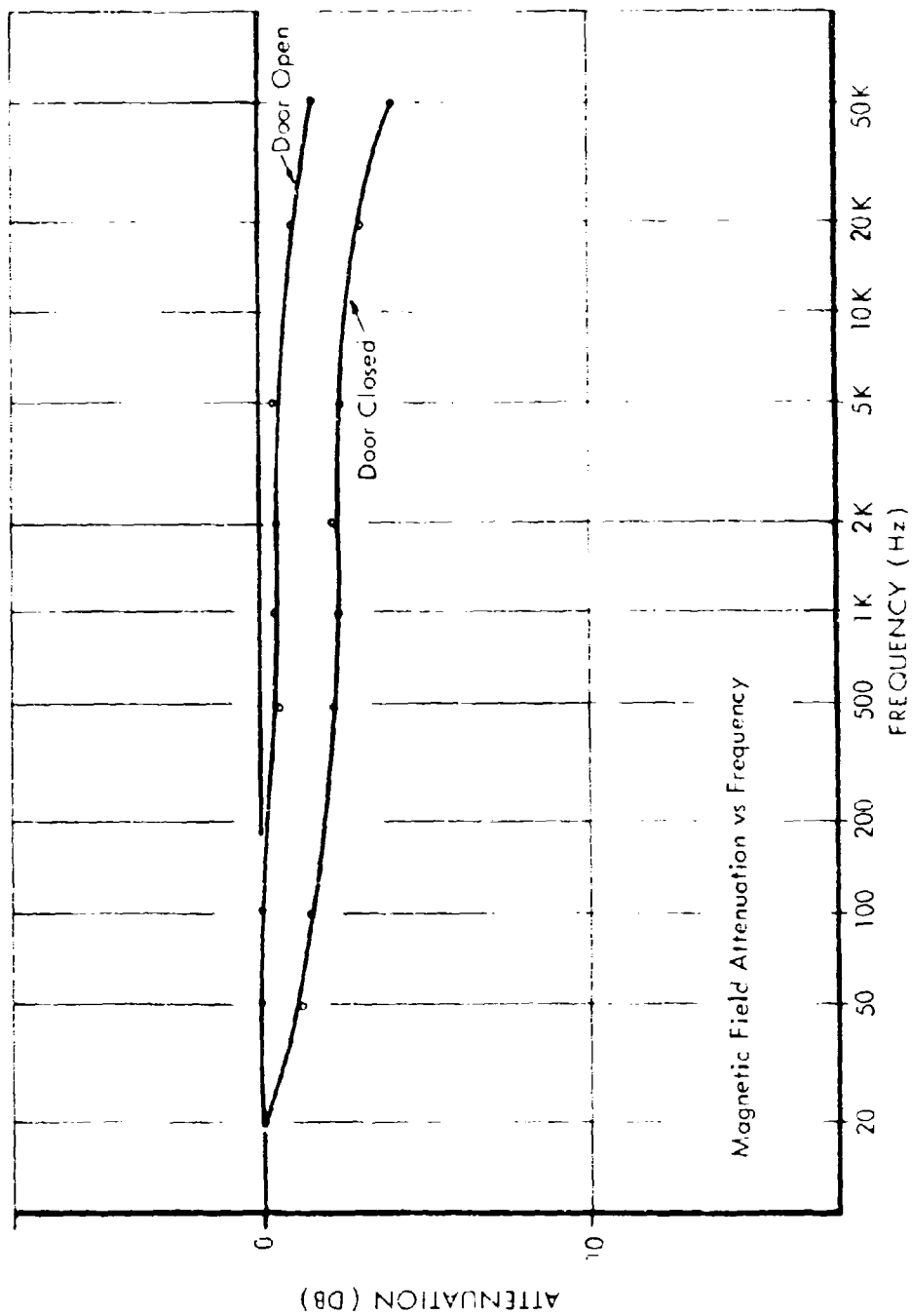


Fig. 13 SE of Plate Glass Door Bordered by an Aluminum Framework

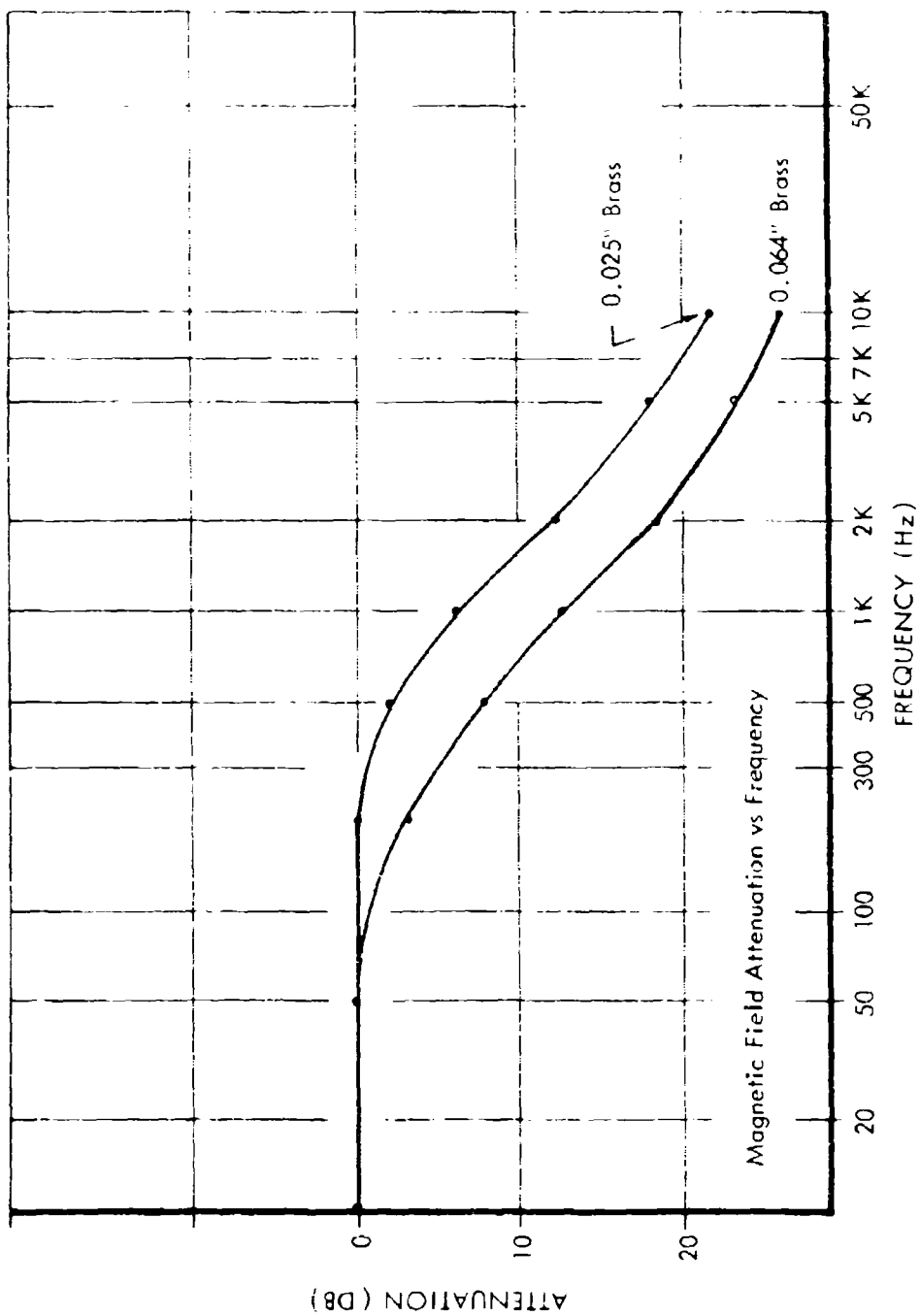


Fig. 14 Curves of SE of Two 1-Foot Square Brass Sheets
(see Fig. 18, pg. 96, for Composite Data Presentation)

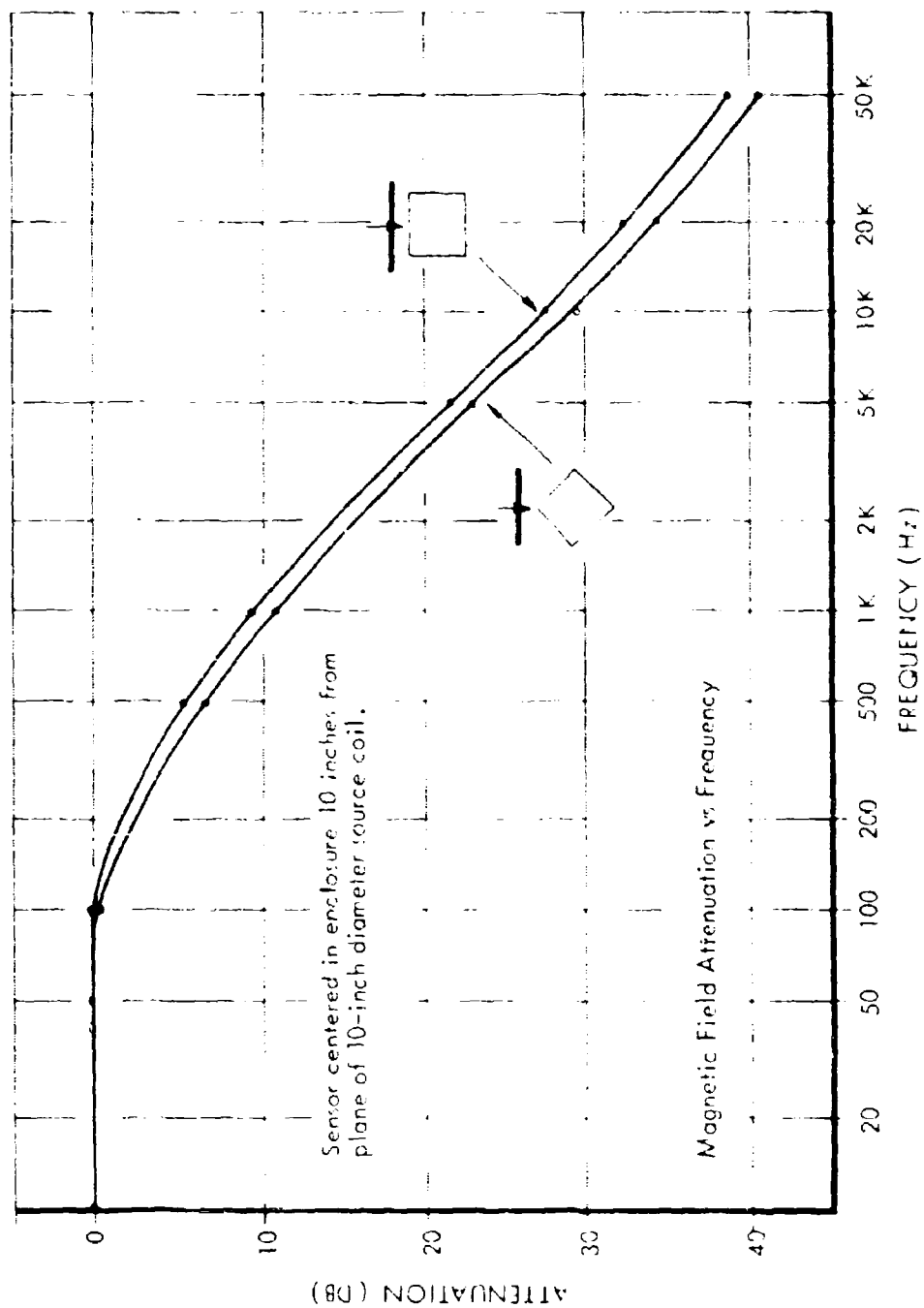


Fig. 15 SE of a 1-Foot Cubed Brass Enclosure Having a 0.025-Inch Wall Thickness with Soldered Seams; Field Orientation Shown

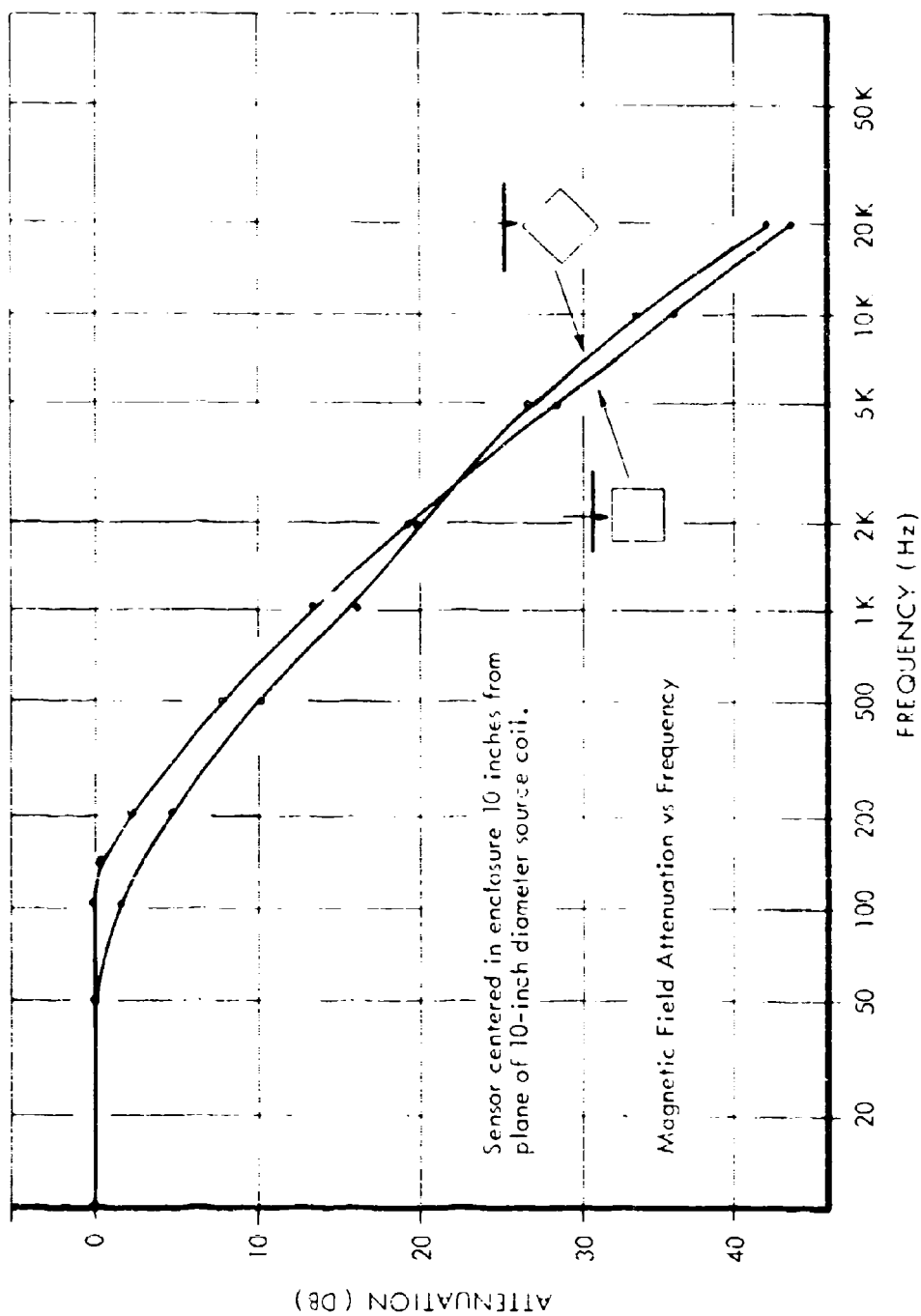


Fig. 16 SE of a 1-Foot Cubed Brass Enclosure Having a 0.064-Inch Wall Thickness
with Soldered Seams, Field Orientation Shown

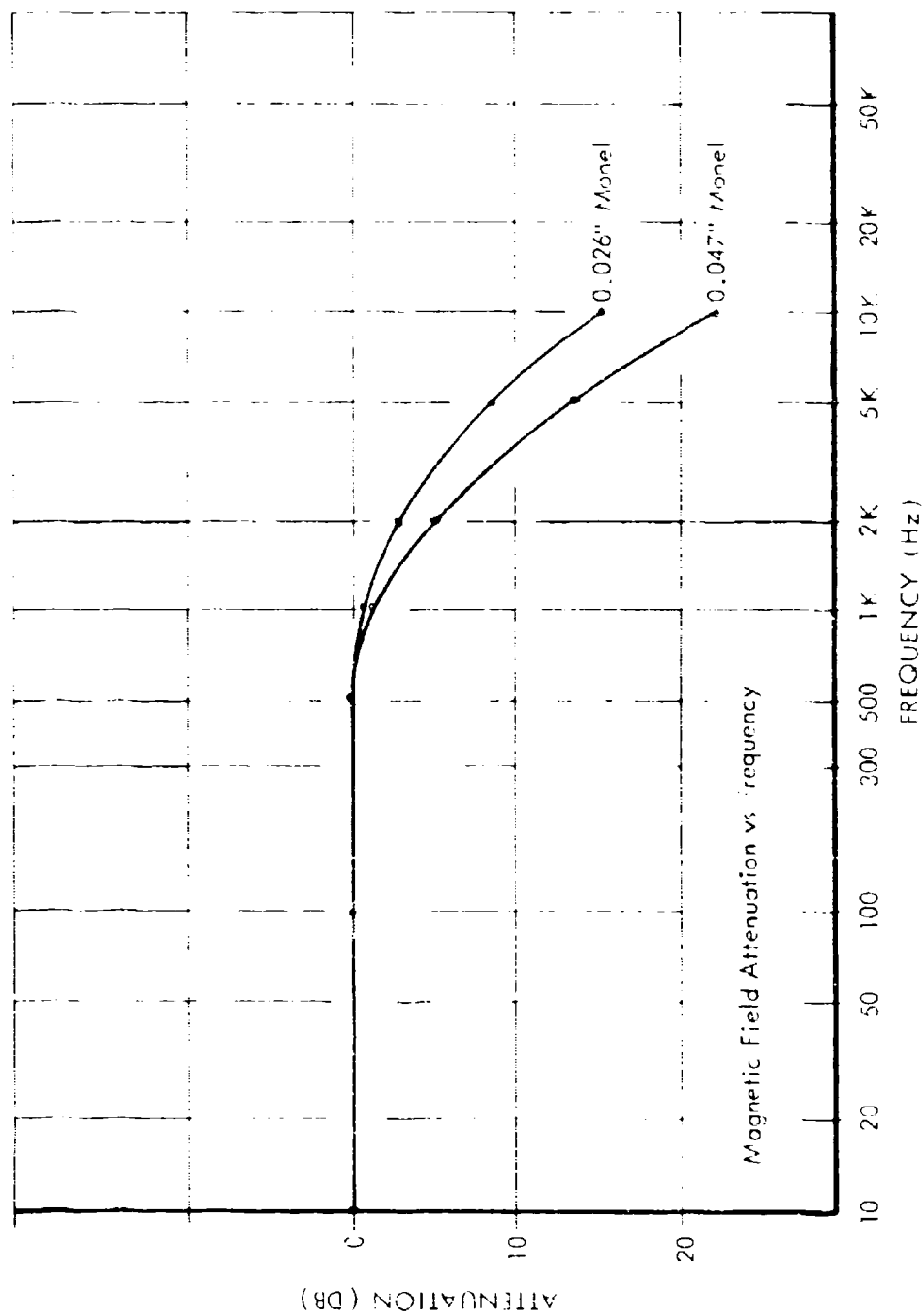


Fig. 17 Curves of SE of Two 1-Foot Square Monel Sheets
(see Fig. 18, pg. 96, for Composite Data Presentation)

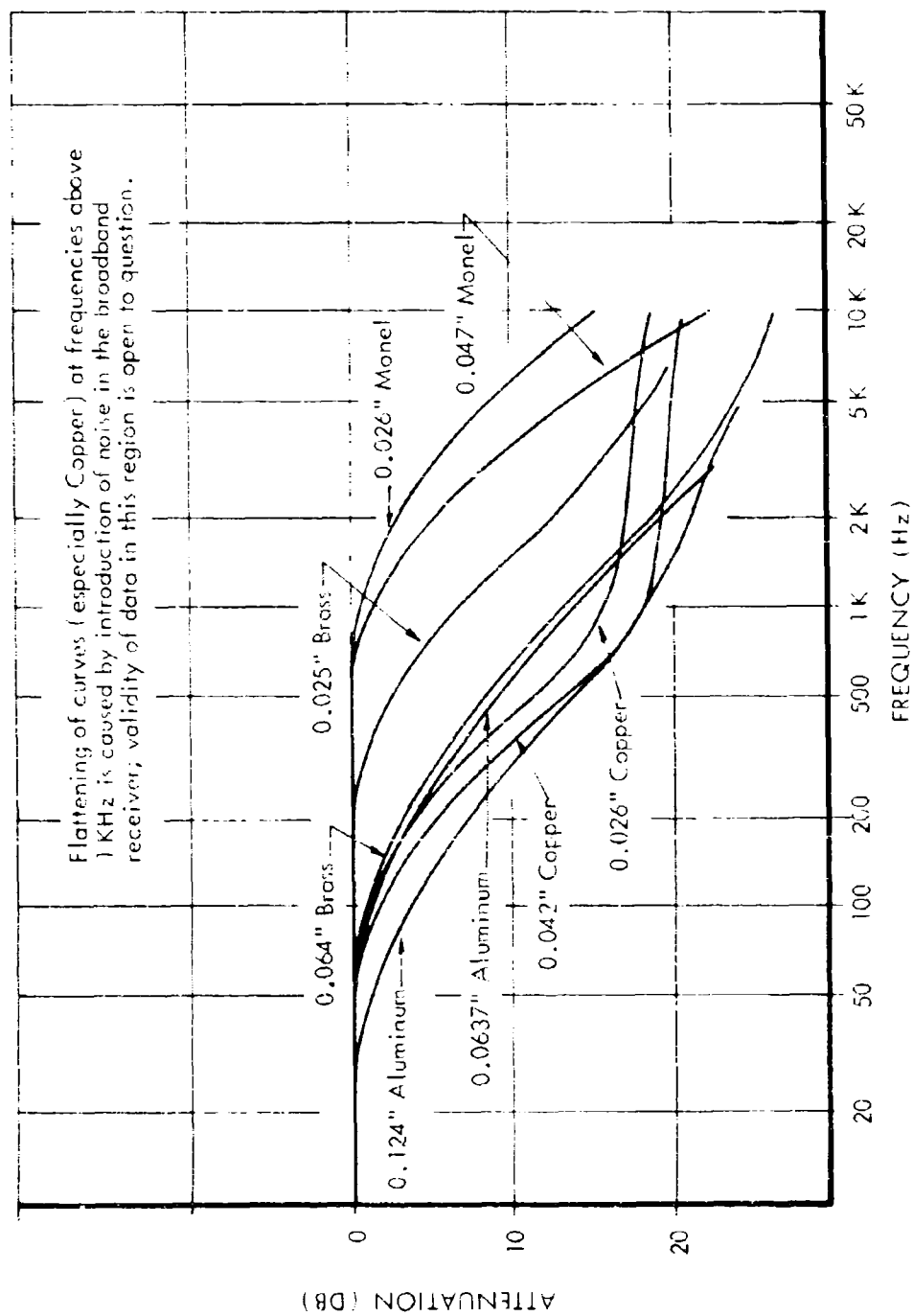


Fig. 18 A Composite Data Presentation of SE of 1-Foot Square Sheets of Various Materials

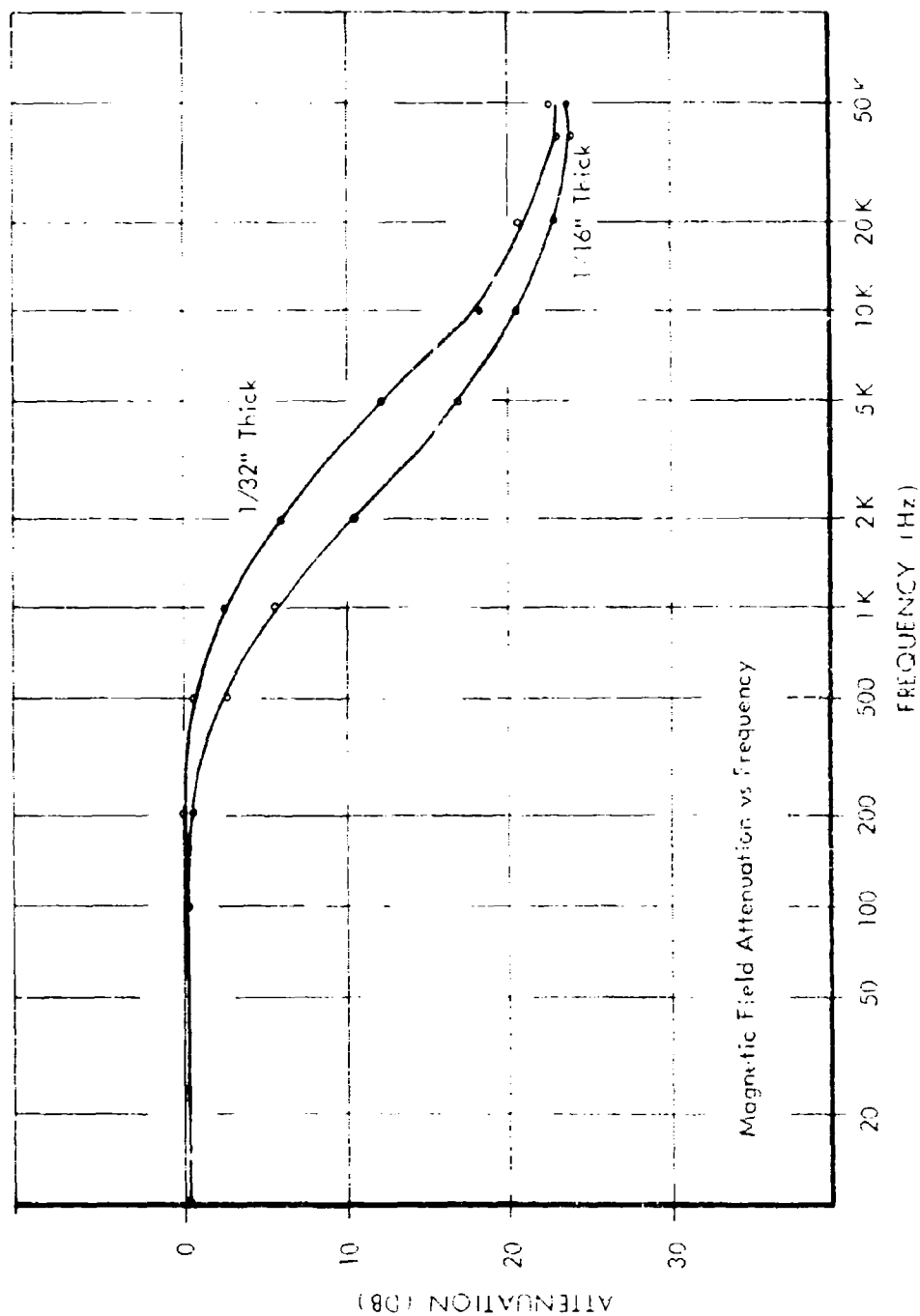


Fig. 19 SE of 3 x 3-Foot Magnet Sheets

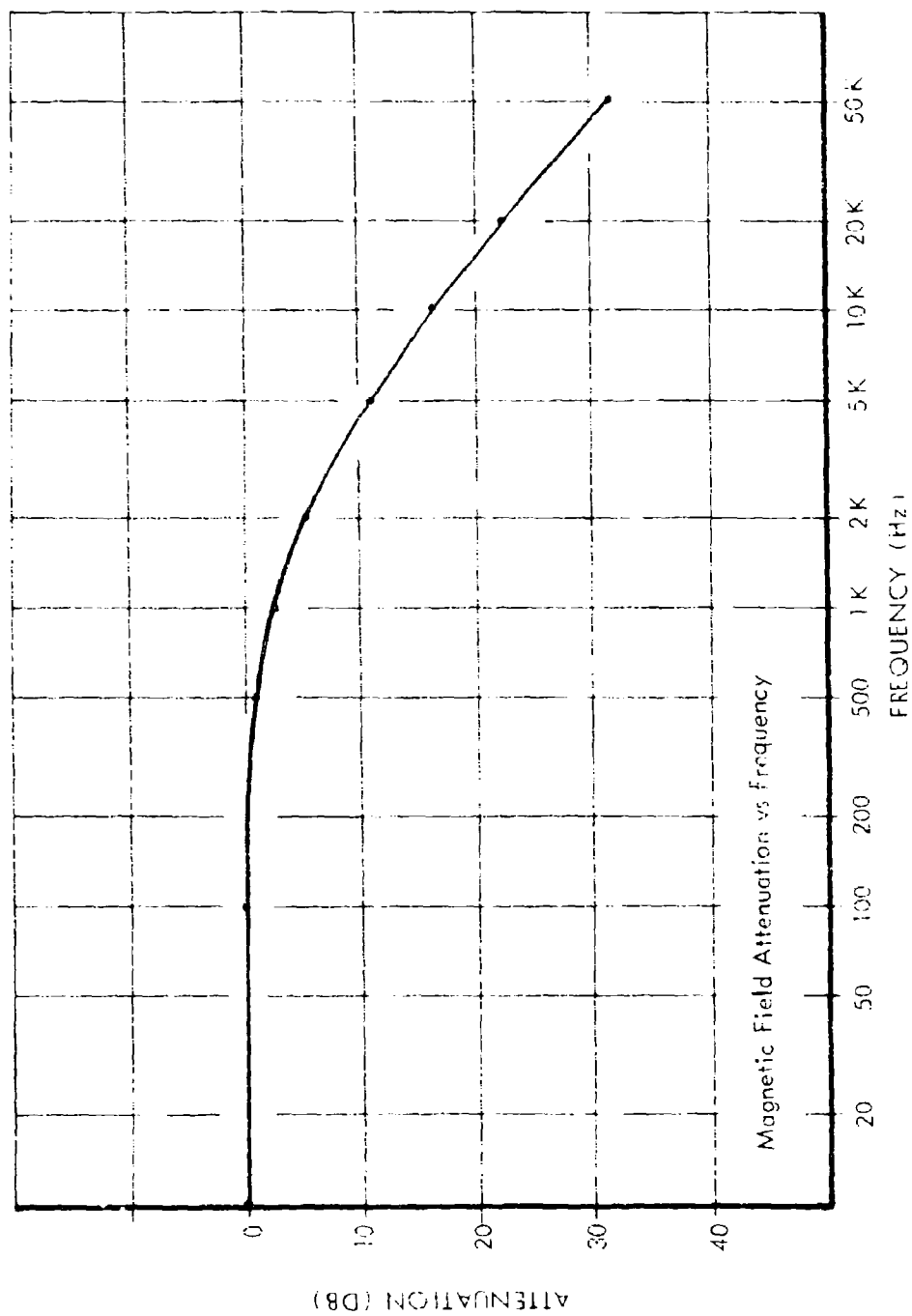


Fig. 20 SE of a 1-Foot Cubed Monel Enclosure Having a 0.026-Inch Wall Thickness
with Soldered Seams

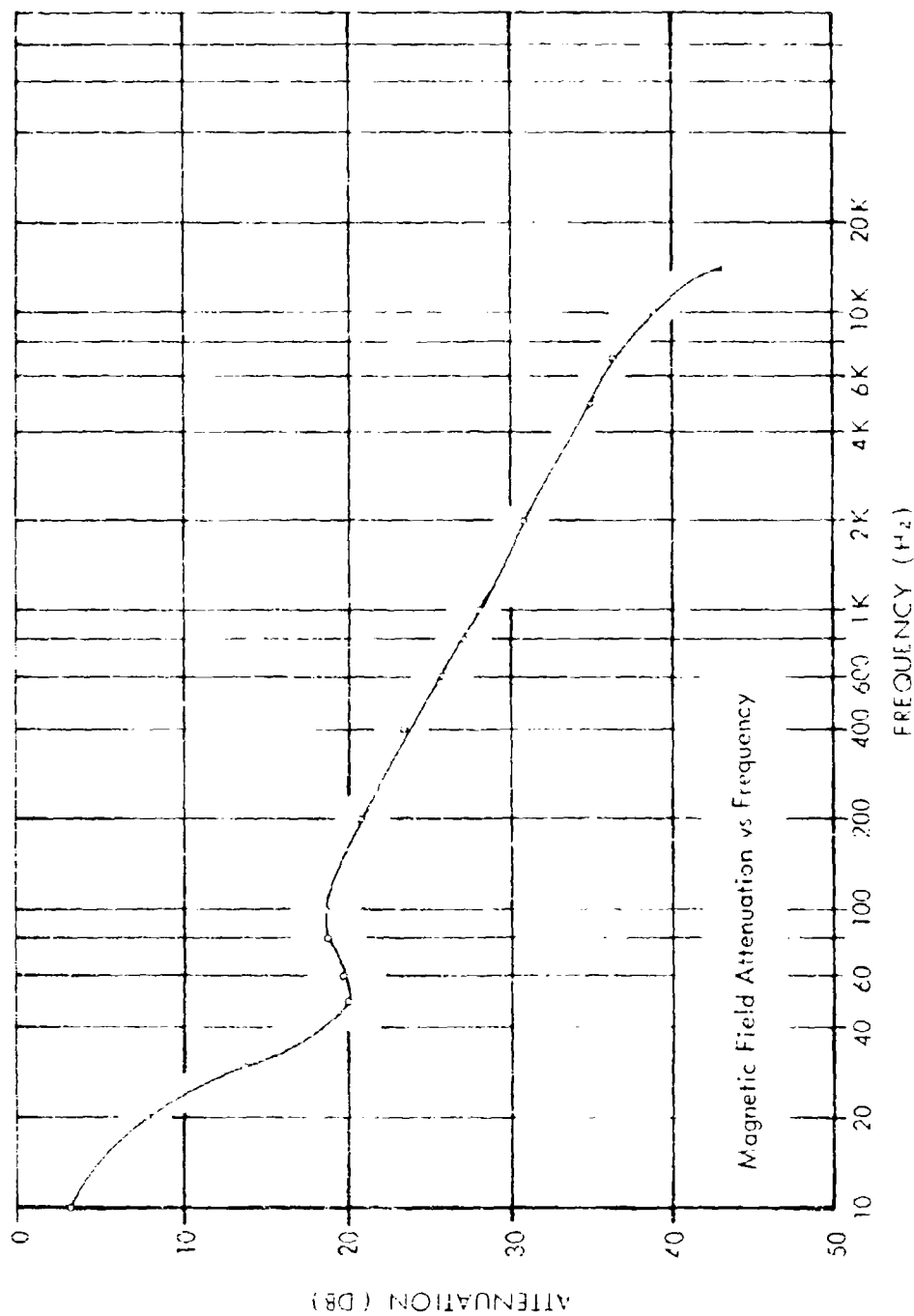


Fig. 21 SE of a 4-Foot Cubed Wrought Iron Enclosure Having a 1/4-Inch Wall Thickness
with Seams Welded and Annealed

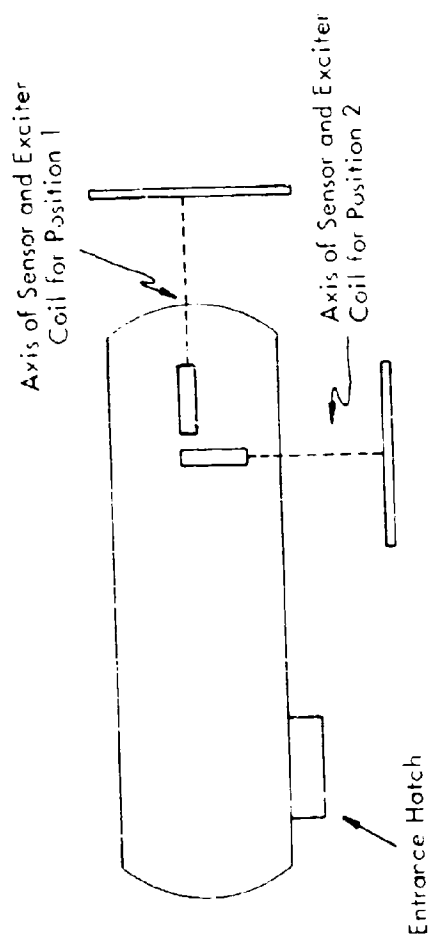


Fig. 22 Sensor and Exciter Coil Orientation for SE Measurements
Made on a Steel Tank Having a 1/2-Inch Wall Thickness

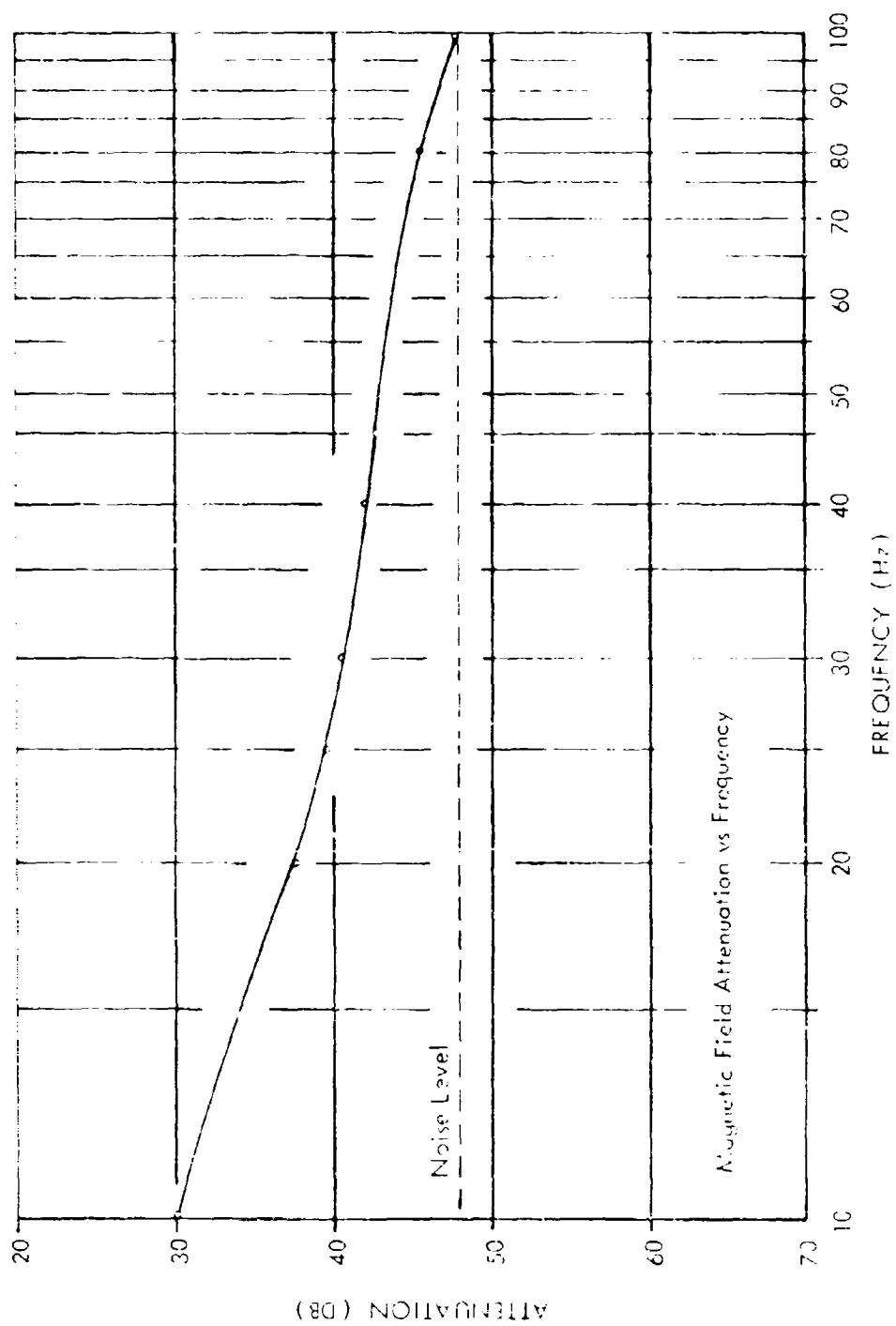


Fig. 23 SE of a Steel Tank with 1/2-Inch Thick Walls (Position I of Fig. 22)

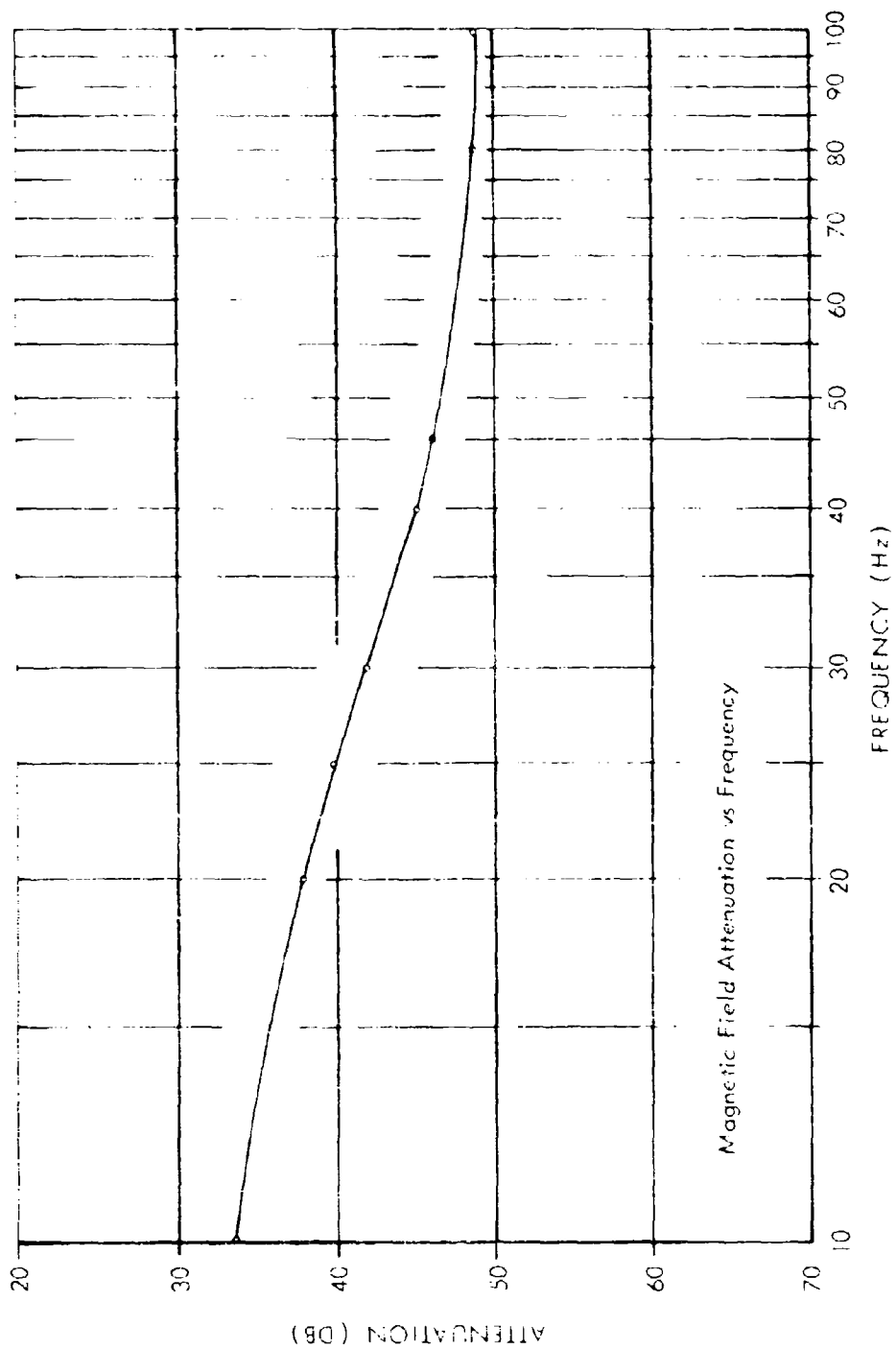


Fig. 24 SE of a Steel Tank with 1/2-Inch Thick Walls (Position 2 of Fig. 22)

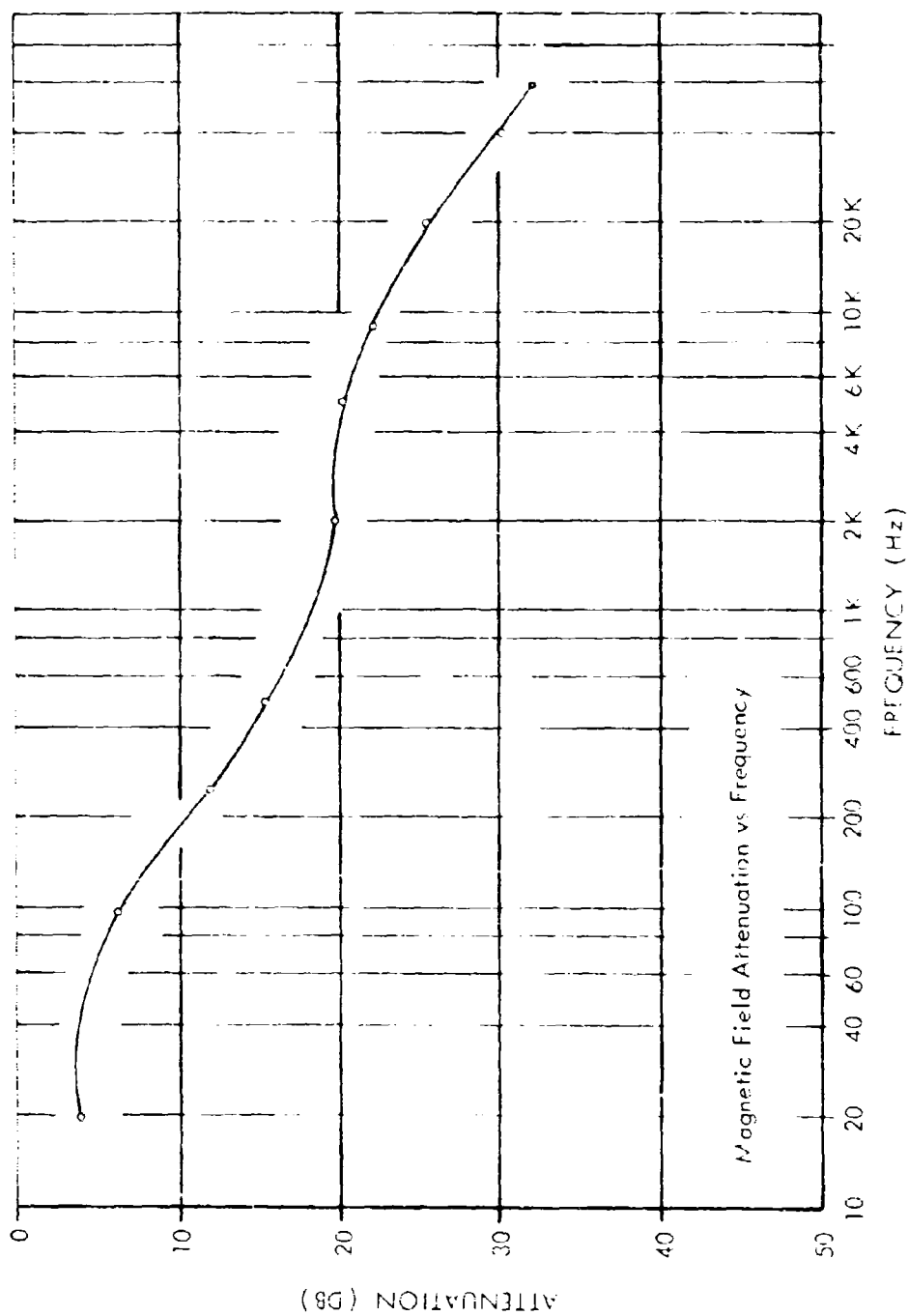


Fig. 25 SE of a 2-Foot Cubed, Mild Steel Sheet Enclosure Having a 0.053-Inch Wall Thickness with Welded Seams

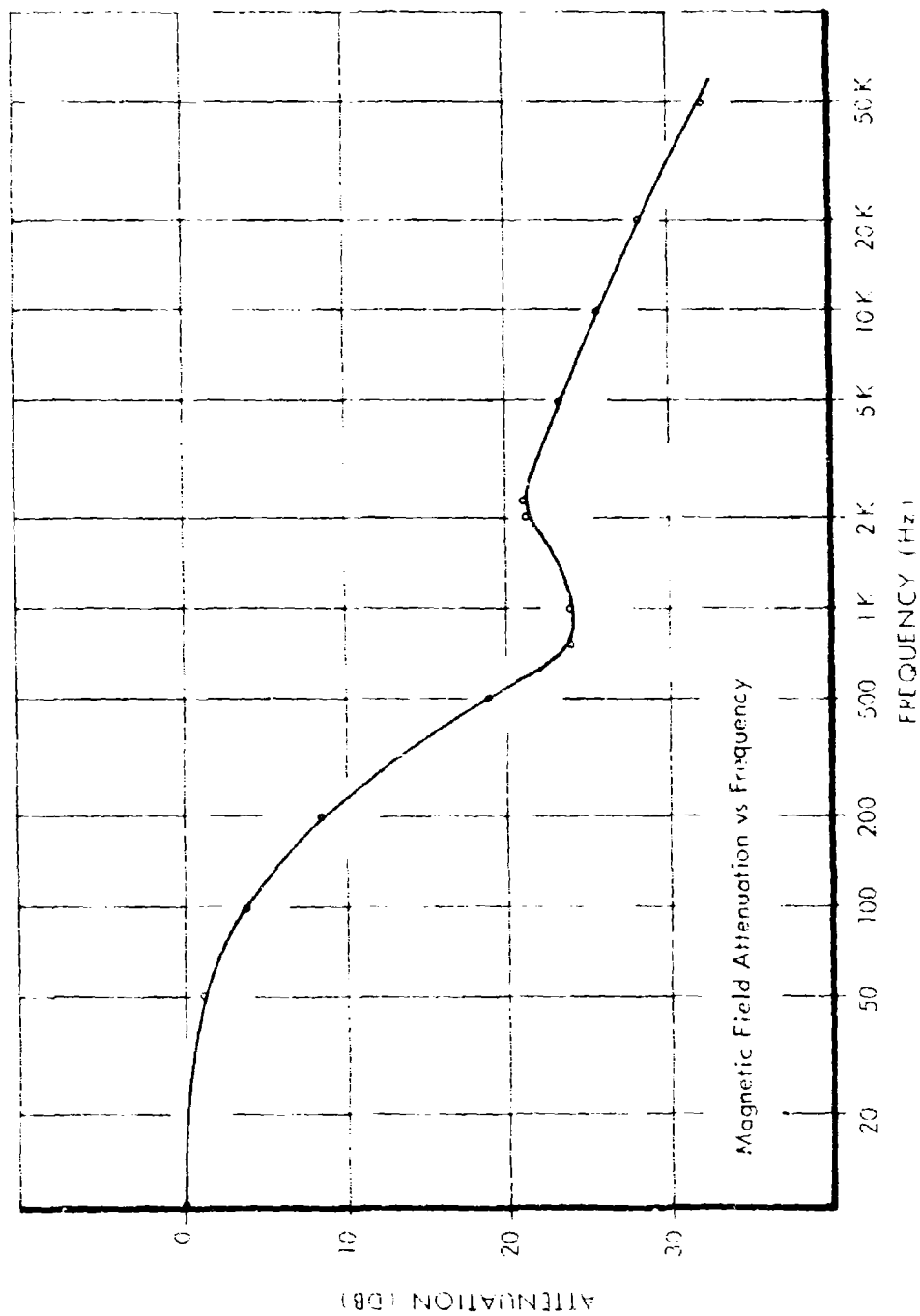


Fig. 26 SE of a 1-Foot Cubed, 18 Gauge Galvanized Steel Enclosure; All Seams Soldered

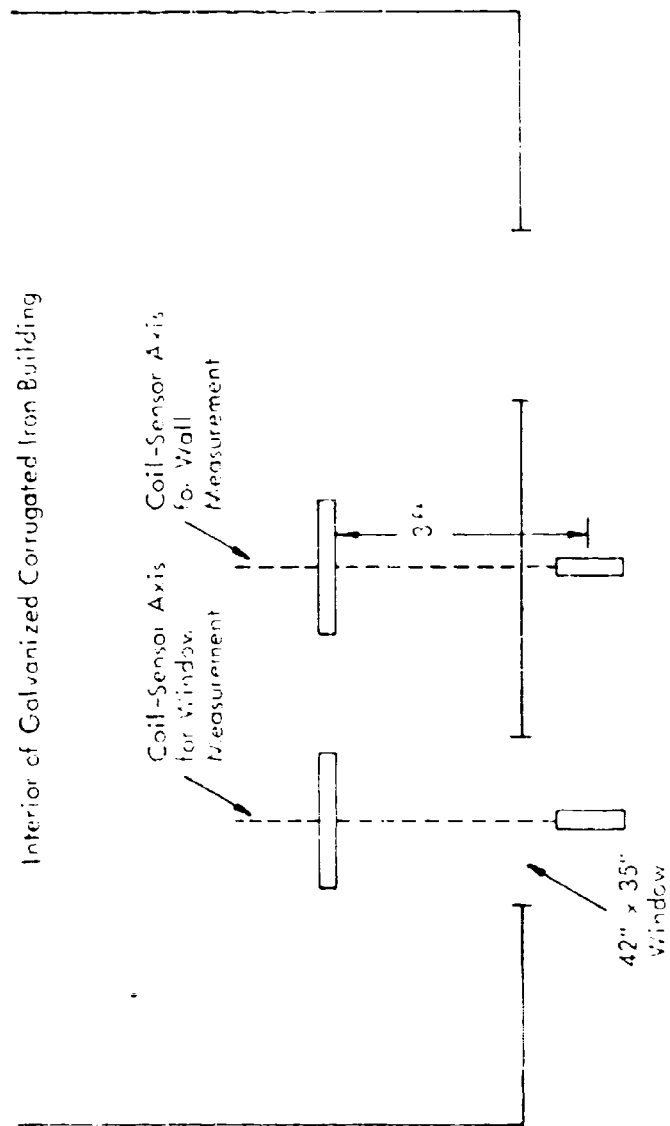


Fig. 27 Measurement Configuration Through Window and Wall of Galvanized Iron Building

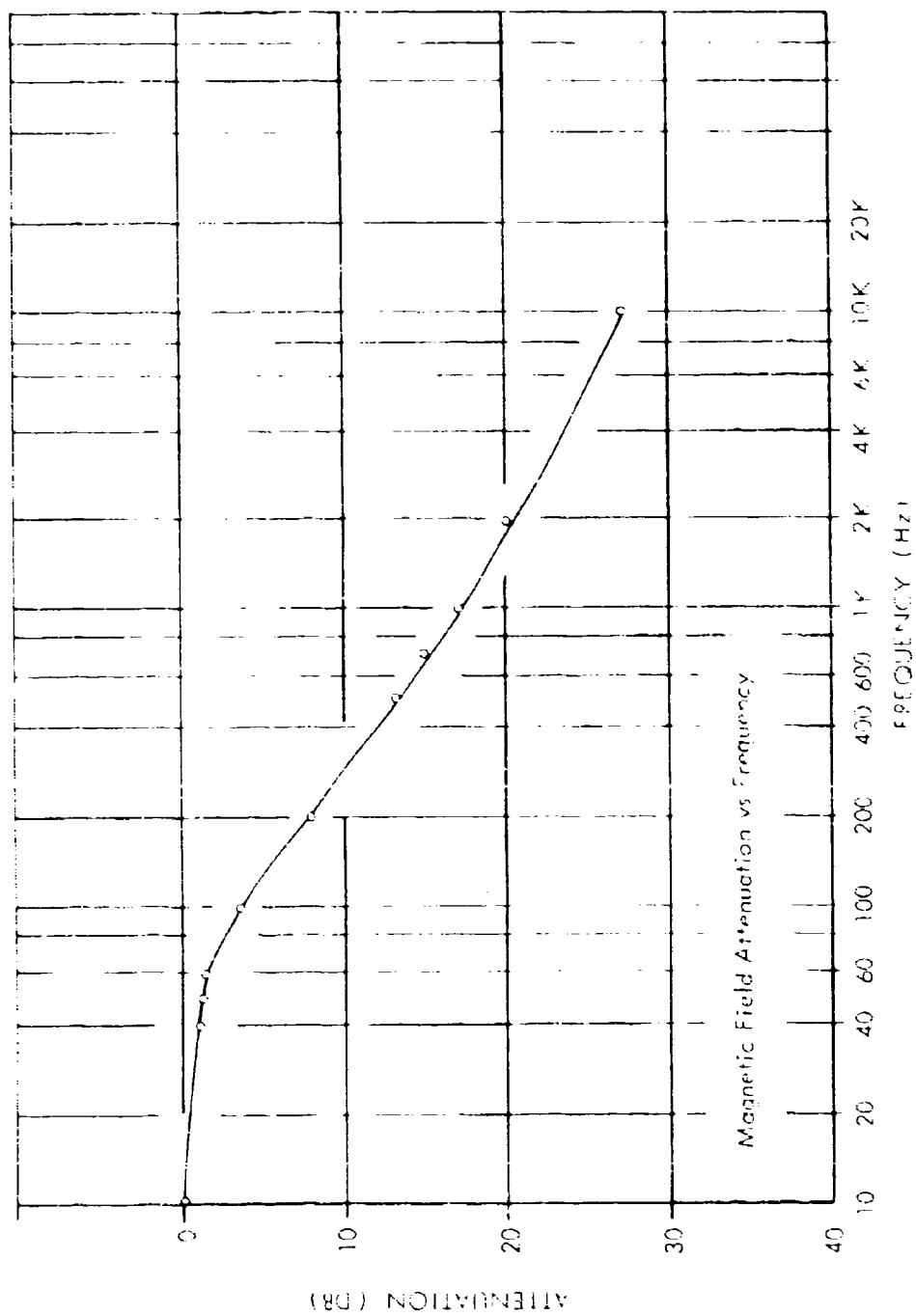


Fig. 28 SE of a Corrugated Galvanized Iron Wall, See Test Configuration in Fig. 27

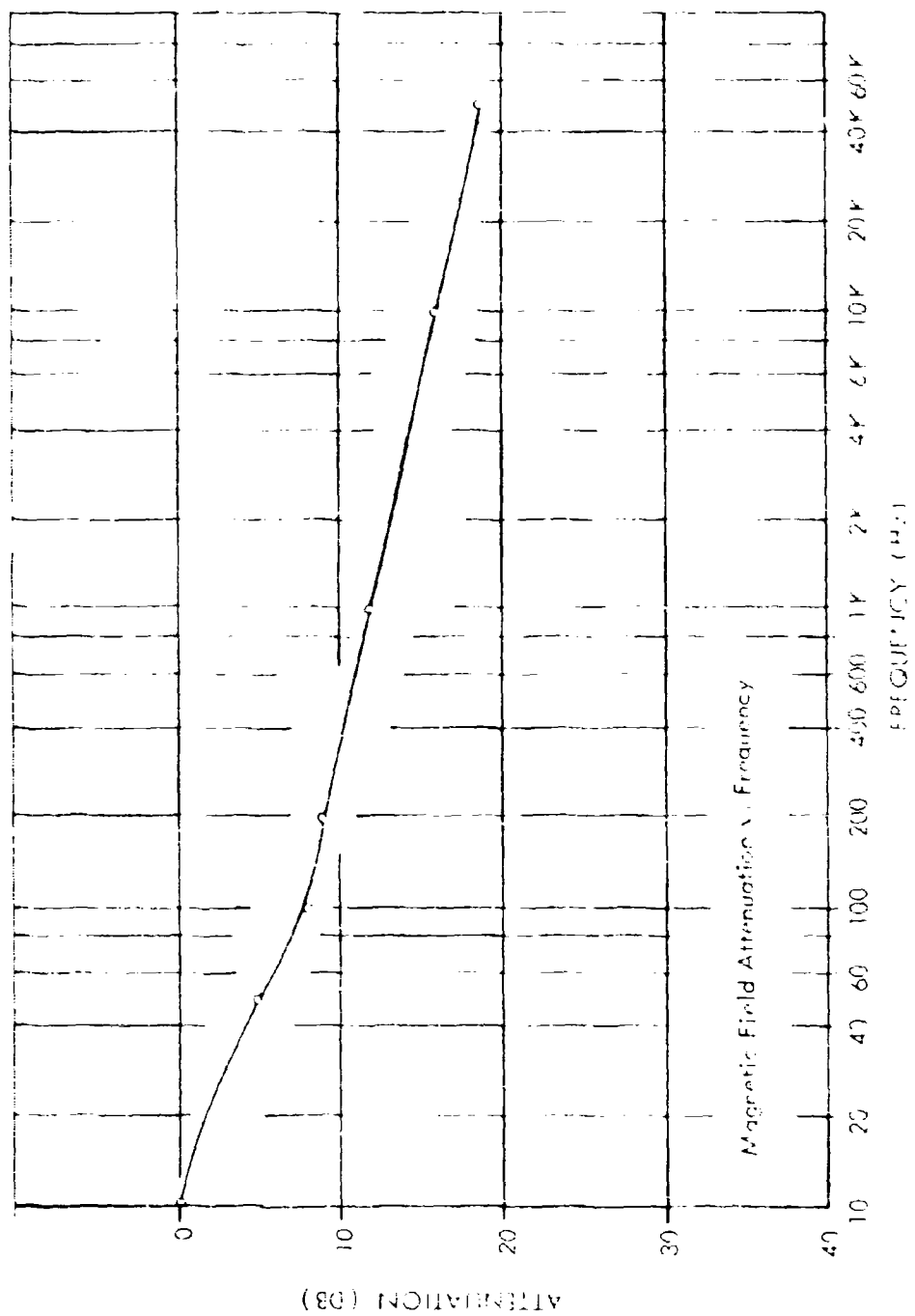


Fig. 29 SE of a 35" x 42" Steel and Glass Window in a Corrugated Iron Wall;
See Test Configuration in Fig. 27

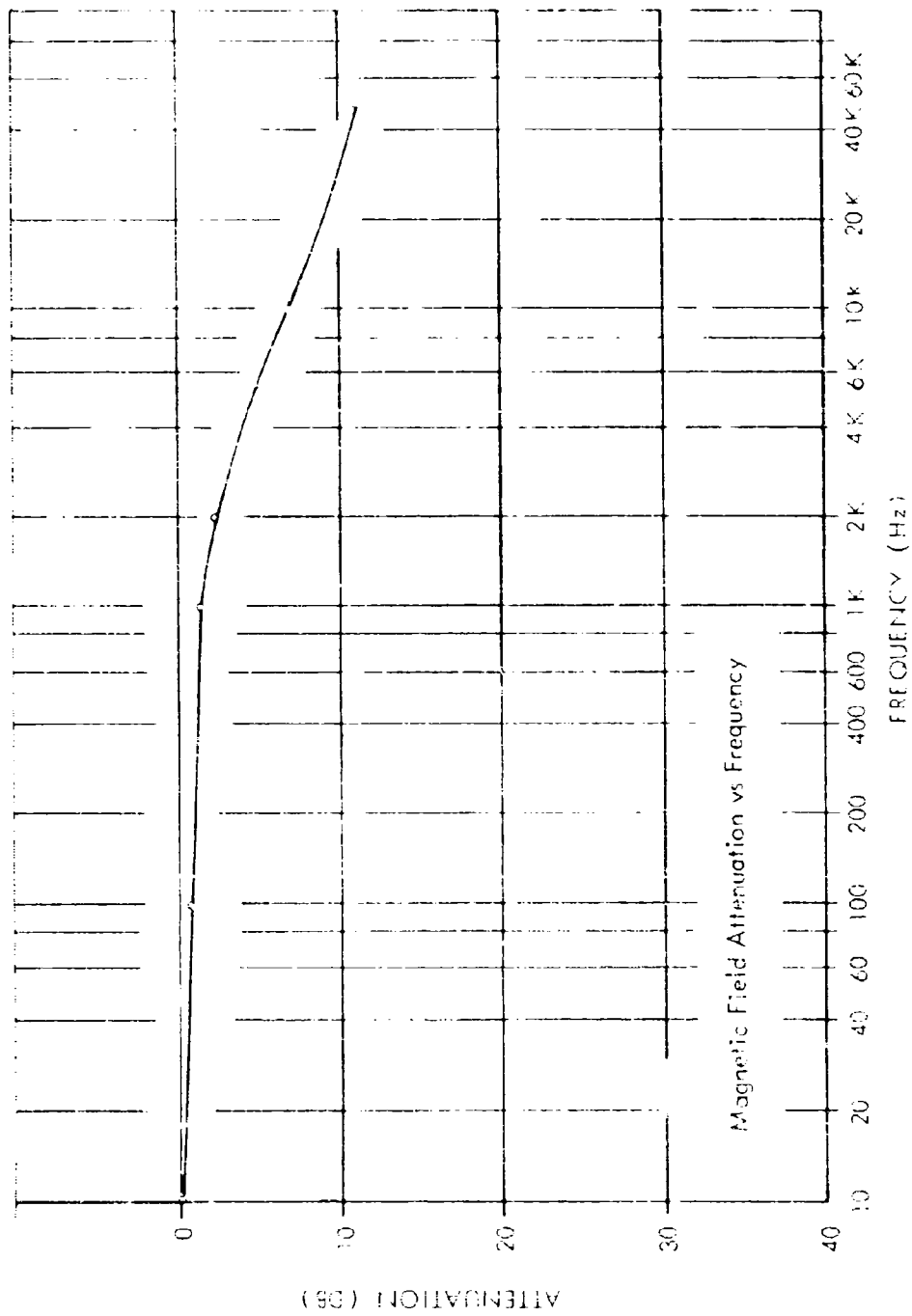


Fig. 30 SE of One Layer of 18 x 14 Mesh Galvanized Iron Wire Screen
in a 2-foot Cubed Configuration, Screen Edges Lapped and Stapled

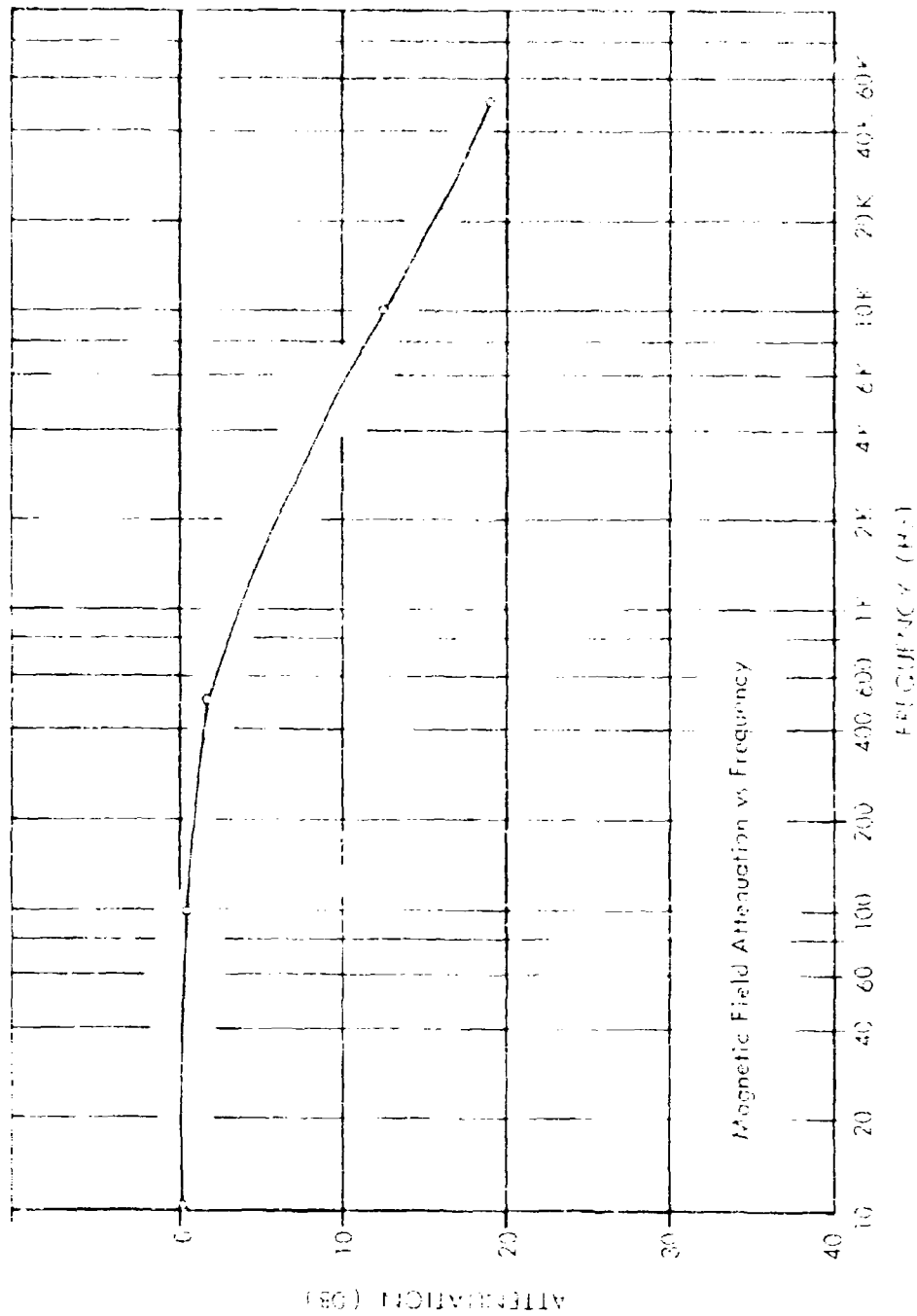


Fig. 21 SE of a 1/4-Inch Mesh, 0.025-Inch Galvanized Iron Wire Hardware Cloth
in a 2-Foot Cubed Enclosure with Edges Lapped and Stapled

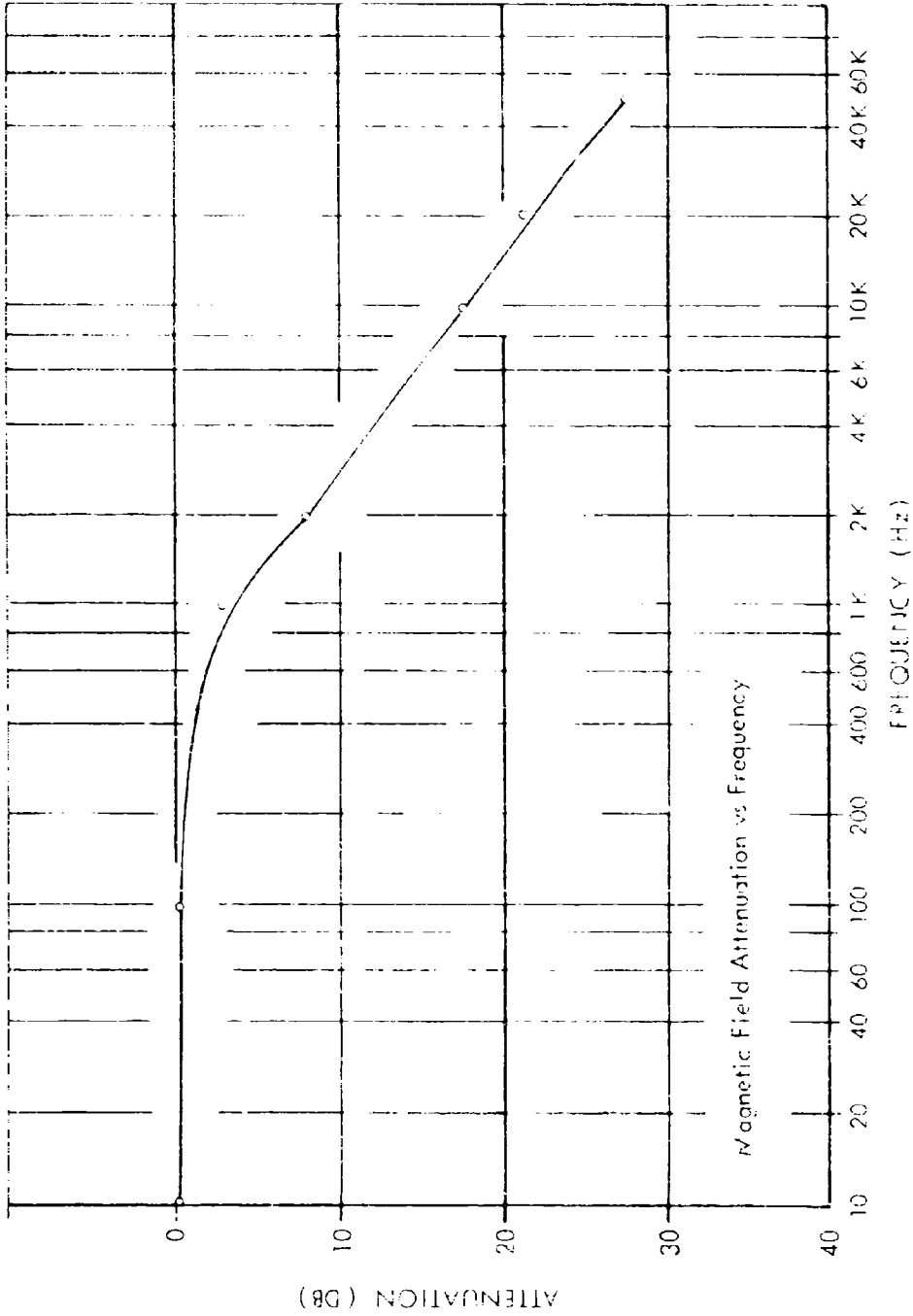


Fig. 32 SE of a 1/2-Inch Mesh, 0.040-Inch Galvanized Iron Wire Hardware Cloth
in a 2-Foot Cubed Enclosure with Edges Lapped and Stapled

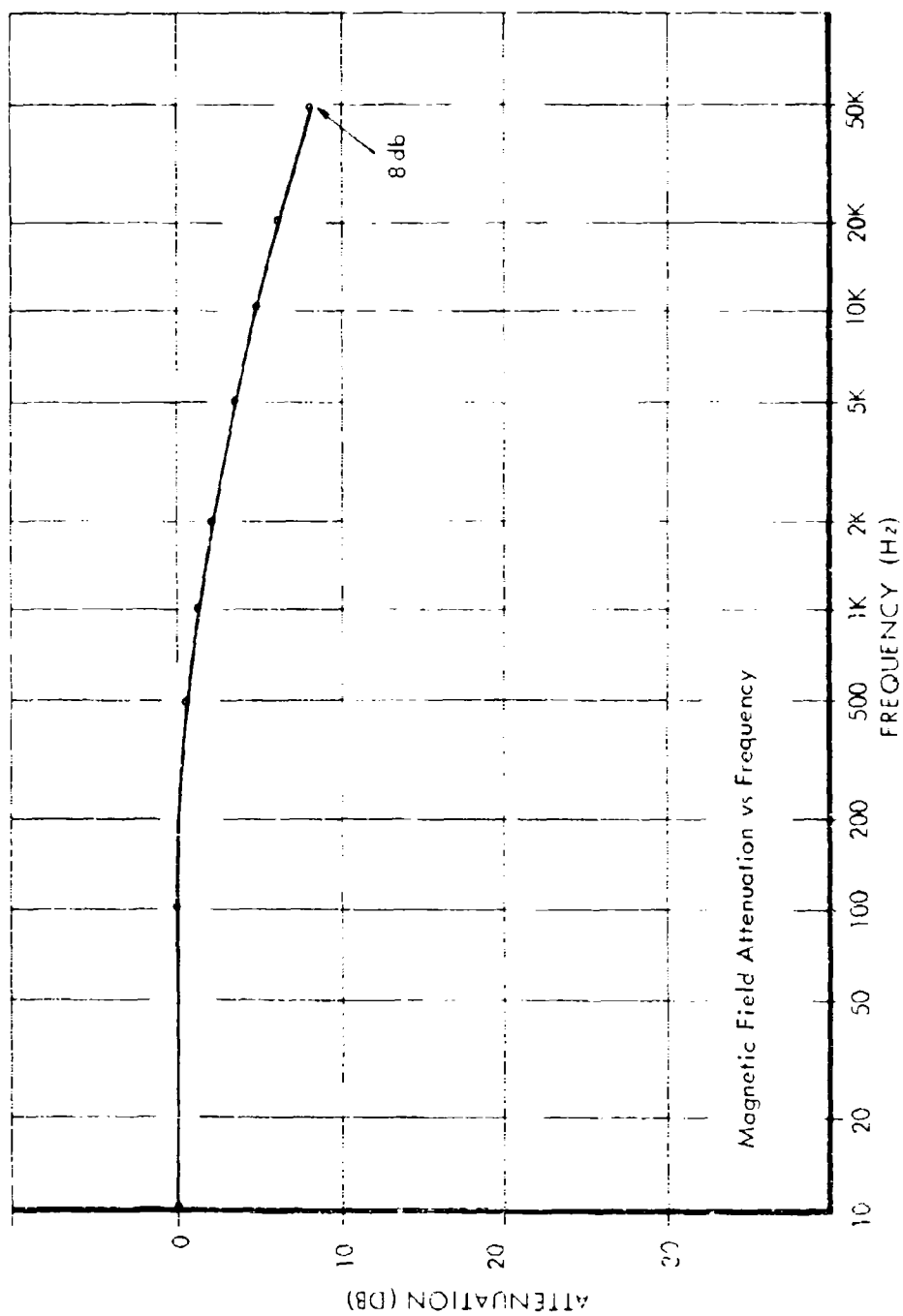


Fig. 33 SE of a 2-Foot Cubed Enclosure of 6" x 6" x 6" No. 10 Reinforcing Steel Wire Mesh
with Edges Wired Together Using Iron Wire

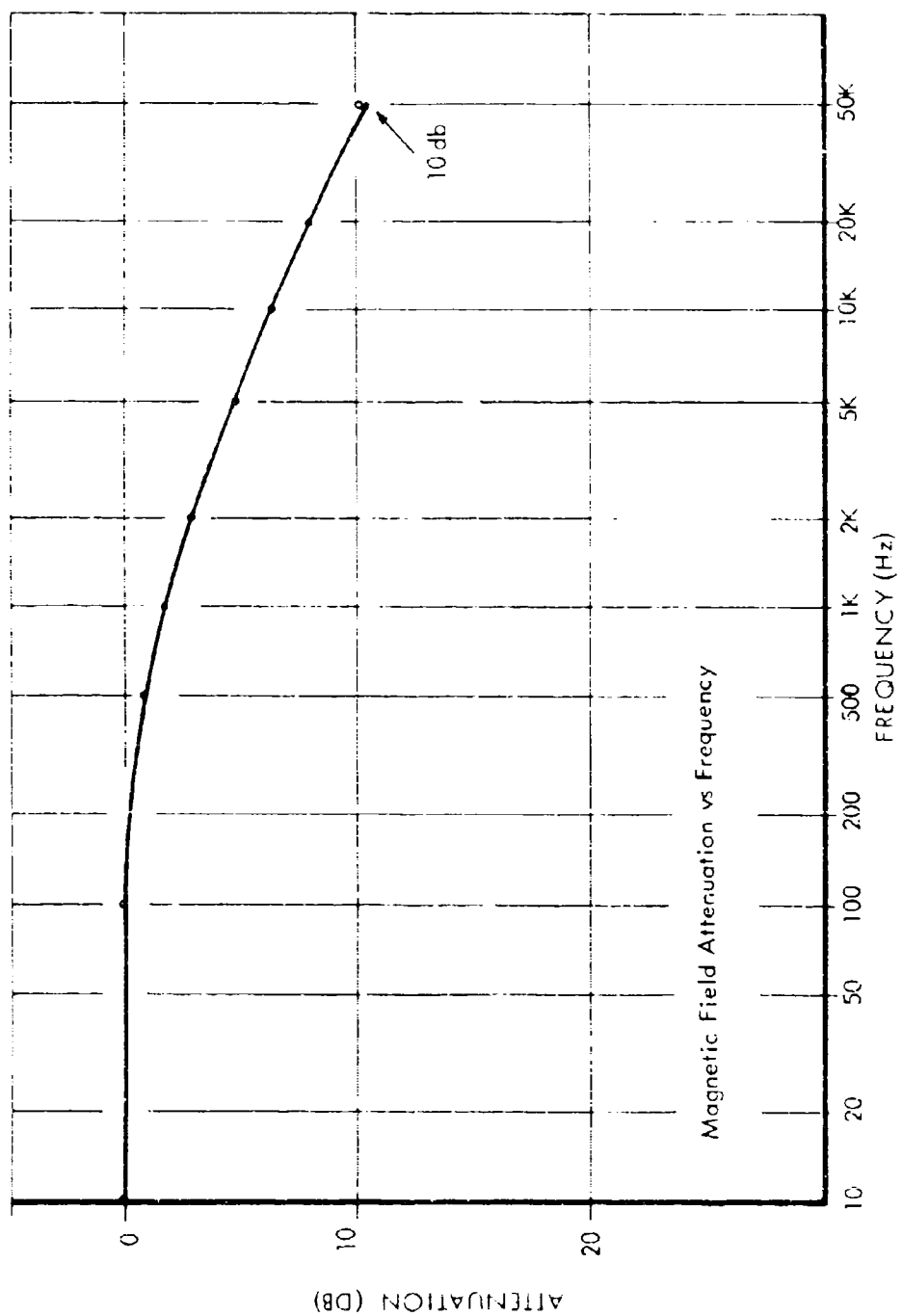


Fig. 34 SE of a 2-Foot Cubed Enclosure of 6" x 6" x No. 6 Reinforcing Steel Wire Mesh
with Edges Wired Together Using Iron Wire

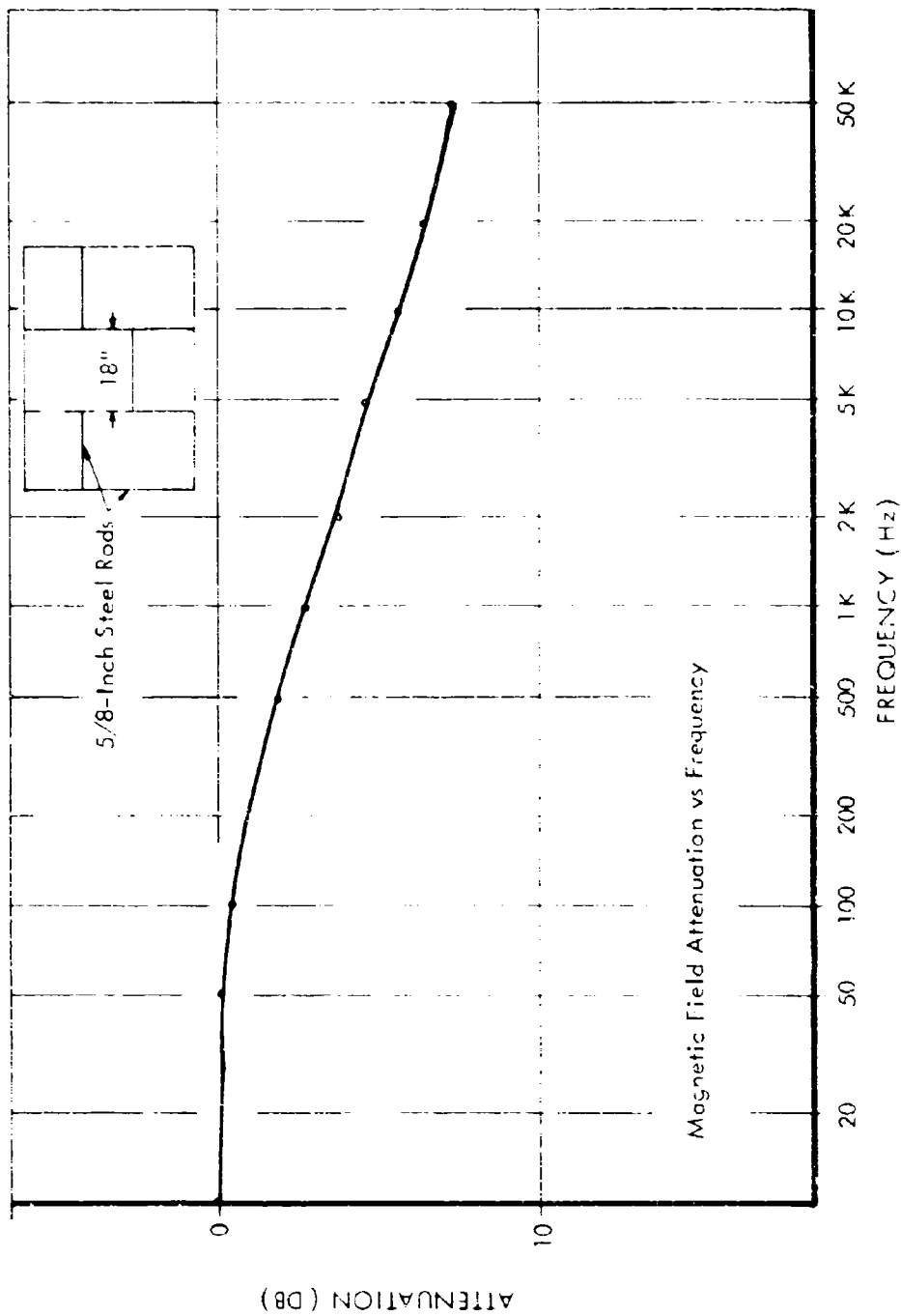


Fig. 35 SE of a 9-Inch Reinforced Concrete Wall (see insert above); at Least One Near-Midsection Cross-Member per Vertical Section with Rods Bent and Tied with Iron Wire at Each Juncture

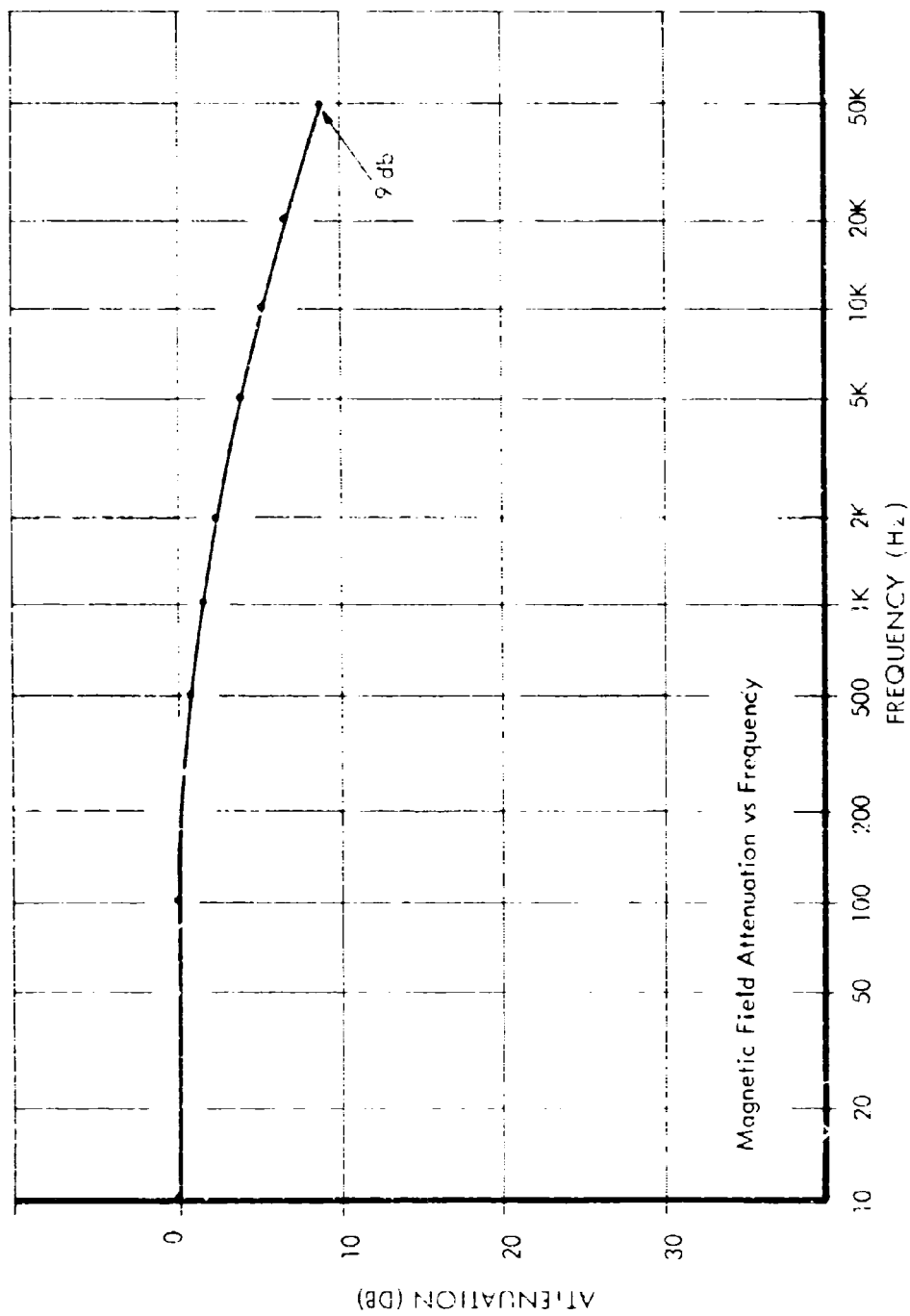
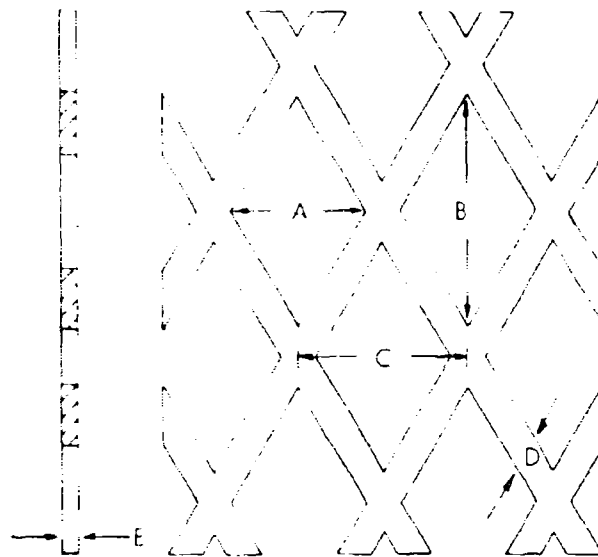


Fig. 36 SE of a 2-Foot Cubed Cage Enclosure of 3/8-Inch Reinforcing Steel Rods Spaced on 6-Inch Centers Both Ways with Steel Welded Cross Points and Corners



- A - Diamond width
- B - Diamond length
- C - Nominal width, center to center of bond
- D - Strand width
- E - Strand thickness

Fig. 37 A Section of Expanded Metal Showing Measured Dimensions

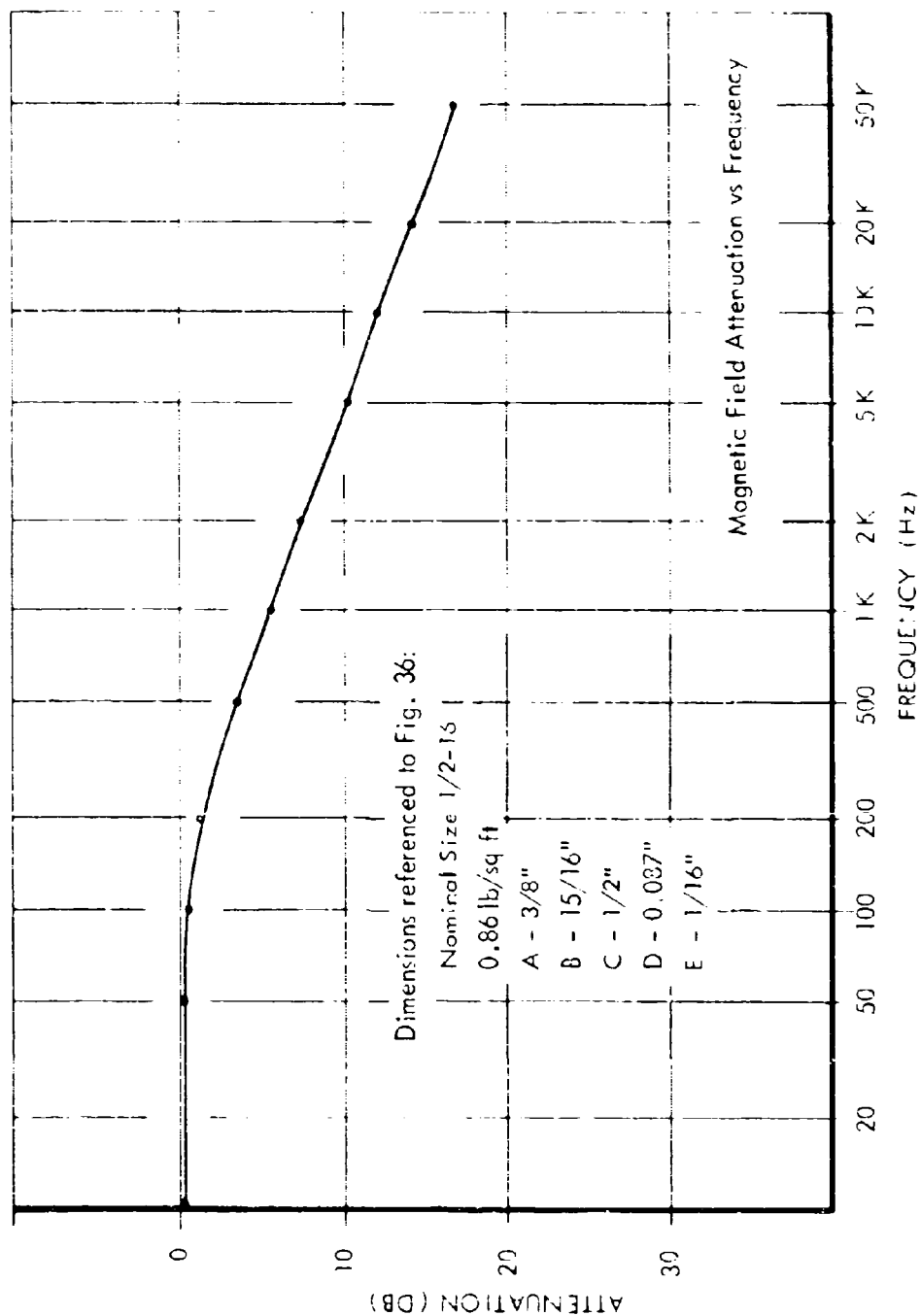


Fig. 38 SE of a 4 x 8-Foot Sheet of 1/2-Inch Safety Mesh Expanded Steel

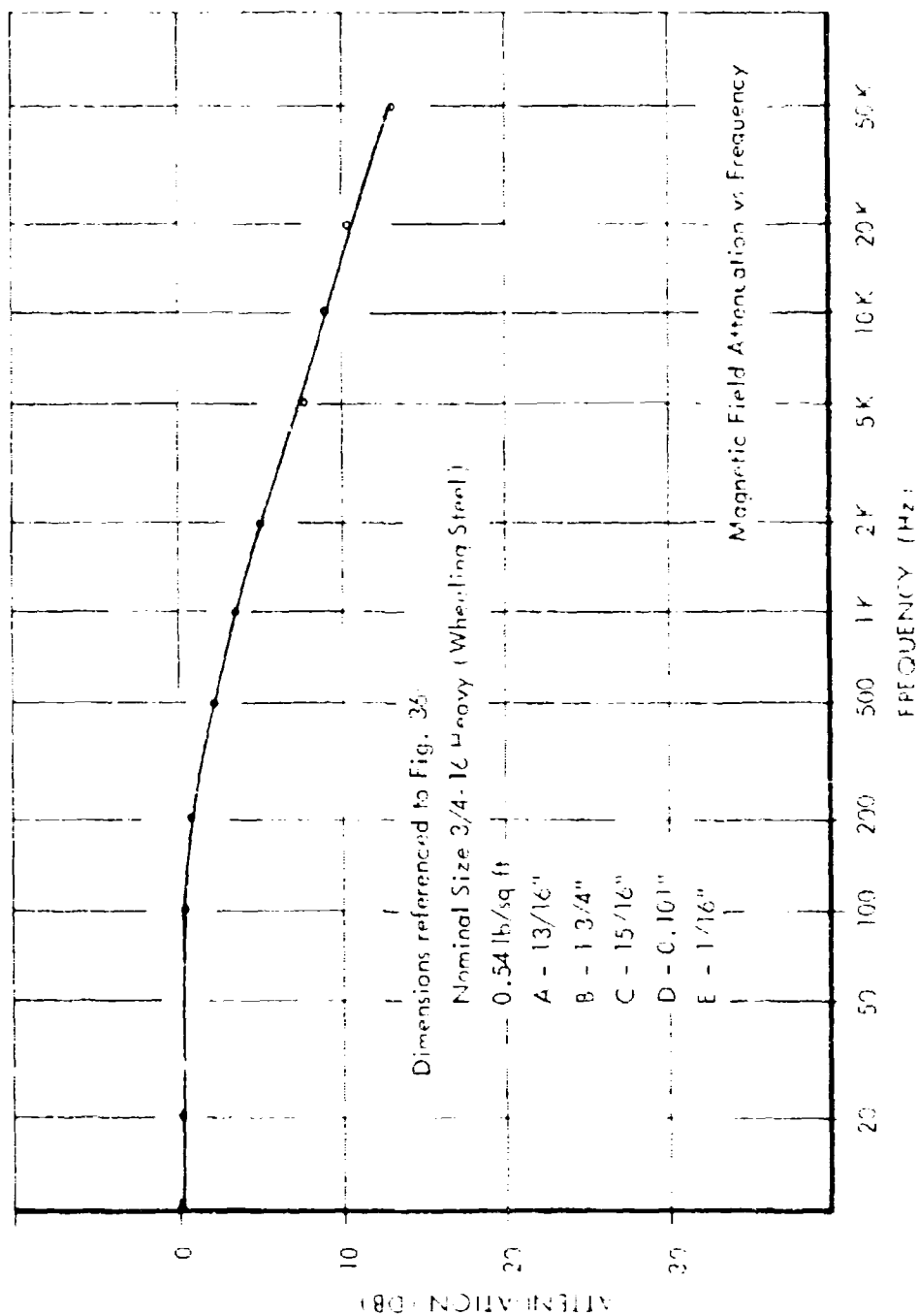


Fig. 39 SE of a 4 x 8-Feet Sheet of 15 1/2-Inch Safety Mesh Expanded Steel

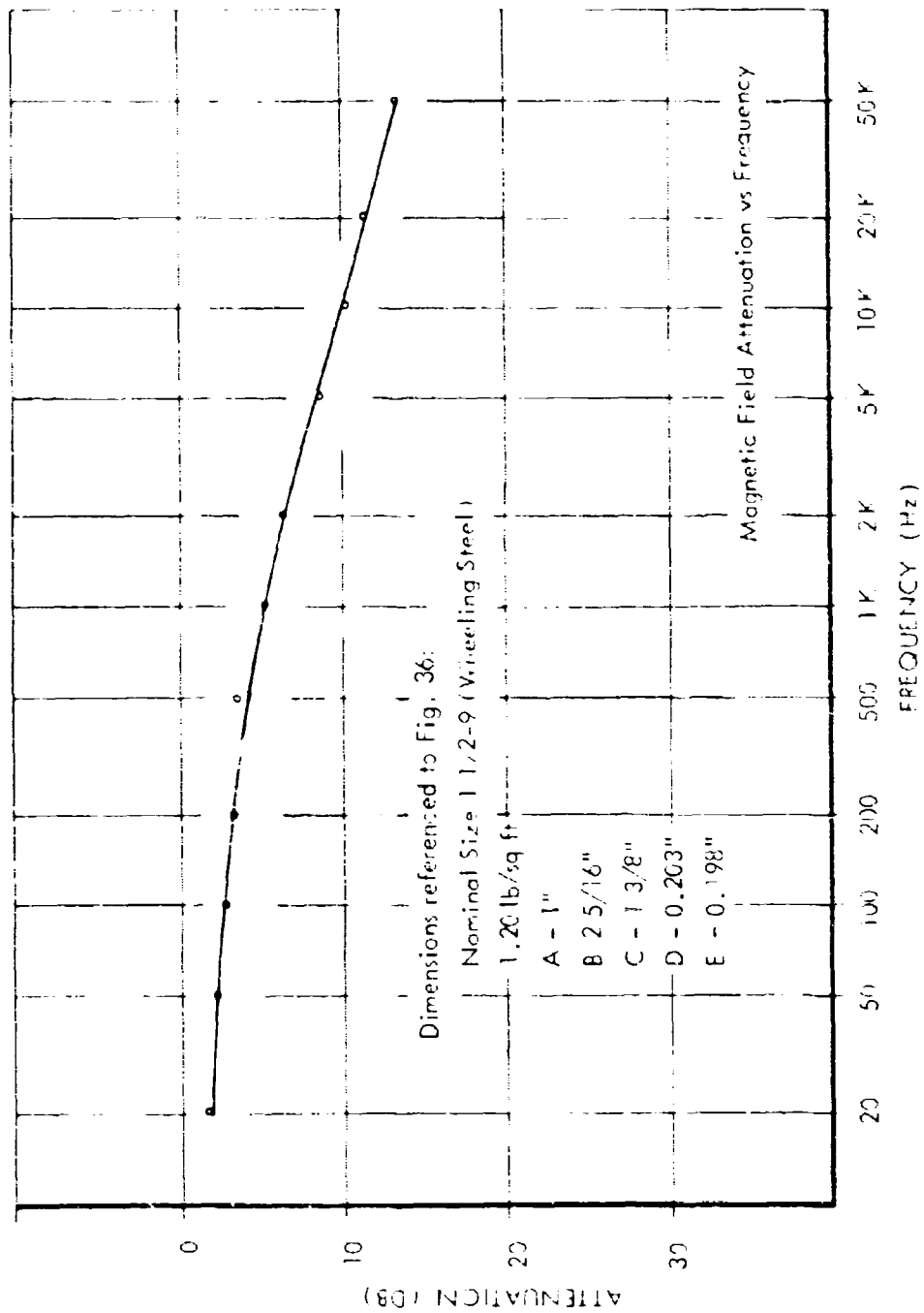


Fig. 40 SE of a 4 x 8-Foot Sheet of 1-3/8-Inch Safety Mesh Expanded Steel

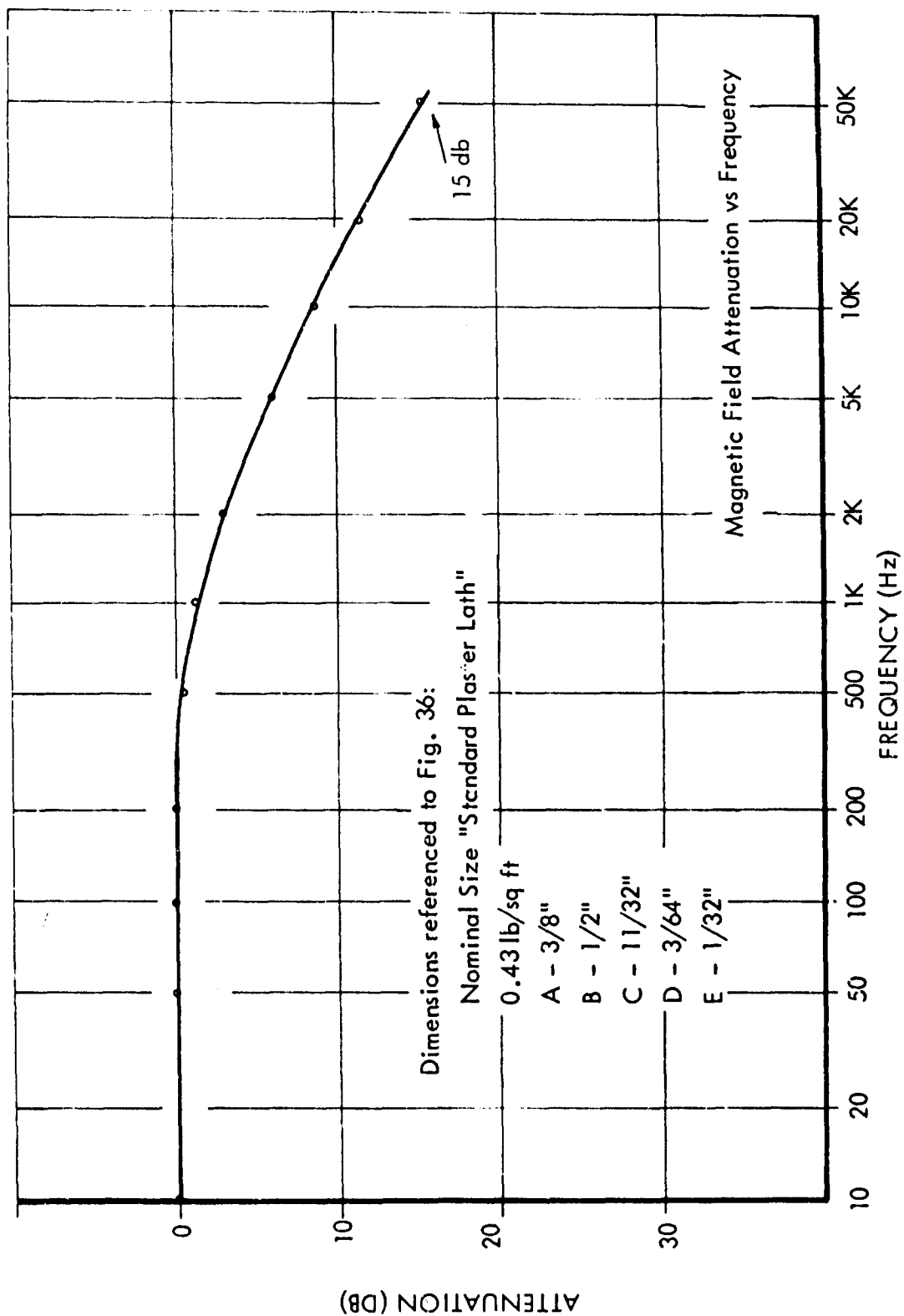


Fig. 41 SE of a 2-Foot Cubed, Plaster Lath Expanded Steel Enclosure Having Lapped and Wired Seams

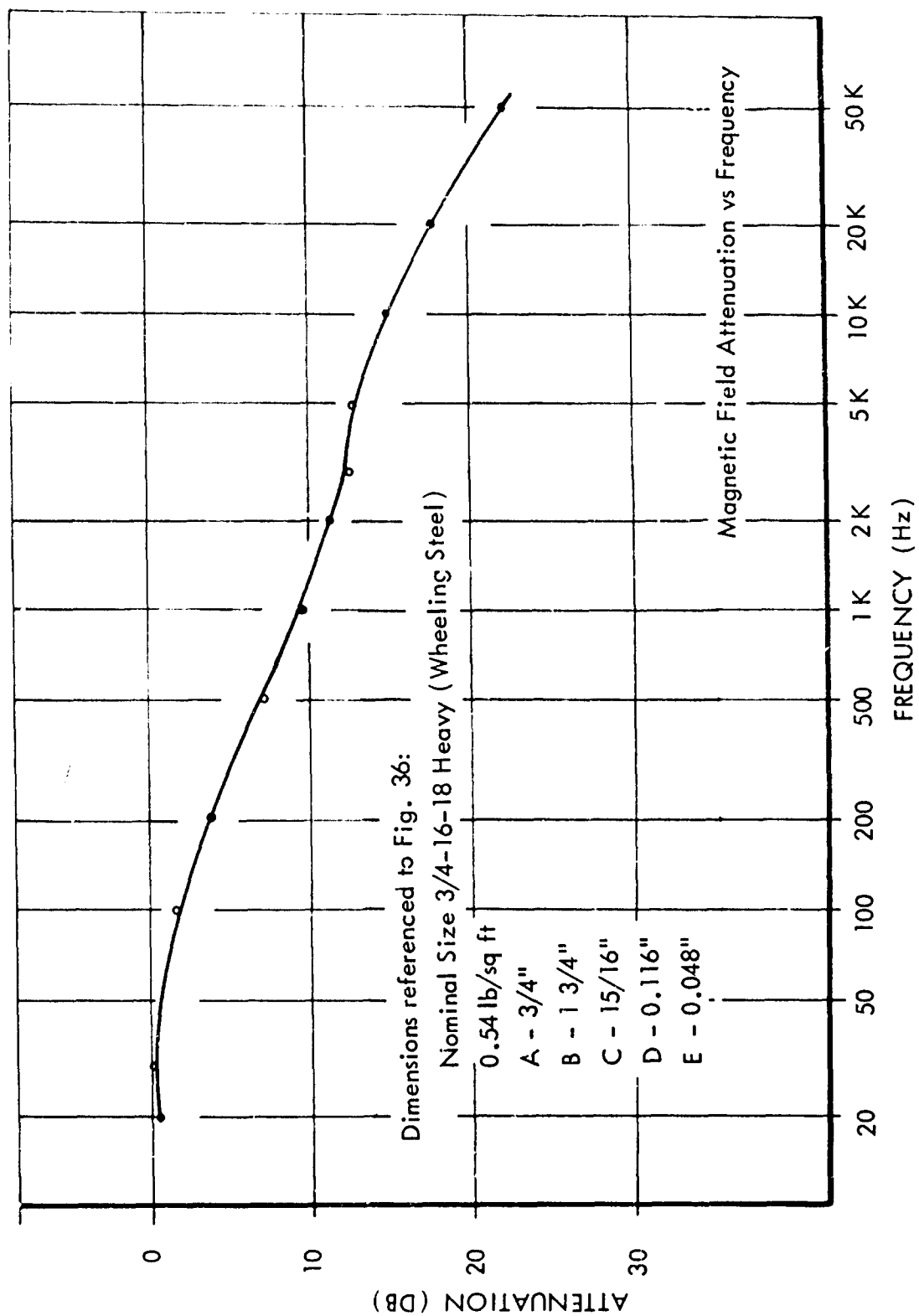


Fig. 42 SE of a Two-Foot Cubical Enclosure of 15/16-Inch Flattened Steel Mesh
With Edges Steel Welded

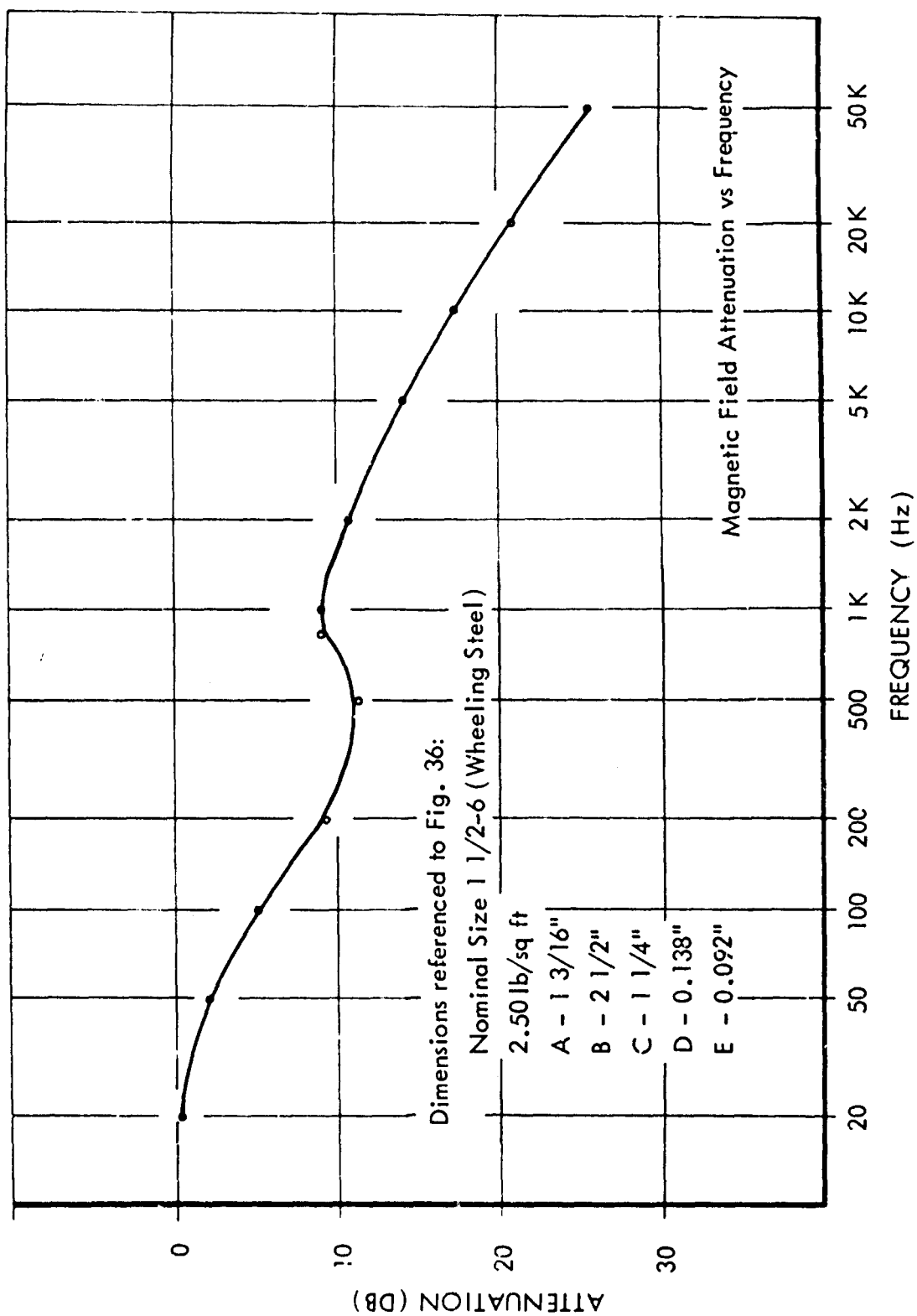


Fig. 43 SE of a Two-Foot Cubical Enclosure of 1/4-Inch Safety Mesh
With Edges Steel Welded

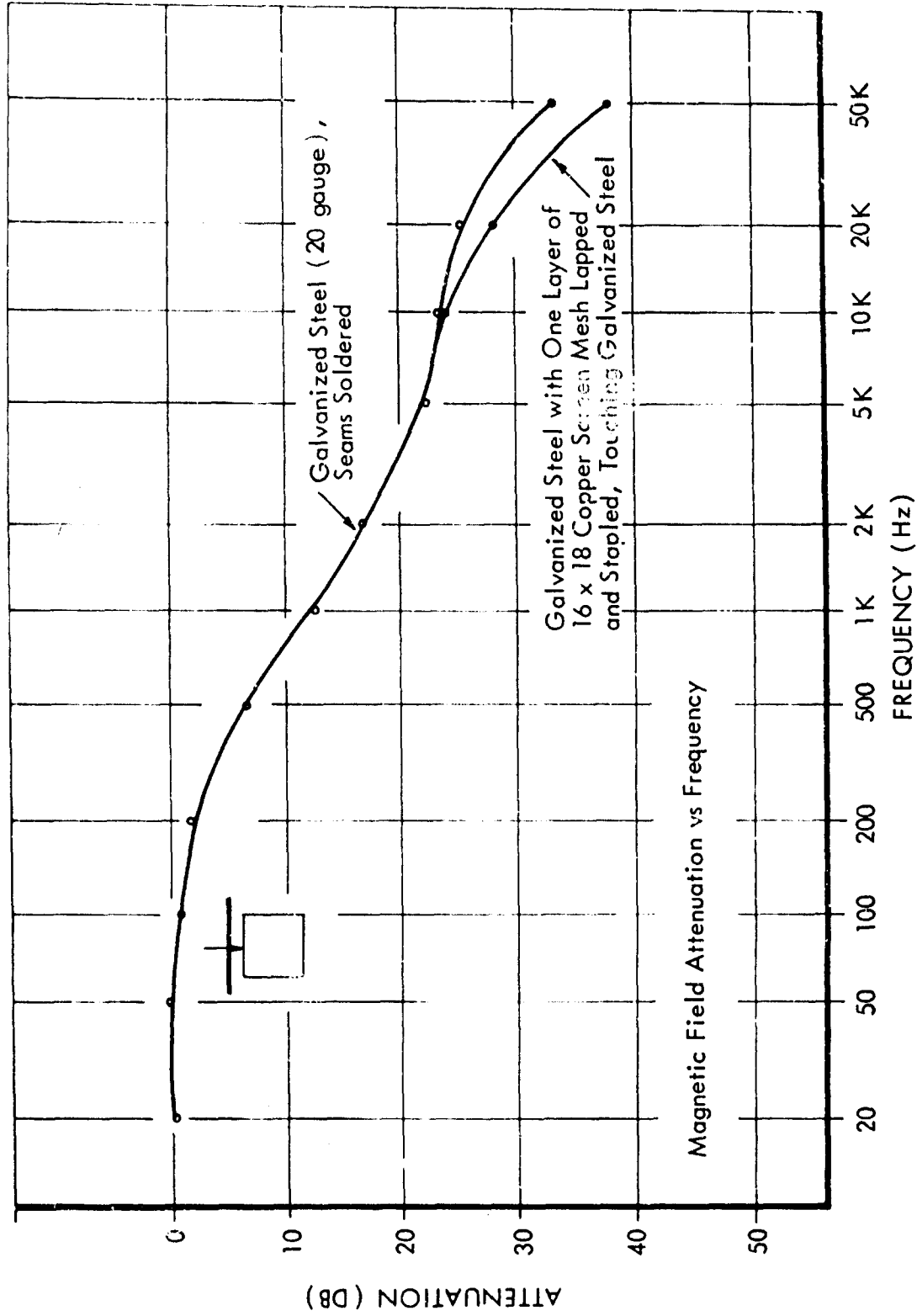


Fig. 44 SE of a Combination of a High Permeability Material and a Highly Conductive Material in a 2-Foot Cubed Configuration with Field Orientation Shown

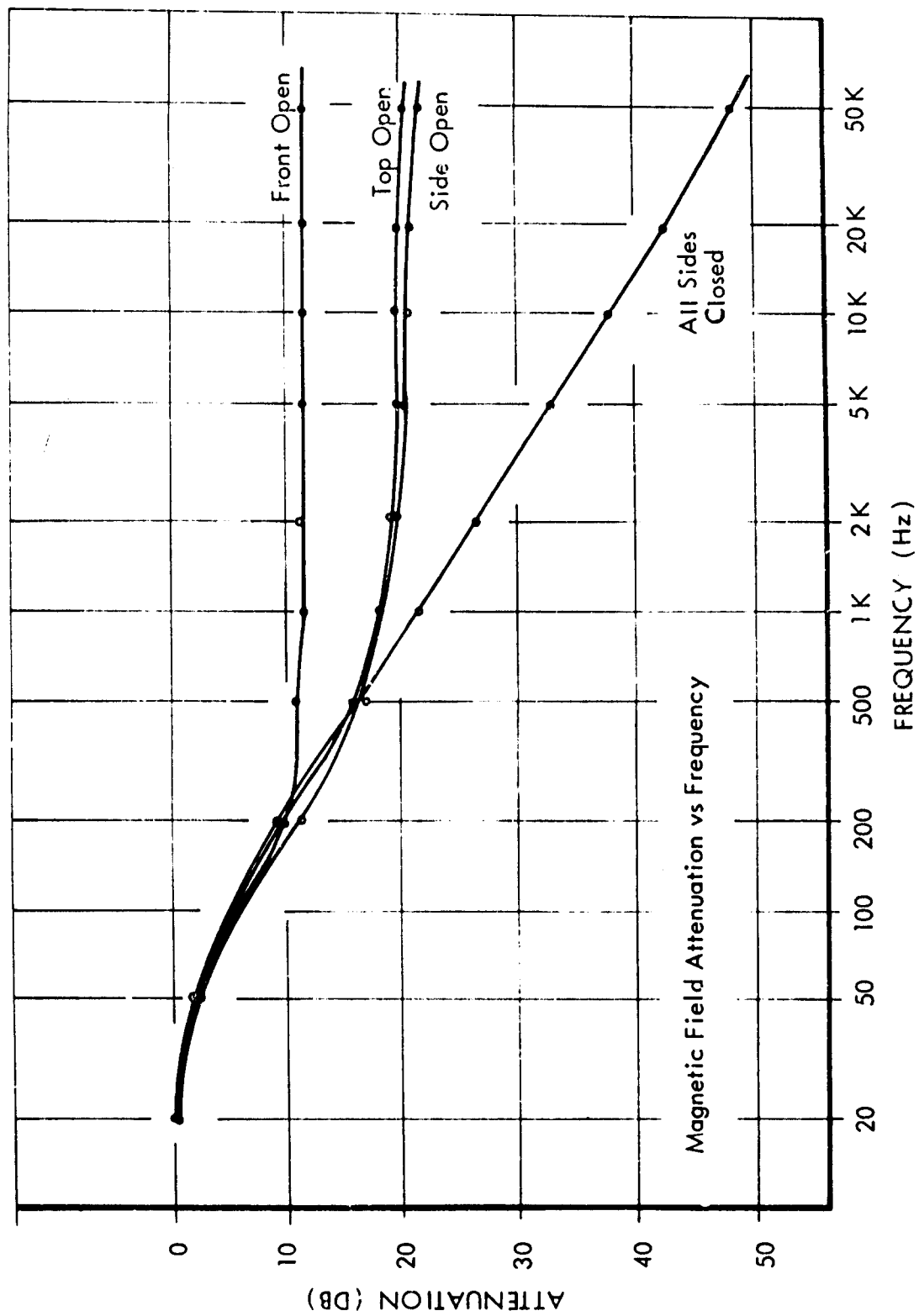


Fig. 45 SE Variations Caused by Removing One Side of a 1-Foot Cubed Sheet Copper Enclosure (Soldered Seams) Having a .026-Inch Wall Thickness

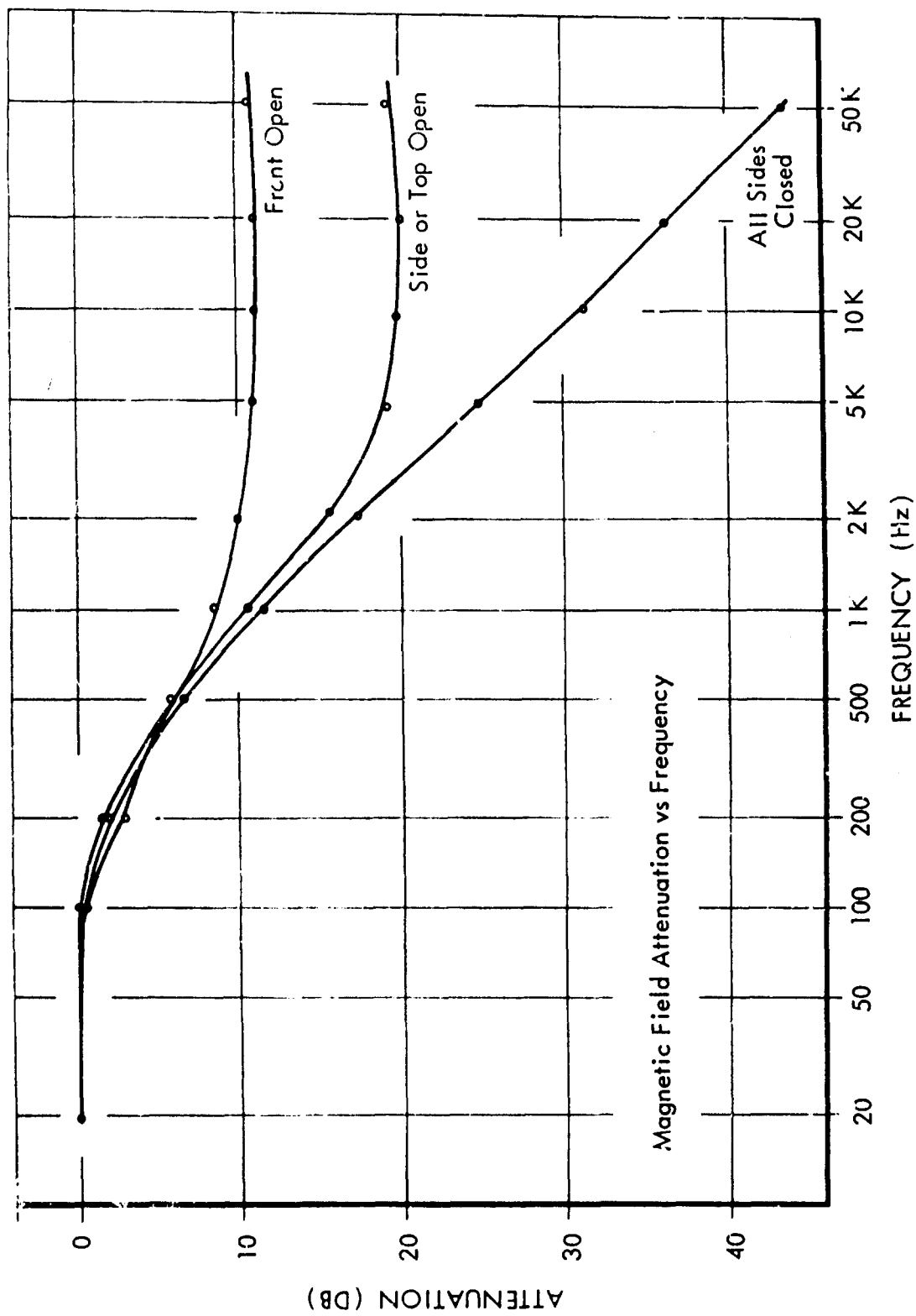


Fig. 46 SE Variations Caused by Removing One Side of a 1-Foot Cubed Sheet Brass Enclosure (Soldered Seams) Having a .025-Inch Wall Thickness

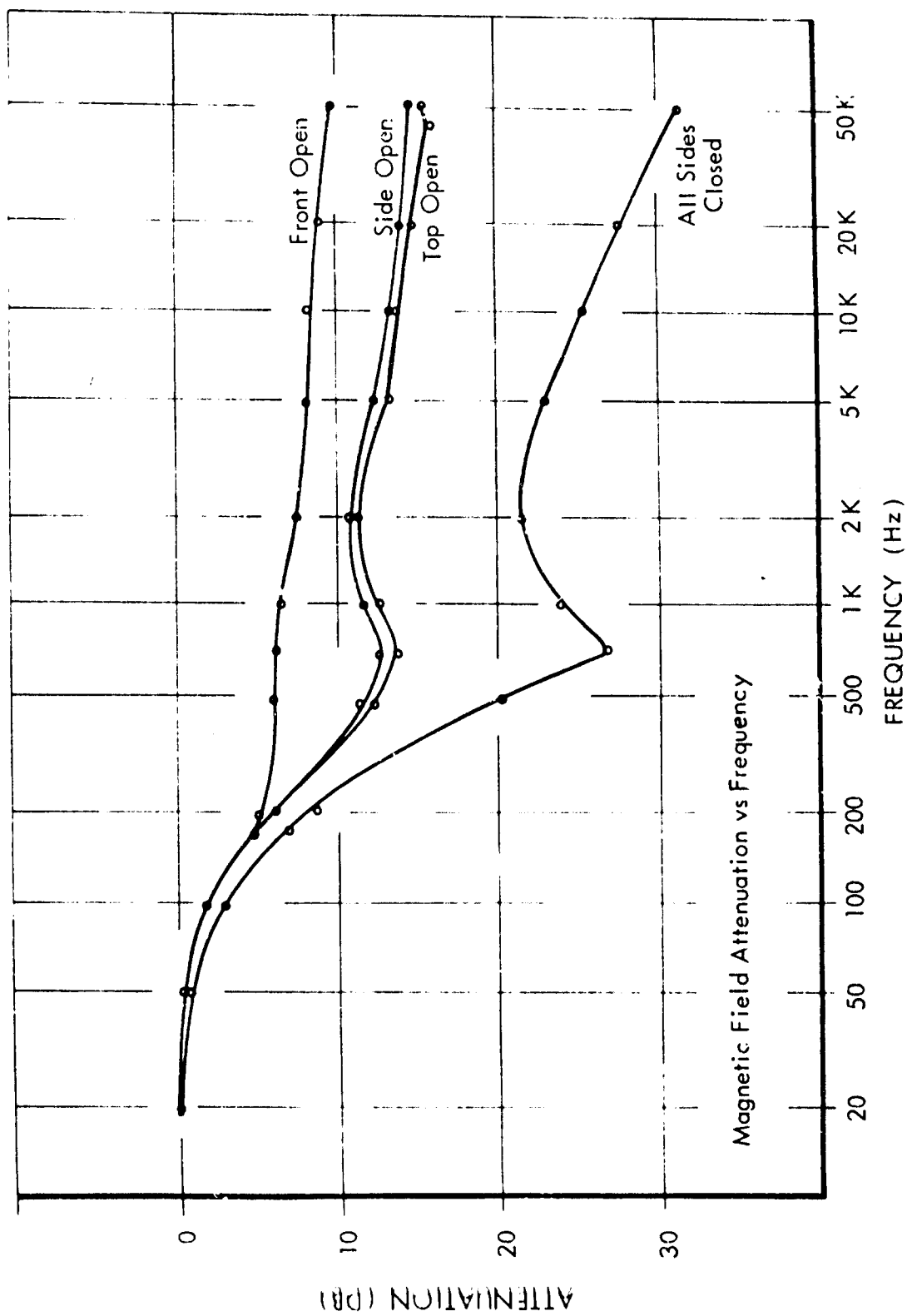


Fig. 47 SE Variations Caused by Removing One Side of a 1-Foot Cubed, 18 Gauge Galvanized Sheet Steel Enclosure; All Seams Soldered

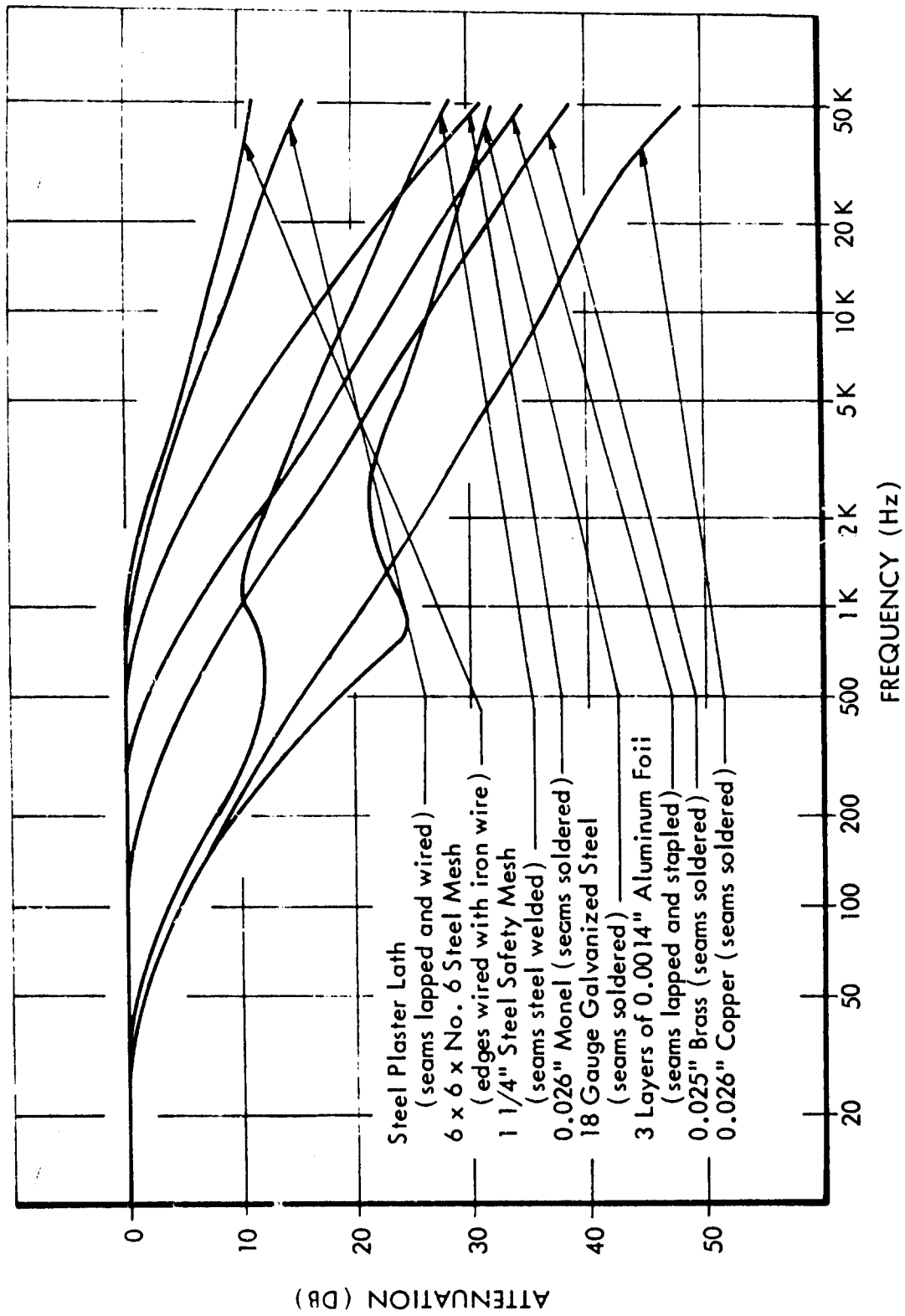


Fig. 48 A Composite Data Presentation of Magnetic Field SE of 1-Foot Cubed Enclosures of Various Metals

Section 3

TABULATED RESULTS OF CONDUCTED MEASUREMENTS

Table of Relative Resistivities of Several Metallic Building Materials
Using Copper as a Standard

Material	Relative Resistivity
Copper	1.00
Aluminum	1.64
Magnesium	2.67
Zinc	3.36
Brass	3.65
Wrought Iron	5.80
Tin	6.67
Cast Iron	6.96
Permalloy	9.30
Mild Steel	11.6
Stainless Steel 404	16.8
Monel	27.8
Stainless Steel 304	30.6
Supermalloy	34.8
Mu Metal	36.0
Titanium	47.8
Nichrome	58.0
Chromel A	62.4

RESULTS OF CONDUCTED MEASUREMENTS

Dry Clay Brick

Frequency (Hz)	Dielectric Constant	Dissipation Factor	Shielding Effectiveness (db/meter)
10	--	--	7.56×10^{-7}
50	--	--	
100	2.8	0.139	
300	2.6	0.435	1.90×10^{-5}
1 K	2.6	0.336	
3	2.5	0.016	
10	2.5	0.015	
30	2.5	0.011	
100	2.4	0.009	
300			
500			
700			
1 M			
3			
5			
7			
10			
20			
40			
60			
100			
200			
500			
700			
1 G			

RESULTS OF CONDUCTED MEASUREMENTS

Moist Clay Brick

Frequency (Hz)	Dielectric Constant	Dissipation Factor	Shielding Effectiveness (db/meter)
10	--	--	8.44×10^{-7}
50	--	--	
100	43.4	0.611	
300	23.7	0.785	
1 K	11.3	0.826	2.24×10^{-5}
3	6.6	0.700	
10	4.4	0.508	
30	3.5	0.463	
100	3.0	0.194	High dissipation factor prevented proper bridge null
300			
500			
700			
1 M			
3			
5			
7			
10			
20			
40			
60	1.7	0.090	
100	1.6	0.080	.58
200	1.5	0.070	
500	1.6	0.060	
700	1.7	0.009	
1 G	1.6	0.008	

RESULTS OF CONDUCTED MEASUREMENTS

Dry Concrete: 5 gal. water per 94 lb sack cement

Portland cement - aggregate ratio: 1/0

Frequency (Hz)	Dielectric Constant	Dissipation Factor	Shielding Effectiveness (db/meter)
10	--	--	8.50×10^{-7}
50	--	--	
100	22.1	0.439	
300	14.0	0.408	1.23×10^{-5}
1 K	9.4	0.416	
3	7.8	0.283	
10	6.9	0.172	
30	6.2	0.117	
100	5.7	0.073	
300			
500			
700			
1 M			
3			
5			
7			
10			
20			
40			
60			
100			
200			
500			
700			
1 G			

RESULTS OF CONDUCTED MEASUREMENTS

Moist Concrete: 5 gal. water per 94 lb sack cement

Portland cement - aggregate ratio: 1/0

Frequency (Hz)	Dielectric Constant	Dissipation Factor	Shielding Effectiveness (db/meter)
10	--	--	4.3×10^{-7}
50	--	--	
100	150.4	0.579	
300	98.9	0.926	
1 K	41.2	0.894	
3	21.3	0.734	1.27×10^{-5}
10	12.7	0.530	
30	9.8	0.369	
100	8.5	0.235	
300	8.2	0.083	
500	7.1	0.053	6.59×10^{-4}
700	8.4	0.021	
1 M	7.9	0.009	
3	7.9	0.009	
5	6.4	0.010	
7	5.8	0.012	
10	4.0	0.014	
20	3.8	0.020	
40	3.7	0.030	
60	3.0	0.050	
100	3.0	0.050	0.56
200	2.9	0.050	
500	2.3	0.040	
700	2.7	0.021	
1 G	2.6	0.010	

RESULTS OF CONDUCTED MEASUREMENTS

Dry Concrete: 6.5 gal. water per 94 lb sack cement

Portland cement - aggregate ratio: 1/0

Frequency (Hz)	Dielectric Constant	Dissipation Factor	Shielding Effectiveness (db/meter)
10	--	--	3×10^{-7}
50	--	--	
100	13.6	0.298	
300	10.0	0.454	1.02×10^{-6}
1K	7.6	0.308	
3	6.5	0.215	
10	5.8	0.136	
30	5.4	0.092	
100	5.1	0.059	
300			
500			
700			
1M			
3			
5			
7			
10			
20			
40			
60			
100			
200			
500			
700			
1G			

RESULTS OF CONDUCTED MEASUREMENTS

Moist Concrete: 6.5 gal. water per 94 lb sack cement

Portland cement - aggregate ratio: 1/0

Frequency (Hz)	Dielectric Constant	Dissipation Factor	Shielding Effectiveness (db/meter)
10	--	--	3.26×10^{-7}
50	--	--	
100	111.3	0.378	
300	105.5	0.567	
1 K	61.6	0.757	
3	32.9	0.772	8.81×10^{-7}
10	17.3	0.627	
30	12.0	0.483	
100	8.9	0.328	
300	7.7	--	
500	--	--	1.40×10^{-4}
700	15.1	0.004	
1 M	10.5	0.005	
3	8.6	0.006	
5	8.6	0.005	
7	7.9	0.009	
10	7.6	0.010	
20	7.3	0.020	
40	7.2	0.035	
60	3.3	0.091	
100	2.9	0.09	
200	2.8	0.09	
500	2.8	0.08	
700	2.8	0.05	
1 G	2.7	0.02	1.11

RESULTS OF CONDUCTED MEASUREMENTS

Dry Concrete: 8 gal. water per 94 lb sack cement

Portland cement - aggregate ratio: 1/0

Frequency (Hz)	Dielectric Constant	Dissipation Factor	Shielding Effectiveness (db/meter)
10	--	--	8.8×10^{-7}
50	--	--	
100	11.5	0.328	
300	8.0	0.315	1.13×10^{-3}
1K	6.2	0.310	
3	5.4	0.204	
10	4.8	0.132	
30	4.5	0.088	
100	4.3	0.057	
300			
500			
700			
1M			
3			
5			
7			
10			
20			
40			
60			
100			
200			
500			
1000			
1C			

RESULTS OF CONDUCTED MEASUREMENTS

Moist Concrete: 8 gal. water per 94 lb sack cement

Portland cement - aggregate ratio: 1/0

Frequency (Hz)	Dielectric Constant	Dissipation Factor	Shielding Effectiveness (db/meter)
10	--	--	7.39×10^{-7}
50	--	--	
100	57.1	0.614	
300	33.2	0.911	
1K	19.4	0.883	
3	15.8	0.743	1.72×10^{-5}
10	9.5	0.535	
30	7.4	0.369	
100	6.1	0.224	
300	5.6	0.013	
500	5.8	0.008	3.92×10^{-4}
700	5.1	0.009	
1M	5.4	0.010	
3	5.4	0.010	
5	5.4	0.010	
7	5.2	0.015	
10	5.8	0.016	
20	5.6	0.029	
40	5.5	0.040	
60	3.7	0.006	
100	2.6	0.040	
200	2.7	0.023	
500	2.8	0.013	
700	2.8	0.053	
1G	2.3	0.090	5.4

RESULTS OF CONDUCTED MEASUREMENTS

Dry Concrete Block (Featherlite)

Frequency (Hz)	Dielectric Constant	Dissipation Factor	Shielding Effectiveness (db/meter)
10	--	--	1.55×10^{-6}
50	--	--	
100	8.6	0.498	
300	6.2	0.427	1.33×10^{-5}
1K	4.6	0.341	
3	4.0	0.237	
10	3.5	0.144	
30	3.3	0.099	
100	3.1	0.068	
300			
500			
700			
1M			
3			
5			
7			
10			
20			
40			
60			
100			
200			
500			
700			
1G			

RESULTS OF CONDUCTED MEASUREMENTS

Moist Concrete Block (Featherlite)

Frequency (Hz)	Dielectric Constant	Dissipation Factor	Shielding Effectiveness (db/meter)
10	--	--	9.23×10^{-7}
50	--	--	
100	36.9	0.616	
300	30.2	0.791	
1K	13.2	0.816	2.04×10^{-5}
3	8.6	0.701	
10	5.9	0.466	
30	4.7	0.315	
100	4.9	0.202	3.86×10^{-4}
300	4.7	0.127	
500	4.6	0.090	
700	4.5	0.091	
1M	4.5	0.090	
3	4.4	0.092	
5	4.1	0.061	
7	3.4	0.044	
10	2.6	0.05	
20	2.6	0.05	
40	2.5	0.06	
60	1.7	0.09	
100	1.6	0.08	5.76
200	1.5	0.07	
500	1.6	0.06	
700	1.7	0.06	
1G	1.6	0.08	

RESULTS OF CONDUCTED MEASUREMENTS

Dry Natural Slab Limestone

Frequency (Hz)	Dielectric Constant	Dissipation Factor	Shielding Effectiveness (db/meter)
10	--	--	5.13×10^{-7}
50	--	--	
100	52.6	0.409	
300	40.5	0.450	7.04×10^{-6}
1k	26.7	0.400	
3	21.1	0.357	
10	16.7	0.276	
30	13.8	0.235	
100	11.6	0.188	
300			
500			
700			
1M			
3			
5			
7			
10			
20			
40			
60			
100			
200			
500			
700			
1G			

RESULTS OF CONDUCTED MEASUREMENTS

Moist Natural Slab Limestone

Frequency (Hz)	Dielectric Constant	Dissipation Factor	Shielding Effectiveness (db/meter)
10	--	--	5.7×10^{-7}
50	--	--	
100	245.3	0.98	
300	219.8	0.884	
1K	155.7	0.603	4.4×10^{-6}
3	98.2	0.694	
10	52.8	0.626	
30	34.9	0.546	
100	23.5	0.402	3.9×10^{-6}
300	17.9	0.032	
500	17.8	0.0010	
700	14.2	0.0012	
1M	12.3	0.0015	
3	11.8	0.0018	
5	11.8	0.0018	
7	10.7	0.0019	
10	9.4	0.0020	
20	8.6	0.0020	
40	6.7	0.0020	
60	4.4	0.0020	
100	4.3	0.0020	
200	4.9	0.0010	0.046
500	4.0	0.0010	
700	4.0	0.0019	
1G	4.0	0.0016	

RESULTS OF CONDUCTED MEASUREMENTS

Dry Mortar: 6.5 gal. water per 94 lb sack cement

Portland cement - aggregate ratio: 1:1

Frequency (Hz)	Dielectric Constant	Dissipation Factor	Shielding Effectiveness (dB/meter)
10	--	--	1.2×10^{-6}
50	--	--	
100	10.1	0.425	
300	8.5	0.332	7.1×10^{-6}
1k	6.9	0.205	
3	6.2	0.149	
10	5.8	0.092	
30	5.5	0.049	
100	5.3	0.044	
300			
500			
700			
1M			
3			
5			
7			
10			
20			
40			
60			
100			
200			
500			
700			
1G			

RESULTS OF CONDUCTED MEASUREMENTS

Moist Mortar: 6.5 gal. water per 94 lb sack cement

Portland cement - aggregate ratio: 1/1

Frequency (Hz)	Dielectric Constant	Dissipation Factor	Shielding Effectiveness (db/meter)
10	--	--	1.53×10^{-6}
50	--	--	
100	33.5	0.974	
300	27.5	0.654	
1K	19.5	0.706	
3	15.9	0.644	1.46×10^{-5}
10	13.1	0.493	
30	10.1	0.365	
100	8.1	0.245	
300	7.1	0.20	
500	6.7	0.09	3.70×10^{-3}
700	5.1	0.09	
1M	4.9	0.09	
3	4.9	0.09	
5	4.6	0.010	
7	4.7	0.010	
10	4.2	0.012	
20	4.3	0.030	
40	4.3	0.070	
60	4.0	0.07	
100	4.0	0.07	
200	3.6	0.06	
500	3.7	0.07	
700	3.2	0.08	
1G	1.8	0.10	6.78

RESULTS OF CONDUCTED MEASUREMENTS

Mortar: 6.5 gal. water per 94 lb sack cement

Portland cement - aggregate ratio: 1/3

Frequency (Hz)	Dielectric Constant	Dissipation Factor	Shielding Effectiveness (db/meter)
10	--	--	1.14×10^{-6}
50	--	--	
100	28.7	0.656	
300	22.9	0.765	
1K	16.8	0.677	1.50×10^{-5}
3	11.4	0.529	
10	8.1	0.383	
30	6.8	0.283	
100	5.7	0.198	3.56×10^{-4}
300	5.1	0.159	
500	5.8	0.005	
700	5.6	0.008	
1M	5.3	0.009	
3	4.9	0.010	
5	4.6	0.015	
7	4.6	0.015	
10	4.5	0.018	
20	4.3	0.030	
40	4.4	0.040	
60	3.8	0.060	
100	3.7	0.040	1.13
200	2.6	0.010	
500	2.6	0.019	
700	2.7	0.020	
1G	2.6	0.020	

RESULTS OF CONDUCTED MEASUREMENTS

Mortar: 9.8 gal. water per 94 lb sack cement

Portland cement - aggregate ratio: 1/3

Frequency (Hz)	Dielectric Constant	Dissipation Factor	Shielding Effectiveness (db/meter)
10	--	--	5.66×10^{-7}
50	--	--	
100	19.1	0.272	
300	15.1	0.396	
1K	9.8	0.414	1.20×10^{-5}
3	7.3	0.392	
10	5.6	0.299	
30	4.8	0.227	
100	4.1	0.161	7.10×10^{-4}
300	3.8	0.021	
500	4.4	0.018	
700	4.3	0.013	
1M	4.2	0.016	
3	4.0	0.009	
5	3.8	0.009	
7	3.6	0.009	
10	3.5	0.009	
20	3.5	0.009	
40	3.4	0.009	
60	2.2	0.009	
100	2.1	0.008	5.59
200	1.5	0.007	
500	1.2	0.05	
700	1.3	0.07	
1G	1.3	0.07	

RESULTS OF CONDUCTED MEASUREMENTS

Dry Plaster of Paris

Frequency (Hz)	Dielectric Constant	Dissipation Factor	Shielding Effectiveness (db/meter)
10	--	--	6.04×10^{-7}
50	--	--	
100	2.8	0.111	
300	2.7	0.082	2.99×10^{-6}
1K	2.6	0.053	
3	2.5	0.0377	
10	2.5	0.020	
30	2.4	0.015	
100	2.4	0.009	
300			
500			
700			
1M			
3			
5			
7			
10			
20			
40			
60			
100			
200			
500			
700			
1G			

RESULTS OF CONDUCTED MEASUREMENTS

Moist Plaster of Paris

Frequency (Hz)	Dielectric Constant	Dissipation Factor	Shielding Effectiveness (db/meter)
10	--	--	1.45×10^{-6}
50	--	--	
100	4.1	0.323	
300	3.8	0.288	
1K	3.2	0.149	
3	3.1	0.107	7.58×10^{-6}
10	2.8	0.055	
30	2.8	0.035	
100	2.7	0.008	
300	2.9	0.008	
500	3.2	0.008	1.50×10^{-4}
700	3.4	0.004	
1M	3.3	0.003	
3	3.3	0.002	
5	3.4	0.0007	
7	3.3	0.0006	
10	3.1	0.0005	
20	3.0	0.0009	
40	3.0	0.0070	
60	3.0	0.0009	
100	2.8	0.0009	0.77
200	2.3	0.0009	
500	1.5	0.0010	
700	1.4	0.0009	
1G	1.4	0.0010	

RESULTS OF CONDUCTED MEASUREMENTS

Acrylic Plastic (Hysol)

Frequency (Hz)	Dielectric Constant	Dissipation Factor	Shielding Effectiveness (db/meter)
10	2.95	0.03	1.31×10^{-6}
50	2.93	0.031	
100	2.79	0.024	
300	2.76	0.014	
1K	2.75	0.007	3.84×10^{-5}
3	2.90	0.009	
10	2.71	0.013	
30	2.69	0.018	
100	2.64	0.022	1.31×10^{-3}
300	2.60	0.026	
500	2.76	0.030	
700	2.76	0.027	
1M	2.76	0.024	
3	2.76	0.020	
5	2.62	0.0100	
7	2.47	0.0058	
10	2.35	0.0038	
20	2.31	0.0030	
40	2.27	0.0020	
60	1.72	0.0017	
100	1.70	0.0016	0.1
200	1.50	0.0015	
500	1.49	0.0012	
700	1.30	0.0012	
1G	1.20	0.0012	

RESULTS OF CONDUCTED MEASUREMENTS

Acrylic Plastic (Lucite)

Frequency (Hz)	Dielectric Constant	Dissipation Factor	Shielding Effectiveness (db/meter)
10	2.90	0.07	3.78×10^{-6}
50	2.85	0.069	
100	2.52	0.066	
300	2.40	0.065	
1 K	2.27	0.062	3.75×10^{-5}
3	2.29	0.055	
10	2.31	0.047	
30	2.15	0.042	
100	2.08	0.038	6.45×10^{-4}
300	2.23	0.020	
500	2.35	0.010	
700	2.03	0.010	
1 M	1.99	0.010	
3	1.95	0.009	
5	1.87	0.009	
7	1.84	0.009	
10	1.77	0.008	
20	1.77	0.008	
40	1.70	0.008	
60	1.80	0.008	
100	1.60	0.007	
200	1.50	0.007	
500	1.49	0.006	
700	1.40	0.006	
1 G	1.30	0.005	0.4

RESULTS OF CONDUCTED MEASUREMENTS

Formica

Frequency (Hz)	Dielectric Constant	Dissipation Factor	Shielding Effectiveness (dB/meter)
10	--	--	9.24×10^{-6}
50	7.	0.27	
100	7.5	0.278	
300	6.4	0.214	
1 K	5.6	0.152	5.84×10^{-6}
3	5.2	0.110	
10	5.2	0.082	
30	6.0	0.065	
100	4.8	0.026	2.86×10^{-4}
300	4.3	0.014	
500	5.1	0.009	
700	5.1	0.008	
1 M	4.9	0.007	
3	4.8	0.007	
5	4.7	0.006	
7	4.6	0.006	
10	4.5	0.008	
20	4.3	0.009	
40	4.2	0.010	
60	1.4	0.010	
100	1.4	0.010	
200	1.4	0.010	
500	1.4	0.010	
700	1.4	0.010	
1 G	1.4	0.010	0.769

RESULTS OF CONDUCTED MEASUREMENTS

Masonite Fiberboard

Frequency (Hz)	Dielectric Constant	Dissipation Factor	Shielding Effectiveness (db/meter)
10	7.	0.8	1.94×10^{-6}
50	6.2	0.601	
100	5.5	0.501	
300	3.9	0.348	
1K	3.5	0.186	
3	3.3	0.109	9.05×10^{-6}
10	3.1	0.063	
30	3.0	0.045	
100	2.9	0.036	
300	2.9	0.018	
500	4.9	0.011	2.06×10^{-4}
700	4.9	0.008	
1M	4.9	0.005	
3	4.9	0.005	
5	4.9	0.004	
7	4.7	0.008	
10	3.9	0.019	
20	3.8	0.030	
40	3.7	0.040	
60	3.9	0.050	
100	3.6	0.045	
200	2.7	0.040	
500	2.8	0.030	
700	2.7	0.010	
1G	2.7	0.030	1.66

RESULTS OF CONDUCTED MEASUREMENTS

Linco Phenolic

Frequency (Hz)	Dielectric Constant	Dissipation Factor	Shielding Effectiveness (dB/meter)
10	--	--	8.05×10^{-6}
50	--	--	
100	12.3	0.310	
300	10.1	0.294	
1K	8.1	0.246	7.87×10^{-5}
3	7.1	0.194	
10	6.2	0.149	
30	5.8	0.120	
100	5.3	0.098	4.66×10^{-5}
300	4.7	0.052	
500	5.8	0.0016	
700	5.5	0.0012	
1M	5.5	0.0012	
3	5.1	0.0030	
5	4.8	0.0044	
7	3.7	0.0037	
10	3.6	0.0056	
20	3.5	0.0070	
40	3.5	0.0079	
60	2.3	0.009	
100	2.2	0.010	4.51
200	2.1	0.040	
500	2.0	0.030	
700	2.0	0.040	
1G	2.0	0.070	

RESULTS OF CONDUCTED MEASUREMENTS

Paper Phenolic

Frequency (Hz)	Dielectric Constant	Dissipation Factor	Shielding Effectiveness (db/meter)
10	--	--	7.09×10^{-6}
50	5.7	0.18	
100	5.7	0.186	
300	5.4	0.096	
1K	5.1	0.061	2.46×10^{-5}
3	4.9	0.042	
10	4.8	0.036	
30	4.7	0.035	
100	4.6	0.036	2.13×10^{-4}
300	4.5	0.014	
500	4.5	0.0051	
700	5.6	0.0051	
1M	5.7	0.0056	
3	5.5	0.0060	
5	4.6	0.0070	
7	4.4	0.0090	
10	3.6	0.0090	
20	3.5	0.0100	
40	3.5	0.0100	
60	3.0	0.01	
100	2.0	0.03	
200	2.0	0.04	
500	1.9	0.085	
700	1.90	0.080	
1G	1.89	0.080	5.30

RESULTS OF CONDUCTED MEASUREMENTS

Vinyl Asbestos Tile

Frequency (Hz)	Dielectric Constant	Dissipation Factor	Shielding Effectiveness (db/meter)
10	--	--	7.75×10^{-6}
50	9.67	0.3	
100	8.98	0.255	
300	7.67	0.215	
1K	6.58	0.166	
3	5.99	0.132	5.89×10^{-5}
10	5.46	0.104	
30	5.19	0.081	
100	5.14	0.041	
300	4.98	0.003	
500	4.84	0.001	
700	4.34	0.001	
1M	4.46	0.001	
3	4.48	0.001	
5	4.78	0.001	
7	4.82	0.001	4.31×10^{-5}
10	4.77	0.001	
20	4.60	0.001	
40	4.54	0.001	
60	1.91	0.02	
100	1.90	0.03	
200	1.80	0.05	
500	1.70	0.04	
700	1.60	0.03	
1G	1.60	0.01	0.72

RESULTS OF CONDUCTED MEASUREMENTS

Balsa wood

Frequency (Hz)	Dielectric Constant	Dissipation Factor	Shielding Effectiveness (db/meter)
10	--	--	6.70×10^{-6}
50	--	--	
100	4.65	1.29	
300	2.58	1.21	
1K	1.59	0.76	5.48×10^{-5}
3	1.27	0.44	
10	1.03	0.29	
30	1.09	0.19	
100	1.02	0.15	1.77×10^{-3}
300	1.04	0.10	
500	1.10	0.0058	
700	1.20	0.0063	
1 M	1.28	0.023	
3	1.24	0.020	
5	1.15	0.019	
7	1.15	0.017	
10	1.07	0.014	
20	1.07	0.020	
40	1.07	0.027	
60	1.13	0.035	
100	1.29	0.040	
200	1.29	0.045	
500	1.24	0.10	
700	1.14	0.12	
1 G	1.12	0.13	11.1

RESULTS OF CONDUCTED MEASUREMENTS

Birch

Frequency (Hz)	Dielectric Constant	Dissipation Factor	Shielding Effectiveness (db/meter)
10	3.85	--	1.39×10^{-6}
50	3.83	0.3	
100	3.71	0.295	
300	3.38	0.173	
1 K	3.12	0.091	4.69×10^{-6}
3	3.02	0.061	
10	2.90	0.042	
30	2.84	0.036	
100	2.73	0.035	1.29×10^{-3}
300	2.65	0.020	
500	2.57	0.014	
700	2.70	0.020	
1 M	2.63	0.023	
3	2.63	0.025	
5	2.63	0.026	
7	2.54	0.027	
10	2.52	0.030	
20	2.49	0.030	
40	2.44	0.030	
60	2.40	0.031	
100	2.40	0.031	
200	2.40	0.036	
500	2.40	0.033	
700	1.92	0.025	2.35
1 G	1.84	0.035	

RESULTS OF CONDUCTED MEASUREMENTS

Cedar (along axis of grain)

Frequency (Hz)	Dielectric Constant	Dissipation Factor	Shielding Effectiveness (db/meter)
10	4.08	0.9	4.20×10^{-6}
50	3.71	0.9	
100	3.56	0.87	
300	3.65	0.64	
1K	3.08	0.343	1.78×10^{-5}
3	2.87	0.199	
10	2.72	0.112	
30	2.64	0.075	
100	2.56	0.057	1.87×10^{-5}
300	2.42	0.040	
500	2.22	0.030	
700	2.18	0.030	
1M	2.13	0.030	
3	2.12	0.029	
5	2.0	0.013	
7	1.79	0.012	
10	1.76	0.015	
20	1.76	0.017	
40	1.75	0.011	
60	1.7	0.022	
100	1.65	0.029	5.0
200	1.48	0.02	
500	1.39	0.02	
700	1.30	0.06	
1G	1.20	0.06	

RESULTS OF CONDUCTED MEASUREMENTS

Douglas Fir

Frequency (Hz)	Dielectric Constant	Dissipation Factor	Shielding Effectiveness (db/meter)
10	5.33	1.0	4.07×10^{-6}
50	4.17	0.91	
100	4.05	0.899	
300	3.22	0.507	
1K	2.73	0.240	1.32×10^{-5}
3	2.55	0.132	
10	2.41	0.073	
30	2.35	0.052	
100	2.27	0.043	4.36×10^{-4}
300	2.46	0.014	
500	2.96	0.009	
700	2.90	0.009	
1M	2.79	0.008	
3	2.74	0.009	
5	2.69	0.009	
7	2.59	0.012	
10	2.49	0.019	
20	2.44	0.019	
40	2.42	0.021	
60	1.90	0.035	
100	1.90	0.030	
200	1.93	0.030	
500	1.82	0.035	
700	1.79	0.027	2.0
1G	1.75	0.029	

RESULTS OF CONDUCTED MEASUREMENTS

Mahogany

Frequency (Hz)	Dielectric Constant	Dissipation Factor	Shielding Effectiveness (db/meter)
10	--	--	3.79×10^{-6}
50	5.84	0.99	
100	5.65	0.989	
300	3.80	0.684	
1 K	2.81	0.393	
3	2.46	0.230	2.13×10^{-5}
10	2.21	0.130	
30	2.11	0.081	
100	2.01	0.063	
300	1.83	--	
500	2.09	0.008	6.48×10^{-4}
700	2.05	0.009	
1 M	1.97	0.010	
3	1.90	0.012	
5	1.88	0.013	
7	1.86	0.014	
10	1.72	0.019	
20	1.69	0.025	
40	1.67	0.022	
60	2.1	0.025	
100	1.82	0.012	
200	1.77	0.017	
500	1.75	0.019	
700	1.69	0.025	
1 G	1.59	0.015	1.08

RESULTS OF CONDUCTED MEASUREMENTS

Mahogany Paneling

Frequency (Hz)	Dielectric Constant	Dissipation Factor	Shielding Effectiveness (db/meter)
10	3.4	0.5	2.44×10^{-6}
50	3.42	0.49	
100	3.33	0.490	
300	2.80	0.325	
1 K	2.40	0.201	1.18×10^{-5}
3	2.19	0.133	
10	2.03	0.089	
30	1.95	0.061	
100	1.88	0.048	8.72×10^{-3}
300	1.84	0.033	
500	2.05	0.010	
700	1.91	0.012	
1 M	1.84	0.013	
3	1.72	0.014	
5	1.69	0.020	
7	1.40	0.025	
10	1.35	0.026	
20	1.32	0.03	
40	1.31	0.037	
60	1.5	0.035	
100	1.46	0.025	
200	1.42	0.030	1.63
500	1.39	0.040	
700	1.29	0.030	
1 G	1.24	0.020	

RESULTS OF CONDUCTED MEASUREMENTS

Mahogany Trim

Frequency (Hz)	Dielectric Constant	Dissipation Factor	Shielding Effectiveness (db/meter)
10	--	--	4.87×10^{-6}
50	--	--	
100	5.82	1.292	
300	3.53	0.899	
1K	3.39	0.559	
3	3.01	0.341	2.76×10^{-5}
10	2.72	0.203	
30	2.58	0.135	
100	2.46	0.095	
300	2.34	0.063	
500	2.59	0.045	2.47×10^{-3}
700	2.49	0.045	
1M	2.40	0.042	
3	2.32	0.041	
5	2.29	0.040	
7	2.28	0.040	
10	2.12	0.039	
20	2.10	0.039	
40	2.06	0.037	
60	2.15	0.025	
100	2.10	0.024	
200	2.05	0.021	
500	2.04	0.023	
700	1.89	0.025	
1G	1.73	0.015	1.03

RESULTS OF CONDUCTED MEASUREMENTS

Oak Flooring

Frequency (Hz)	Dielectric Constant	Dissipation Factor	Shielding Effectiveness (dB/meter)
10	--	--	2.60×10^{-6}
50	--	--	
100	13.29	1.041	
300	7.39	0.847	
1 K	5.13	0.498	2.00×10^{-5}
3	4.30	0.312	
10	3.70	0.185	
30	3.44	0.124	
100	3.20	0.087	6.14×10^{-4}
300	3.15	0.066	
500	2.81	0.010	
700	2.71	0.011	
1 M	2.66	0.011	
3	2.56	0.011	
5	2.34	0.011	
7	2.31	0.011	
10	2.19	0.011	
20	2.17	0.012	
40	2.16	0.017	
60	2.10	0.019	
100	1.80	0.02	
200	1.70	0.02	
500	1.70	0.032	
700	1.60	0.03	2.88
1 G	1.60	0.04	

RESULTS OF CONDUCTED MEASUREMENTS

Yellow Pine

Frequency (Hz)	Dielectric Constant	Dissipation Factor	Shielding Effectiveness (db/meter)
10	--	--	3.80×10^{-6}
50	--	--	
100	5.26	0.957	
300	3.88	0.580	
1K	3.07	0.308	1.60×10^{-5}
3	2.75	0.184	
10	2.45	0.108	
30	2.42	0.070	
100	2.32	0.064	3.14×10^{-3}
300	2.29	0.058	
500	2.35	0.054	
700	2.30	0.053	
1M	2.27	0.052	
3	2.19	0.052	
5	2.16	0.061	
7	1.94	0.042	
10	1.82	0.044	
20	1.80	0.041	
40	1.66	0.038	
60	1.50	0.035	
100	1.48	0.030	
200	1.46	0.026	1.50
500	1.31	0.025	
700	1.30	0.020	
1G	1.20	0.018	

RESULTS OF CONDUCTED MEASUREMENTS

Fir Plywood

Frequency (Hz)	Dielectric Constant	Dissipation Factor	Shielding Effectiveness (db/meter)
10	--	--	2.65×10^{-6}
50	--	--	
100	10.25	0.932	
300	6.45	0.729	
1 K	4.68	0.464	
3	3.51	0.341	1.95×10^{-5}
10	2.92	0.217	
30	2.67	0.151	
100	2.43	0.116	
300	3.08	0.044	
500	3.08	0.014	8.34×10^{-4}
700	3.08	0.014	
1 M	3.05	0.016	
3	2.79	0.018	
5	2.36	0.019	
7	2.23	0.019	
10	2.16	0.020	
20	2.16	0.025	
40	2.16	0.030	
60	1.96	0.036	
100	1.60	0.030	2.62
200	1.86	0.025	
500	1.78	0.031	
700	1.52	0.034	
1 G	1.57	0.036	

RESULTS OF CONDUCTED MEASUREMENTS

Asbestos Shingle

Frequency (Hz)	Dielectric Constant	Dissipation Factor	Shielding Effectiveness (db/meter)
10	--	--	1.66×10^{-7}
50	--	--	
100	25.3	0.092	
300	23.9	0.105	
1K	22.1	0.118	2.28×10^{-6}
3	20.4	0.148	
10	17.6	0.190	
30	15.6	0.096	
100	12.5	0.078	2.76×10^{-4}
300	12.1	0.043	
500	11.9	0.019	
700	11.9	0.011	
1M	10.9	0.010	
3	9.7	0.009	
5	9.4	0.009	
7	8.5	0.009	
10	7.9	0.009	
20	7.1	0.009	
40	6.8	0.010	
60	5.2	0.010	
100	4.1	0.010	
200	4.1	0.010	
500	3.7	0.010	
700	3.6	0.010	.49
1G	3.5	0.010	

RESULTS OF CONDUCTED MEASUREMENTS

Dark Beeswax
(Used with Paper Materials as a Moisture Barrier)

Frequency (Hz)	Dielectric Constant	Dissipation Factor	Shielding Effectiveness (db/meter)
10	2.9	--	1.98×10^{-7}
50	2.92	0.041	
100	2.90	0.037	
300	2.87	0.027	
1K	2.84	0.026	1.4×10^{-6}
3	2.81	0.014	
10	2.73	0.013	
30	2.64	0.009	
100	2.57	0.009	4.02×10^{-4}
300	2.57	0.008	
500	2.57	0.007	
700	2.57	0.008	
1M	2.51	0.007	
3	2.50	0.007	
5	2.49	0.008	
7	2.49	0.009	
10	2.49	0.0015	
20	2.38	0.030	
40	2.35	0.040	
60	2.59	0.049	
100	2.52	0.050	
200	2.50	0.050	
500	2.50	0.050	
700	2.50	0.050	2.76
1G	2.40	0.047	

RESULTS OF CONDUCTED MEASUREMENTS

Light Beeswax

(Used with Paper Materials as a Moisture Barrier)

Frequency (Hz)	Dielectric Constant	Dissipation Factor	Shielding Effectiveness (db/meter)
10	--	--	8.67×10^{-8}
50	2.83	0.02	
100	2.82	0.016	
300	2.82	0.027	
1 K	2.79	0.015	
3	2.78	0.030	8.17×10^{-7}
10	2.72	0.051	
30	2.64	0.049	
100	2.58	0.031	
300	2.56	0.013	
500	2.52	0.005	
700	2.52	0.005	
1 M	2.52	0.005	
3	2.52	0.008	
5	2.52	0.009	
7	2.52	0.012	2.87×10^{-4}
10	2.52	0.014	
20	2.52	0.030	
40	2.52	0.050	
60	2.48	0.084	
100	2.50	0.070	
200	2.50	0.060	
500	2.50	0.057	
700	2.49	0.050	
1 G	2.48	0.042	2.43

RESULTS OF CONDUCTED MEASUREMENTS

Cardboard

Frequency (Hz)	Dielectric Constant	Dissipation Factor	Shielding Effectiveness (db/meter)
10	2.2	0.5	2.56×10^{-6}
50	2.15	0.41	
100	2.05	0.403	
300	1.68	0.275	
1K	1.45	0.168	
3	1.35	0.104	1.27×10^{-5}
10	1.38	0.067	
30	1.34	0.048	
100	1.29	0.078	
300	1.26	0.020	
500	1.23	0.009	7.9×10^{-4}
700	1.23	0.007	
1M	1.31	0.016	
3	1.41	0.022	
5	1.42	0.035	
7	1.46	0.042	
10	1.44	0.041	
20	1.37	0.070	
40	1.21	0.090	
60	1.19	0.120	
100	1.20	0.100	6.79
200	1.25	0.120	
500	1.19	0.090	
700	1.15	0.090	
1G	1.15	0.080	

RESULTS OF CONDUCTED MEASUREMENTS

Glass

Frequency (Hz)	Dielectric Constant	Dissipation Factor	Shielding Effectiveness (db/meter)
10	8.0	--	2.37×10^{-4}
50	7.48	0.011	
100	7.22	0.007	
300	7.07	0.0051	
1 K	6.91	0.0036	1.35×10^{-7}
3	6.85	0.0034	
10	6.81	0.0039	
30	6.69	0.0042	
100	6.14	0.0062	2.88×10^{-4}
300	5.83	0.005	
500	6.50	0.0074	
700	6.61	0.0082	
1 M	6.53	0.0081	
3	6.52	0.0086	
5	6.44	0.009	
7	6.40	0.011	
10	6.40	0.011	
20	6.26	0.013	
40	5.76	0.022	
60	4.62	0.020	
100	5.15	0.01	
200	5.30	0.01	0.504
500	5.03	0.01	
700	3.61	0.01	
1 G	3.26	0.01	

RESULTS OF CONDUCTED MEASUREMENTS

Dry Corrugated Pasteboard

Frequency (Hz)	Dielectric Constant	Dissipation Factor	Shielding Effectiveness (db/meter)
10	--	--	3.8×10^{-6}
50	--	--	
100	1.27	0.47	
300	1.24	0.097	
1 K	1.24	0.067	5.48×10^{-6}
3	1.22	0.054	
10	1.22	0.045	
30	1.21	0.039	
100	1.20	0.043	
300			
500			
700			
1 M			
3			
5			
7			
10			
20			
40			
60			
100			
200			
500			
700			
1 G			

RESULTS OF CONDUCTED MEASUREMENTS

Moist Corrugated Pasteboard

Frequency (Hz)	Dielectric Constant	Dissipation Factor	Shielding Effectiveness (dB/meter)
10	--	--	2.40×10^{-6}
50	--	--	
100	14.1	0.99	
300	6.1	0.95	
1 K	2.2	0.95	
3	1.3	0.96	5.83×10^{-5}
10	1.8	0.61	
30	1.6	0.31	
100	1.5	0.22	
300	1.3	0.091	
500	1.21	0.063	3.35×10^{-3}
700	1.18	0.068	
1 M	1.18	0.040	
3	1.16	0.012	
5	1.06	0.013	
7	1.06	0.012	
10	1.02	0.012	
20	1.02	0.018	
40	1.02	0.019	
60	1.25	0.023	
100	1.30	0.020	
200	1.30	0.019	
500	1.25	0.020	
700	1.12	0.013	
1 G	1.10	0.009	0.78

RESULTS OF CONDUCTED MEASUREMENTS

Tar Paper

Frequency (Hz)	Dielectric Constant	Dissipation Factor	Shielding Effectiveness (db/meter)
10	2.0	0.4	1.96×10^{-6}
50	1.7	0.313	
100	1.6	0.273	
300	1.6	0.193	
1K	1.45	0.117	8.84×10^{-6}
3	1.4	0.078	
10	1.3	0.052	
30	1.3	0.038	
100	1.3	0.029	1.34×10^{-4}
300	1.2	0.019	
500	1.3	0.014	
700	1.4	0.014	
1M	1.4	0.015	
3	1.4	0.016	
5	1.5	0.017	
7	1.5	0.018	
10	1.5	0.018	
20	1.5	0.030	
40	1.4	0.050	
60	1.5	0.080	
100	1.5	0.095	
200	1.4	0.080	
500	1.3	0.080	
700	1.2	0.070	5.21
1G	1.1	0.060	

UNCLASSIFIED

Security Classification

DOCUMENT CONTROL DATA - R & D

(Security classification of title, body of abstract and indexing annotation must be entered when the overall report is classified)

1. ORIGINATING ACTIVITY (Corporate author) The Electro-Mechanics Co. P.O. Box 1546 Austin, Texas 78767		2a. REPORT SECURITY CLASSIFICATION UNCLASSIFIED	
3. REPORT TITLE EM Shielding of Building Materials		2b. GROUP	
4. DESCRIPTIVE NOTES (Type of report and inclusive dates) Final Report (May 66 to June 67)			
5. AUTHOR(S) (First name, middle initial, last name) C. M. Brennan G. F. Roberts C. C. Lambert W. T. Flannery C. G. Conner F. J. Morris			
6. REPORT DATE February 1968		7a. TOTAL NO. OF PAGES 188	7b. NO. OF REFS None
8a. CONTRACT OR GRANT NO. AF30(602)4275		9a. ORIGINATOR'S REPORT NUMBER(S)	
b. PROJECT NO. 4540			
c. Task 454003		9b. OTHER REPORT NO(S) (Any other numbers that may be assigned this report) RADC-TR-67-446	
10. DISTRIBUTION STATEMENT This document has been approved for public release and sale; its distribution is unlimited.			
11. SUPPLEMENTARY NOTES		12. SPONSORING MILITARY ACTIVITY Rome Air Development Center (EMCVI-2) Griffiss AFB, N.Y. 13440	
13. ABSTRACT This report covers the results of a program for measuring the Shielding Effectiveness (S. E.) of Building Materials. Part I of the report describes a number of techniques which were used to make radiated measurements of magnetic field SE from 10 Hz to 50 kHz and conductive measurements from 10 Hz to 1 GHz. A method was introduced for plotting the low frequency field distribution about various shaped ferromagnetic enclosures. Part II contains a group of the significant results of the radiated measurements on a variety of building materials. A collection of tables shows the measured electrical parameters and the calculated shielding obtainable from a cross-section of dielectric building materials.			

DD FORM 1473

UNCLASSIFIED

Security Classification

UNCLASSIFIED

Security Classification

14	KEY WORDS	LINK A		LINK B		LINK C	
		ROLE	WT	ROLE	WT	ROLE	WT
	Electromagnetic Shielding Radio Frequency Interference Dielectrics Magnetic materials.						

UNCLASSIFIED

Security Classification